CORRECTIONS for M.Sc Thesis of S.A.French.

Page No.	Line	Fault	Correction
9	13	Table 2.2.	Table 2.1.
17	4	hi	Li
	4	Yes	No (Semiconductors)
19	12	studies	studied
21	23	verying	varying
(23	11	Evidently	It is evident that)
29	15	abour	about
(29	9 - 10	all mono-kinetic electrons leaving the source, which	all electrons leaving the source, with the energy for which the spectrometer is focused, which are ...
45	11	Insert	$\pi\sqrt{2}$
51		Insert	Kelvin Varley Slide
70	8	hysterisis	hysteresis
73	2	Figure 3.	Figure 3.11.
		Insert	Earth
83	6	Supply	Switch
107	4	$C_1 = 2.1 \times 10^2 \mu F$	$C_1 = 2.1 \mu F$
120	16		Insert $1 \sim 10^{-4}$ mm.
126			Fluting (no.14) should be perpendicular to direction indicated.
135	19	2 seconds	2τ seconds
143	23	2τ and ...	τ and...
145	11	t	τ
153	3	C = 0	$C = \infty$
167	1	Insert	Ω
176	17	(33K)	(33 L)
178	7	Insert	β
	15	CeCl	$CeCl_3$
180	6	fig 6.2.	fig 6.3.
199	26	de Vriss	de Vries

STUDIES IN β-RAY SPECTROMETRY

A Thesis submitted by

SARAH ANNE FRENCH

for the

DEGREE OF MASTER OF SCIENCE

in the

UNIVERSITY OF LONDON

Bedford College

August, 1966.

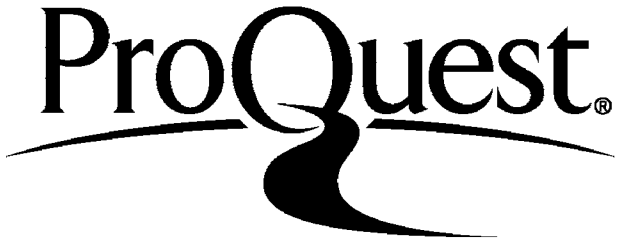

ABSTRACT

A brief survey of the field of β ray spectrometry has been made, particular attention being given to the use of magnetic spectrometers. The performance of various instruments is compared and the principles of operation of different automatic systems are discussed.

An automatic system for a prolate spheroidal field spectrometer was constructed. Details of construction and testing are described and improvements suggested.

Efforts were made to increase the signal to noise ratio of a scintillation detector system, by cooling the photomultiplier tube. The various effects observed are considered in relation to results reported by other workers.

Coincidence circuitry using fast avalanche transistors was constructed and tested. Limiters employing two rather than one transistor had better performance, particularly for the lower electron energies.

Some β - β coincidences in the decay of Ce^{144} were investigated with a view to deciding between the different decay schemes which have been proposed. The 53 keV - 80 keV cascade was identified, but in the case of the proposed 33 keV - 133 keV cascade, the results were inconclusive.

Acknowledgements

I have great pleasure in thanking Professor Richardson for his constant help and encouragement during the course of the work contained in this thesis. I am happy too to acknowledge my debt to Dr. P. Rice-Evans and Mr. R.N.Thomas of Bedford College, and to Dr. D. Michelson of Brunel College for their interest and much useful advice.

My sincere thanks are due to Miss Franklin for typing the thesis as well as to Mr. W. Baldock and the other members of the technical and workshop staff of the Physics Department at Bedford College for their frequent assistance with the experimental work.

I am grateful to Dr. D. Michelson for permission to reproduce Figure 3.1 from her doctoral thesis (Michelson 1960), and to Impex Electrical Ltd. for Figure 3.4; also to the British Institute of Radio Engineers for Figure 3.19 (Bertoya 1963), to the Physical Society for the essentials of Figure 2.5 (Symonds 1955), and to the Institute of Physics, Uppsala for Figure 2.4 (Petterson 1964).

List of Contents — Page No.

List of Figures and Tables

Chapter 4.

Chapter 5.

CHAPTER I

Introductory Survey of β-ray Spectrometry

1.1. The Scope of the Subject

The field of β-ray spectrometry is a central one in low energy nuclear physics. The term "spectrometry" is used in analogy with its use in optics: just as optical spectrometry consists in an analysis of electromagnetic radiation in terms of the frequency (or alternatively of the photon energy $E = h\nu$), so β-ray spectrometry consists in an analysis of β-radiation in terms of momentum or energy. Classification of the characteristic lines in the optical spectra of atoms and molecules leads to the assignment of electron energy levels and the deduction of other of their properties. Similarly the analysis of β-ray spectra permits the assignment of energies and other parameters to nuclear excited states and the testing of many assumptions in nuclear theory.

There are two important classes of β-radiation resulting from different types of nuclear event. There are those electrons which arise within the nucleus itself in the process of β-decay and whose emission causes a change in the atomic number of the nucleus; these electrons have a continuous energy distribution whose characteristic shape, end-point energy and relative strength are important

objects of measurement and analysis in β-ray spectrometry.

The internal conversion lines on the other hand do not come from within the nucleus; they are ejected from an atomic shell as a direct result of the de-excitation of the nucleus and as an alternative to its de- excitation by γ - emission. Conversion electrons have well defined energies equal to the difference between the energy of de-excitation of the nucleus, and the binding energy of the atomic level from which they have been ejected. Measurement of their positions and relative intensities leads to the identification and classification of the excited states of nuclei. Care has to be taken to distinguish low energy internal conversion lines from Auger electrons which often accompany radioactive decay, being emitted in competition with X-rays in the process of atomic de- excitation.

The scope of β-ray spectrometry has enlarged considerably since the original identification of the β-rays, found in the emanation from radioactive matter, with the known "cathode" rays or electrons. The subject may be said to have originated when early investigators "examined by a photographic method the spectrum in a magnetic field of the β-rays expelled from thin films of radioactive matter." (Rutherford 1912). The fundamental distinction between the continuous spectrum and the homogeneous sets of β-rays was recognized early on, and by the beginning of the 1930s

the characteristic features of the 18 or so known β- emitters had been investigated. Study of the continuous spectra led to Pauli's postulate of the neutrino (1931) and Fermi's theory of β-decay (1934), and also contributed to the development of the various nuclear models. The homogeneous lines were attributed to a direct coupling mechanism between the excited nucleus and the atomic electrons by Taylor and Mott in 1933.

The field of study was enlarged with the discovery of artificial radioactivity, and in particular when a plentiful supply of different isotopes was made available from nuclear reactors. Several hundred β-emitters are now known and the need to make precise studies of their decay schemes has led to the development of much improved instruments and techniques.

β-ray spectrometry is primarily concerned with the measurement and analysis of the momentum distribution of the electrons emitted by these nuclides, and in this introductory chapter the chief methods of measurement will be reviewed, together with the type of information which can be deduced from them. Often, however, the term is extended to include the measurement of quantities such as the life-times of excited states and the angular correlation between cascade emissions; these provide useful complementary information in establishing and interpreting the energy level schemes for the decaying nuclides. Further information about the excited states may be obtained when they are excited by coulomb excitation, or radiative capture; the methods of β-ray spectrometry are applied to

measurement of electron energies in these and many other cases, both within nuclear physics and outside it. These topics, however, lie outside the scope of the present thesis.

1.2. Methods of β-ray Spectrometry.

1.2.1. Spectrometers.

Various types of spectrometer are available. Of these the magnetic spectrometers are easily the most precise though their efficiency is poor. Others with less good resolving powers can have efficiencies approaching 100%. The choice of spectrometer depends on the type of measurement required, on the strength and half- life of the source available, as well as on other factors. Magnetic spectrometers are fully considered in the next chapter; the salient properties of the other types are mentioned here. The data assembled in Table 1.1. provides a rough basis for comparison.

(a) Scintillators. The combination of a scintillator, a photomultiplier and a multichannel pulse height analyser provides a β-ray spectrometer which is quick and easy to use, and in which the whole spectrum is recorded simultaneously. Such counters have in general good efficiency which makes them useful for short lived isotopes. Cramer (Cramer 1962) has used a specially designed spectrometer for such isotopes in the region of

TABLE 1.1. Comparison of Properties of β-ray Spectrometers

Spectrometer Type	Energy E per ion pair	Line width $\Delta W_{1/2}$	Geometry	Stopping Power (rough classification)	Speed of Response	Energy Range	Affected by Magnetic Field
Scintillator	500 eV (per photoelectron)	100 keV	Approx. 4π for split crystal arrangement	good	2 n.s.	100 keV–13 MeV	Yes
Gas Proportional Counter	30 eV	27 keV	2π or 4π for source mounted internally	poor	1 μs (100 μs dead-time)	< 1 keV–100 keV	No
Semiconductor	3.5 eV	5 keV	Small area; mosaic of counters used to improve geometry.	Poor	3 n.s.	50 keV–1 MeV (hi-drifted type for high energies	Yes
Magnetic (see Table 2.1)	-	~0.01% ~1.5%	Efficiency $\sim 10^{-3}$% ~ 5%		Depends on detector	0–Several MeV Pre-acceleration for very low energies	-

energy greater than 3 MeV and his results compare favourably with those obtained by magnetic analysis.

The distorting effects which back-scattering and incomplete absorption may have on the line shape can be minimized by careful design and by using a phosphor of low atomic number. The pulse height is proportional to energy over a wide range. The gain depends sensitively on the voltage applied to the photomultiplier tube and is also temperature-dependent (see Chapter 4). The limit of resolution is about 8% for 1 MeV electrons and worse for low energy particles. The counters are capable of extremely good time resolution, if plastic phosphors and specially designed photo-multiplier tubes are used.

(b) Gas counters, which are operated in the "proportional" region such that the output pulse is proportional to the energy of the incident particle are also used as spectrometers. They are preferred to scintillation spectrometers for low energy β-rays owing to their better resolution and the greater possibility of discriminating against background or noise pulses. Gas flow proportional counters have been used to investigate the β-spectrum of Tritium whose end-point energy is only 18.5 KeV. On the

other hand the poor stopping power of even large volume counters makes them unsuitable for energy determinations above about 100 KeV. With large volume counters special precautions have to be taken to reduce the background counting rate. Gaseous sources are often used; they may be mounted internally thereby eliminating the need for thin end windows and for supporting films, and thus enhancing the performance of the counters for weak sources and low energy rays.

(c) Semiconductor devices are very compact and the complete spectrum may be studies simultaneously using a multichannel analyser. Their speed of response is comparable with that of scintillation counters but their energy resolution is considerably better.

In these counters, as in scintillation or gas counters, statistical fluctuations in the multiplicative processes make a major contribution to the line width and thus to the resolution. The magnitude of the effect depends on the number of primary ion-pairs formed by the β-ray, or in the case of the scintillation counter, on the number of photo-electrons emitted from the photo-cathode. Thus the resolution, or line width (fwhm). $\Delta W_{\frac{1}{2}}$, depends on the energy

E of the incident β-rays necessary to liberate one secondary electron in the medium of the counter. Comparative values of E and $\Delta W_{\frac{1}{2}}$ are given in Table 1.1 and indicate the superiority of semiconductor spectrometers over the scintillation or gas types. In practice the resolution of a semiconductor is also limited by current leakage in the crystal and by noise in the sensitive pre-amplifier.

The small sensitive thicknesses available limit the usefulness of semiconductor devices for resolving the energy of fast β-rays. The specially constructed lithium drift detectors have much larger sensitive volumes but they are very expensive and their performance deteriorates with time, also their response times are slower than for the surface barrier type. Semiconductor counters are being used increasingly as β-particle spectrometers and it is to be expected that with the large amount of research on them which is being pursued, leading to improvements in properties and performance, their application will become even more widespread.

1.2.2. Source Preparation.

The preparation of suitable sources requires very careful attention especially when low energy β-rays are being

studied. The problem is avoided when the source is incorporated in the medium of the counter. In other cases a very thin layer of the isotope is deposited on a suitable backing. The backing must be thin and of low atomic number so as to reduce back-scattering; the source layer itself must be thin so as to minimize absorption. Aluminium leaf or films of organic materials are usually used for backing; VYNS resin (Yaffe 1962) has been found particularly suitable. The thickness of the films may be measured by various techniques; interferometric methods are capable of good accuracy but methods involving the absorption of α or β rays in matter have found wide acceptance. A very simple method using α-particle absorption is described in Chapter 4. When insulating backing materials are used some thin metallic or graphite stripshould be used to connect the source to ground thus preventing distortion of the spectrum due to charging up of the source.

The most usual methods for depositing the source in a thin uniform layer have been surveyed by Parker and Slätis (Parker 1965); of these electro-deposition in vacuum and electro-static spraying are among the most popular.

1.3. Information yielded by study of β-ray spectra.

Many conclusions at verying levels of abstraction have been deduced from the body of precise measurements of β-ray

spectra which has been accumulated. At the same time the experimental data has been a starting point and an important point of reference for many hypotheses and theories in nuclear physics. The increasing quantity and precision of the experimental results justify increasing detail and rigour in the theoretical treatment.

1.3.1. Nuclear Decay Schemes.

Analysis of the β-ray spectrum of a β-emitting isotope often permits an unambiguous assignment of its decay scheme, including the identification of some of the excited states of the daughter nucleus. In complex cases additional information such as is derivable from coincidence measurements may be required. Complementary information is obtained in the special cases when different parent nuclei both give rise to the same daughter nucleus, one by the emission of an electron and the other by the emission of a positron; the accompanying conversion line spectrum is in either case that of the daughter nucleus.

The energy loss of a nucleus in a β-decay is obtained from the Fermi-Curie Plot by measurement of the end-point energy. The energy of de-excitation is obtained from the energies of the group of internal conversion lines associated with a given transition combined with a knowledge of the binding energies of the electrons in the K, L, M

atomic shells; alternatively, it may be obtained by measurement of the corresponding γ- ray energy.

Working out the decay scheme on the basis of the spectroscopic data is often a lengthy and painstaking procedure, especially when, as for example is the case with the isotope Au^{194}, many hundreds of lines, corresponding to more than a hundred γ-transitions are observed. Mitchell (Mitchell 1965) has summarized the chief methods used in the analysis of different types of spectra. He points out the need for the complementary information which different instruments and methods yield. Evidently the analysis is facilitated if the data are both reliable and precise.

1.3.2. Multipolarities of Transitions.

In many cases the multipolarity of a nuclear transition can be determined by comparing the measured values for the relative intensities of the conversion lines with the theoretical values computed by Sliv and Rose and their coworkers. At low energies the ratio of the line intensities in a given subshell e.g. $L_1 : L_3$, when these have been resolved, is a sensitive function of the multipolarity whether it be a pure or a mixed transition. At higher energies and for lighter elements it is often easier to use the K internal conversion co-efficient α_K. This is defined

by the relation

$$\alpha_K = \frac{N_k}{N_\gamma}$$

where N_k is the number of electrons emitted as the result of internal conversion in the K shell and N_γ is the number of γ-photons corresponding to the same nuclear transition emitted in the same interval of time.

1.3.3. Spins and Parities of States.

Different lines of evidence lead to the assignment of the spins and parities to nuclear energy states.

(i) Internal Conversion Line Data; having decided the multipolarity of a certain transition the theory of the electromagnetic field gives directly the change of spin and parity involved.

(ii) The Classification of β-transitions; once β-decay processes have been classified, as allowed, first forbidden or second forbidden, the Fermi theory of β-decay may permit the change of angular momentum to be deduced. The classification is made on the basis either of the ft.- values, or of the shape of the continuous β-spectrum. In the latter case the evidence is not always unambiguous.

(iii) Other indications of angular momentum can be obtained from, for example, angular correlations or such

observations as the total absence of a γ-ray corresponding to well-defined internal conversion lines, which would indicate a 0 - 0 transition.

In general, the absolute assignment of spins and parities of nuclear states may be made with a reasonable degree of accuracy once sufficient information has been accumulated as to the way in which they change.

1.3.4. Nuclear Models

Once the energy levels of a nuclide, together with their spins and parities are known with a reasonable degree of certainty they can be used as a test for the various nuclear models and, in particular, to disginguish between the single-particle and the collective-nucleus types of model. In certain nuclear transitions the whole nucleus appears to be involved collectively, while in others it is probable that only individual nucleons are affected.

The transition probabilities or the life-times for γ-decay or for the emission of conversion electrons give additional evidence on the relevance of particular models. In general short life-times are characteristic of processes in which the whole nucleus is involved.

1.3.5. β-Decay Theory.

Measurement of the shape and end-point energy of the continuous β-spectrum permit the investigation of various

aspects of Fermi's theory of β-decay. An upper limit can be set to the rest mass of the neutrino and the coupling constant g of the weak interaction can be estimated. The final evidence in favour of the vector and axial vector type of β-interaction was obtained from experiments on nuclear recoil.

1.4. Situating the Present Thesis

The preceding section indicated the considerable contribution of β-spectrometry to our knowledge of the nucleus. While the predominant decay modes of the many β-emitters are known, yet many ambiguities and discrepancies in the experimental evidence remain and work is in progress on many fronts to try to resolve these differences. Much depends on the experimental techniques which are available. Better resolutions should help both in distinguishing closely spaced β or γ transitions and also in resolving conversion lines of the same nuclear transition due to the ejection of electrons from different atomic shells. Improved techniques should also permit the extension of the investigation in various respects: to short-lived isotopes and weak sources as well as to low energy transitions.

The great emphasis on nuclear techniques in recent years is evidenced by the publication of journals devoted exclusively to them, such as, for example, Nuclear Instruments and Methods, first published by the North Holland Publishing Company in 1957. It is interesting to note that techniques which have been developed in connection with β-ray spectrometry are now finding application in other fields. Ewan and Graham (Ewan 1965), for example, list many applications of high resolution magnetic spectrometers to problems in atomic physics. For example, electron spectroscopic methods have been used at Uppsala to draw up a table of electron binding energies, whose accuracy, the authors claim, compares favourably with that obtained by the previous X-ray method.(Hagstrom 1965).

It is in the context of the importance of refined techniques for extending our knowledge of different decay processes that this thesis must take its place. Various modifications and improvements have been made to the two magnetic spectrometers in this laboratory with a view to investigating β-β coincidences. A start has been made on such a study of the isotope Ce^{144} and this is reported in chapter 6. Many of the levels of this isotope are low lying and there is still dispute as to the existence of some of the weaker transitions and the arrangement of the

energy levels. The automatic system, described in chapter 3, was constructed so as to reduce the tedium involved in counting rare coincidences. It was hoped that by improving the detection system of the small spectrometer (chapter 4) the signal to noise ratio could be enhanced, thus facilitating the study of low energy lines. The fast coincidence circuitry was constructed in order to reduce the time resolution of the system, thereby improving the ratio of true to random coincidences; the performance of the coincidence system is treated in chapter 5.

CHAPTER 2

Magnetic Spectrometry

2.1. Important Properties of a Spectrometer

The two fundamental properties of a spectrometer are its Momentum or Energy Resolution and its Transmission or Collecting Power. The Resolution of a spectrometer determines its ability to distinguish electrons with small momentum differences and is measured in terms of the relative line width, the line width being usually measured at half the maximum height. $R = \Delta_{1/2} B\rho / B\rho$, and is constant for a spectrometer of fixed geometry. The Transmission is defined as the fraction of all mono-kinetic electrons leaving the source which are counted in the detector.

Owing to the inevitable presence of aberrations, the requirements of good transmission and good resolution tend to conflict; an optimum ratio of abour 1 for the value of the transmission to that of the resolution is obtained for good instruments. The flux of particles arriving at the detector depends not only on the transmission but on the activity of the source: this is determined both by its specific activity and by its area. The source thickness must always be kept vanishingly small to reduce the distorting effects of absorption and back-scattering on the spectrum.

However, increasing the source area only leads to a

deterioration in the resolution, for a spectrometer of given design and overall dimensions. Thus a compromise between the resolution on the one hand and the transmission and source area, which together determine the counting rate, on the other, must be arrived at for any particular experiment. It can then be understood why a further parameter the luminosity defined as the product of the transmission and the source area, is often preferred to the transmission as being more relevant to the description of the performance of a spectrometer.

Other features of a spectrometer which are of particular relevance in special applications are:-

(i) The precision with which the magnetic field and hence the momentum of the electrons can be determined.

(ii) The absolute accuracy of momentum determination.

(iii) The sensitivity of the spectrometer field to ambient magnetic fields.

(iv) The escape of magnetic flux from the spectrometer, which might interfere with ancillary equipment.

(v) Ease of access to source and detector.

(vi) Proportional dependence of the magnetic field and thus of the momentum of the focused electrons on current.

(vii) Possibility of shielding the detector so as to exclude background radiation.

(viii) The dispersion, dispersion being defined as the change in position of the electron - optical image for a small change in the magnetic rigidity of the electrons; this parameter is closely related to the resolution and transmission, it decreases as the size of source is increased.

(ix) The magnitude of the spherical aberration, where spherical aberration is defined as the spread in image position for electrons of the same rigidity. Even when, with the use of baffles, electrons of different rigidity can be excluded from the detector, still the aberration will necessitate the use of a large detector.

2.2 Types of Spectrometers

A convenient though not a rigorous classification of spectrometers is that which divides them into Flat and Helical types. In Flat spectrometers the field is perpendicular to the direction of travel of the particles; in Helical instruments the two are parallel. Further distinctions depend on the type of focusing, whether or not iron is used to produce the field as well as other factors. A brief description of the chief types will be given together with an estimation of their relative merits.

2.2.1. Flat Spectrometers

(a) The Semicircular Spectrometer is the prototype of β-spectrometers and has been used since 1912. The electrons are detected after completing a semi-circular path perpendicular to a uniform magnetic field (fig.2.1a). One dimensional focusing is achieved in this way but any electrons which leave the source at an angle to the median plane will not be brought to a focus.

The resolution depends inversely on the radius of the orbit but the lack of focusing, giving rise to very low transmissions, limits the extent to which the resolution can be improved by increasing the radius. However, the possibility of making long photographic exposures of the spectrum and of

Fig. 2.1. Ray Paths in "Flat" Spectrometers

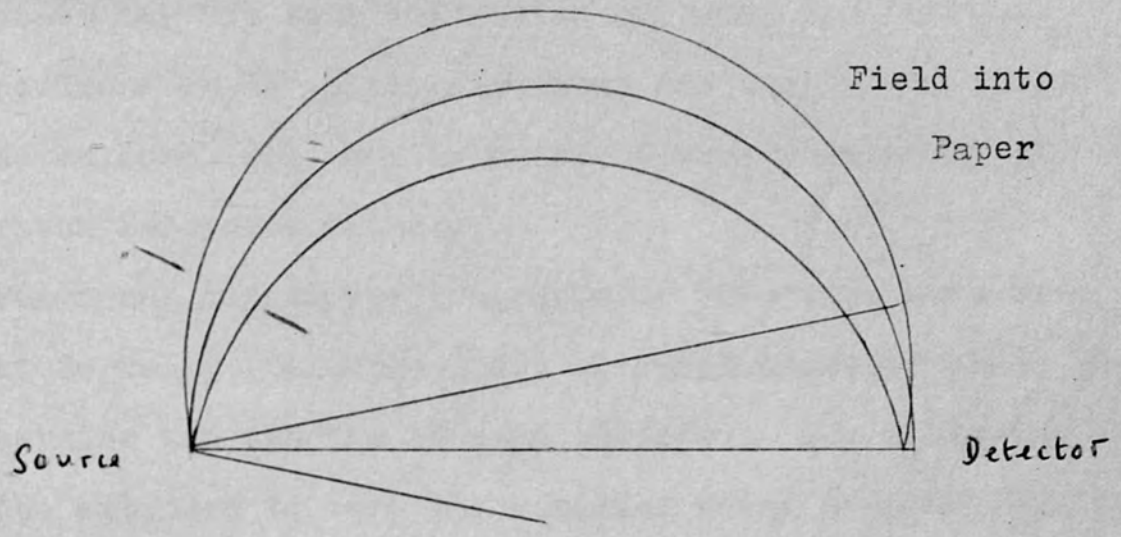

(a) Semicircular Spectrometer: Uniform Field.

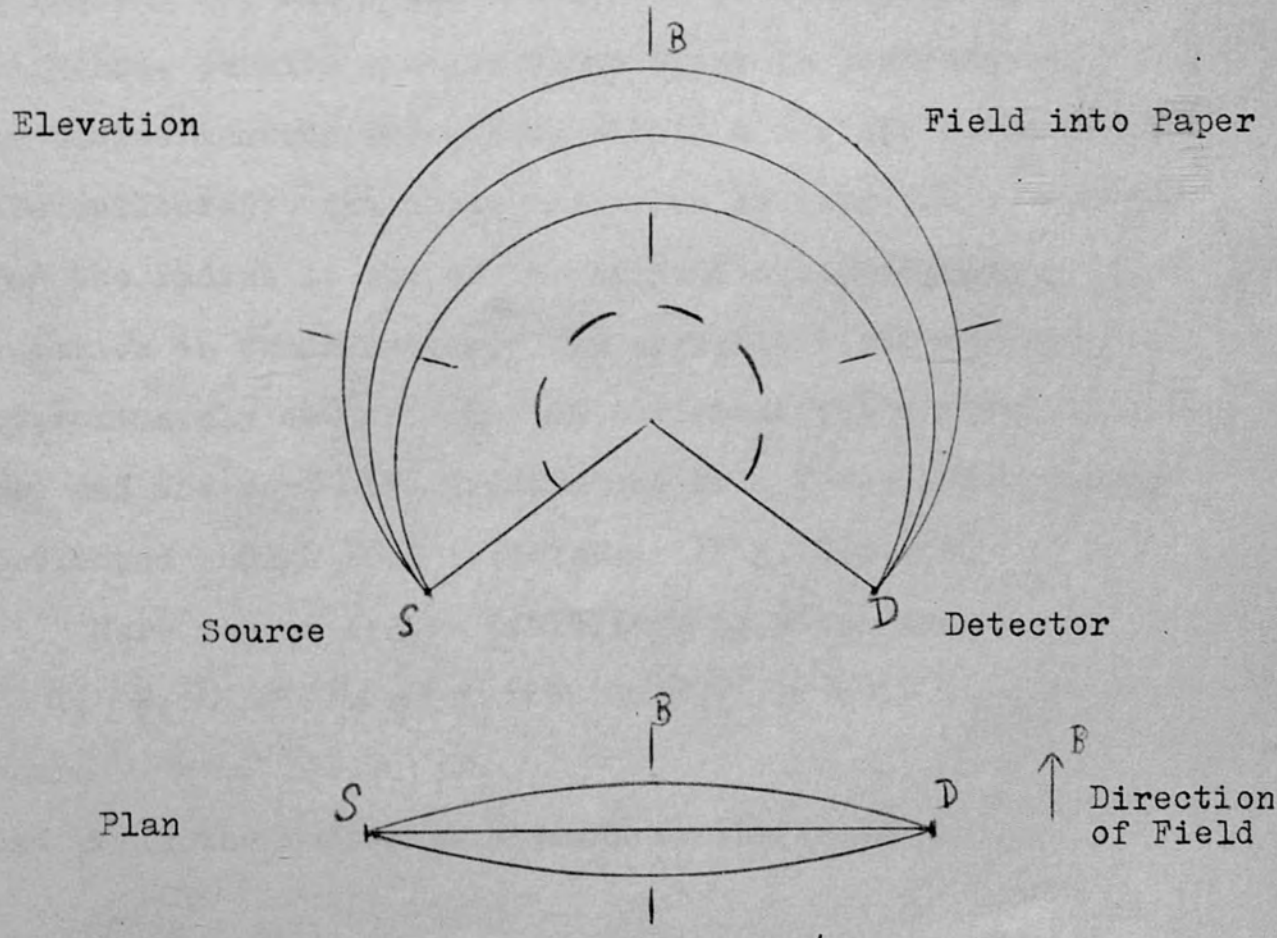

(b) $\pi\sqrt{2}$ Spectrometer: Field Varies as $1/\sqrt{e}$

studying a range of momentum values simultaneously partly compensate for the poor collection efficiency. Further, the spectrometer is relatively cheap and easy to construct and the uniform field can be measured very accurately by the proton resonance method.

Permanent magnet spectrographs of this type have been used at Berkeley (Valentin 1962) at resolutions of about 1% to determine the spectra of many isotopes. The analysis has been extended to very low energies using pre-acceleration techniques, with photographic detection.

(b) The Double Focusing Spectrometer, the underlying principle for which was discovered by Svartholm and Siegbahn, permits a major improvement in performance. All particles leaving the source within a certain solid angle are collected; the resolutions can be improved by increasing the radius of the orbit, without a corresponding deterioration in transmission. The magnetic field varies approximately as $1/\sqrt{\rho}$ in the region of the central trajectory and the particles are brought to a focus after being deflected through $\pi\sqrt{2}$ radians. (fig. 2.1.(b)).

More generally the field form is given by

$$B_z(\rho, 0) = B_0 \{1 + \alpha\eta + \beta\eta^2 + \gamma\eta^3 + \cdots\}$$

where $\eta = (\rho - \rho_0)/\rho_0$

and ρ is the radius at a point in the field

ρ_0 is the radius at the central trajectory

α, β, γ are constants to be determined to minimise aberration.

Usually $\alpha = -\frac{1}{2}$ and either $\beta = 3/8$, in which case the resolution is independent of the length of the source, or $\beta = 1/8$ when it is independent of its width; thus a line rather than a point source may be used which permits a corresponding improvement in the luminosity.

The required field shape can be achieved either with or without the use of iron. The chief advantage of using iron is that the spectrometer field is shielded from external fields, and the flux leakage from the spectrometer can be reduced. Such a field is relatively insensitive to temperature fluctuations and further, the power consumption is small. Such instruments suffer, however, from the disadvantage that the field is not strictly proportional to the current and also the field form is a function of the field strength. This means that the field at a particular point in the spectrometer as determined using a probe is not necessarily a very accurate measure of the field actually at the electron orbit. The accuracy with which the momentum of β-ray lines can be determined is thus limited, particularly at low energies where the effect of the magnetic

retention of the iron is particularly marked.

Two principal configurations have been used to produce the required field shape. In the "double mushroom" type there is easy access to source and detector, and to the field for measurement purposes; on the other hand, the fringing fluxes are more easily controlled in the "inside out" design in which the field is completely enclosed by iron.

A precision instrument of the first type, referred to in a later section (2.3.2.), is in use at Uppsala. (Backström 1962).

Bartlett and his co-workers at Colorado (Bartlett 1962) preferred the "inside out" design; their instrument has the additional advantage that the field parameters can be altered by varying the current configuration in the coils. Typical performance data for the spectrometers are given in table 2.1.

There is a limit to the extent to which the resolution of an"iron" spectrometer can be improved by increasing the radius of the orbit; as the field necessary to focus the electrons decreases the adverse effects of hysteresis become increasingly noticeable. This does not arise with iron free spectrometers which are thus preferred for high resolution

work. In this case, however, care must be taken to make accurate compensation for the earth's field and a site is chosen as far as possible from local magnetic disturbances. Iron must be excluded from the vicinity so that certain experiments, such as those requiring a flux of neutrons from a reactor, are immediately excluded. Temperature compensation is necessary to allow for any change in the coil dimensions.

A special iron free building was constructed in a carefully chosen site to house the 100 cm $\pi\sqrt{2}$ spectrometer at Chalk River and elaborate degaussing facilities were provided. Even very small magnetic disturbances are significant as fields of the order of only a few gauss are sufficient to focus even 100 kev electrons. The resolving power of this instrument is among the highest available going as low as 0.01% at a luminosity of 10^{-5} cm^2. However, such resolution is not often required and it is usually run at lower resolutions and correspondingly higher luminosities.

(c) Sector Spectrometers have the advantage, especially for coincidence work, that both source and detector can be placed outside the field.

(i) The radial variation of the field in the sectors may be $1/\sqrt{e}$ as in the case of the double focusing instruments described above; the fringing fields cause defocusing unless the aperture is kept small; thus in general the transmission

of such instruments is low.

(ii) Other workers have used fields varying as $1/\rho$; Kofoed-Hansen and co-workers were first to arrange several such sectors as a group of"orange segments", around source and detector, thus greatly improving the solid angle of collection. The sectors must be identical and this is most easily achieved using iron-free torroidal coils. Transmissions as high as 20% for resolutions of the order of 1% have been achieved at the Argonne laboratory. (Freedman 1960).

(iii) Kelman et al (Kelman 1962) have used a single sector as part of a prism spectrometer, which also employs collimating and focusing "lenses" in analogy with an optical spectrometer. An advantage is that focusing and dispersion are performed by separate electron optical systems. Also the source and detector may be removed to considerable distances from the deflecting magnet, thus permitting good shielding of detector with consequent reduction in background counting rate.

2.2.2. Lens Spectrometers

In general the performance data for the lens type of spectrometer are less good than those for the double focusing instruments. They are capable of high transmission but the luminosity at a given resolution is lower owing to the need for a point rather than a line source.

The Short Lens Spectrometer consisting of a single short solenoid is simple to construct and permits easy access to source and detector. It has, however, largely been superseded for precision work.

The Long Solenoid Spectrometer has better performance data. The source and detector are both inside the homogeneous solenoid field in which the electrons describe helical trajectories. A carefully constructed ring focus is needed to define the momentum of the beam reaching the detector; there is a considerable spherical aberration, however, and a large detector is needed if the spectrometer is to have a good collection efficiency. In practice the transmission is limited to about 5% or less. An advantage is the precision with which the field can be determined using the proton resonance method. Jungerman achieved a precision of a few parts in 10^5 in the absolute determination of the energy of certain lines in the spectrum of Th.B., using such a spectrometer. (Jungerman 1962).

The aberrations present in the lens spectrometer can be reduced by suitable shaping of the field.

In the Intermediate Image Spectrometer due to Slätis and Siegbahn the field has a concave form, reaching a minimum at the centre where there is an intermediate ring focus. The aberration is reduced compared to the long lens spectrometer but good transmission is maintained; however, the resolution falls off badly as the source diameter is increased. Typical figures of merit are R = 3% and T = 8%.

An intermediate ring focus also exists in the Prolate Spheroidal Field Spectrometer in use at Bedford College. The rays are strongly bent after passing through the ring slit (see figure 2.2) and a concentrated beam reaches the detector which may be small without loss in transmission. Freeman (Freeman 1960) compared the effect of increasing the source area on the resolution in this case and also in the case of the Concave Field type above; the effect was worse in the latter case though the radius of the orbit was smaller which would at least partly account for it. It has been shown (Richardson 1963) that the luminosity is not so favourable as for a uniform field spectrometer of the same size, but that for thin sources of small diameter the Prolate Spheroidal field can give a larger transmission for the same resolution.

Fig, 2.2. Ray Paths in Lens Spectrometers.

(a) Prolate Spheroidal Field

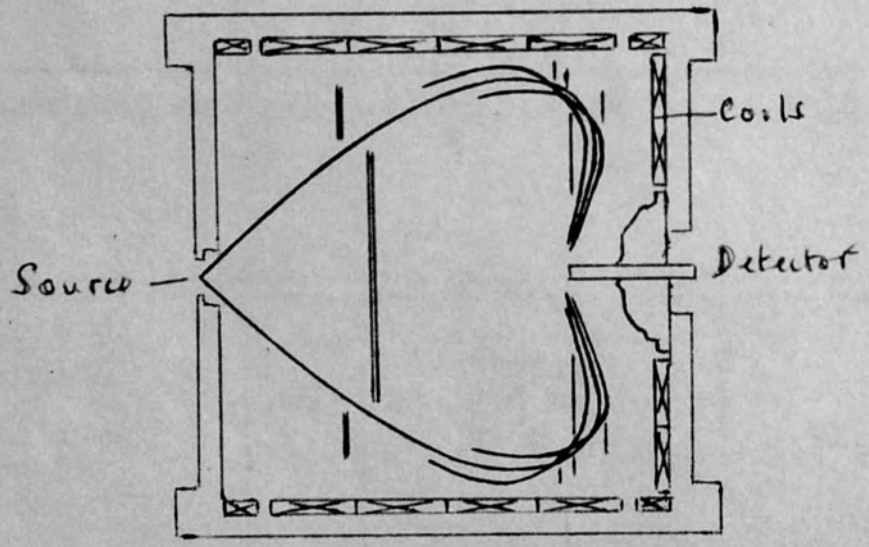

(b) Long Lens Spectrometer

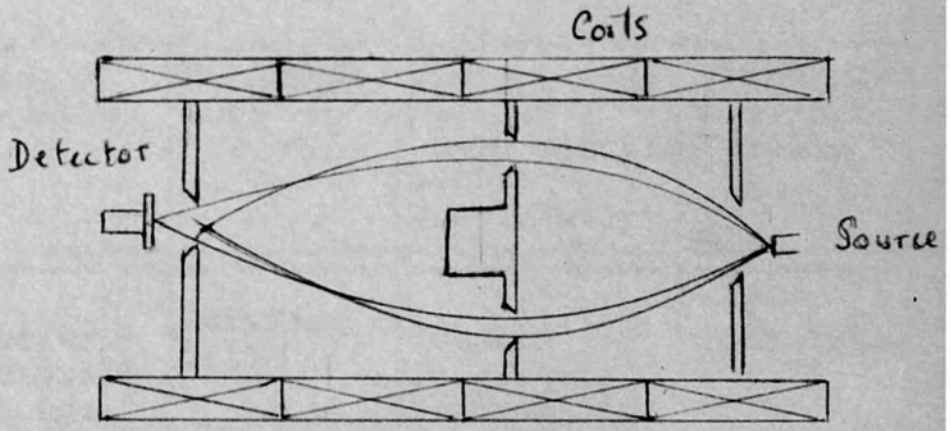

TABLE 2.1

Spectrometer Type	R %	T %	Source dimensions	Spectrometer dimensions	Particle detector	Measurement of Magnetic Field	Application; other remarks	Reference
Semicircular	0.1		fine wire d < 1/4 mm	$r \sim 20$ cm	Photographic recording at constant field.		Used for relative $B\rho$ measurements	Valentin (1962)
Semicircular	.25	.07	5 x .1cm	$r \sim 30.5$cm	Geiger counter	Rotating Coil	Energy range 0-4 Mev using electrostatic accelerator	Geoffrion & Giroux (1956)
Double Focusing $\pi\sqrt{2}$ With iron "double mushroom"	.05	.2	Strips 2.8 mm x 50 mm	50	Geiger & Scintillation Counters	Rotating Coil	Spectra following neutron capture by target nuclei; energies up to 12 Mev	Bäckström (1962)
With iron "inside out"	1.5 .07	5 .5	width .02" .02	30	Geiger Counter	Peaking Strip		Bartlett (1962)

Spectrometer Type	R %	T %	Source dimensions	Spectrometer dimensions	Particle detector	Measurement of Magnetic Field	Application; other remarks	Reference
Iron free	.01 .1	luminosity 10^{-5} cm^2 5×10^{-3} cm^2		100 cm	Continuous flow proportional Counter		Very high resolution studies.	Graham (1960)
Iron free; concentric solenoids	.1 .045	.1 .05	~ .1 mm	50 cm	G.M. tube. Semiconductor Counter.	Hall generator	Applied to electron binding energy measurements & other "atomic" problems.	Siegbahn (1964)
Sector Magnets Field varies as $1/\sqrt{e}$	.27 .4	1 .02	-	15 cm	-	-	Coincidence work	Bergström (1963)
Field varies as $1/e$. Orange segment arrangement	1 0.2	20 2.8	1/8"	100 cm diameter	Scintillation Counter		Two used for β-β coincidences	Freedman (1960)

Spectrometer Type	R %	T %	Source dimensions	Spectrometer dimensions	Particle detector	Measurement of Magnetic Field	Application other remarks	Reference
Prism	.014 .2	.015 .8	.4 mm 1 mm		G.M. Counter	Gate Magnetometer	Suitable for correlations. Low background	Kelman (1964)
Lens Spectrometer Uniform Field.	0.05 .018	.36 .04		l = 2m d = 60cm	Geiger Counter	Proton Resonance	Absolute Measurement of rigidity of Th.B. lines.	Jungerman (1962)
Intermediate Image: Concave Field Form	1.5 1	4 8		l = 5½" d = 18"	Scintillation and Geiger Counter		Used as Pair Spectrometer	Alburger (1956)
Prolate Spheroidal Field.	1.5 .4	4.5 .7	d = 1mm	38 cm	Plastic Scintillator	Rotating Coil	$\beta - \gamma$, $\beta - \beta$ Coincidences	Evans (1958)

Discussion

The resolution and luminosities of different instruments are compared in figure 2.3. The diagram is based on a similar one given by Graham (Graham 1960), but with certain modifications. The relevant data for the Prolate Spheroidal Field Spectrometer at Bedford College are included. The best resolution is probably still that obtainable with the iron free spectrometer at Chalk River; this can be matched by Kelman's prism spectrometer or by de Vries in Amsterdam with a $\pi\sqrt{2}$ iron free instrument, though at lower luminosities. At less good resolutions (0.1% approximately) both Kelman's Spectrometer and the iron-clad instrument of Bartlett have better luminosity than that at Chalk River. Bartlett (Bartlett 1962) shows how if scaled to the size of the Chalk River Spectrometer his design would give considerably better luminosity at all resolutions.

Resolution and luminosity are, however, not the only criteria of performance. For particular applications such as coincidence or correlation studies, other requirements must be met and instruments with less striking performance figures may be of more practical use. The table summarizes the properties of some instruments of the different types and indicates the work for which they have been found particularly useful.

Fig. 2.3. Comparison of Properties of Magnetic Spectrometers.
Resolution Plotted Against Luminosity

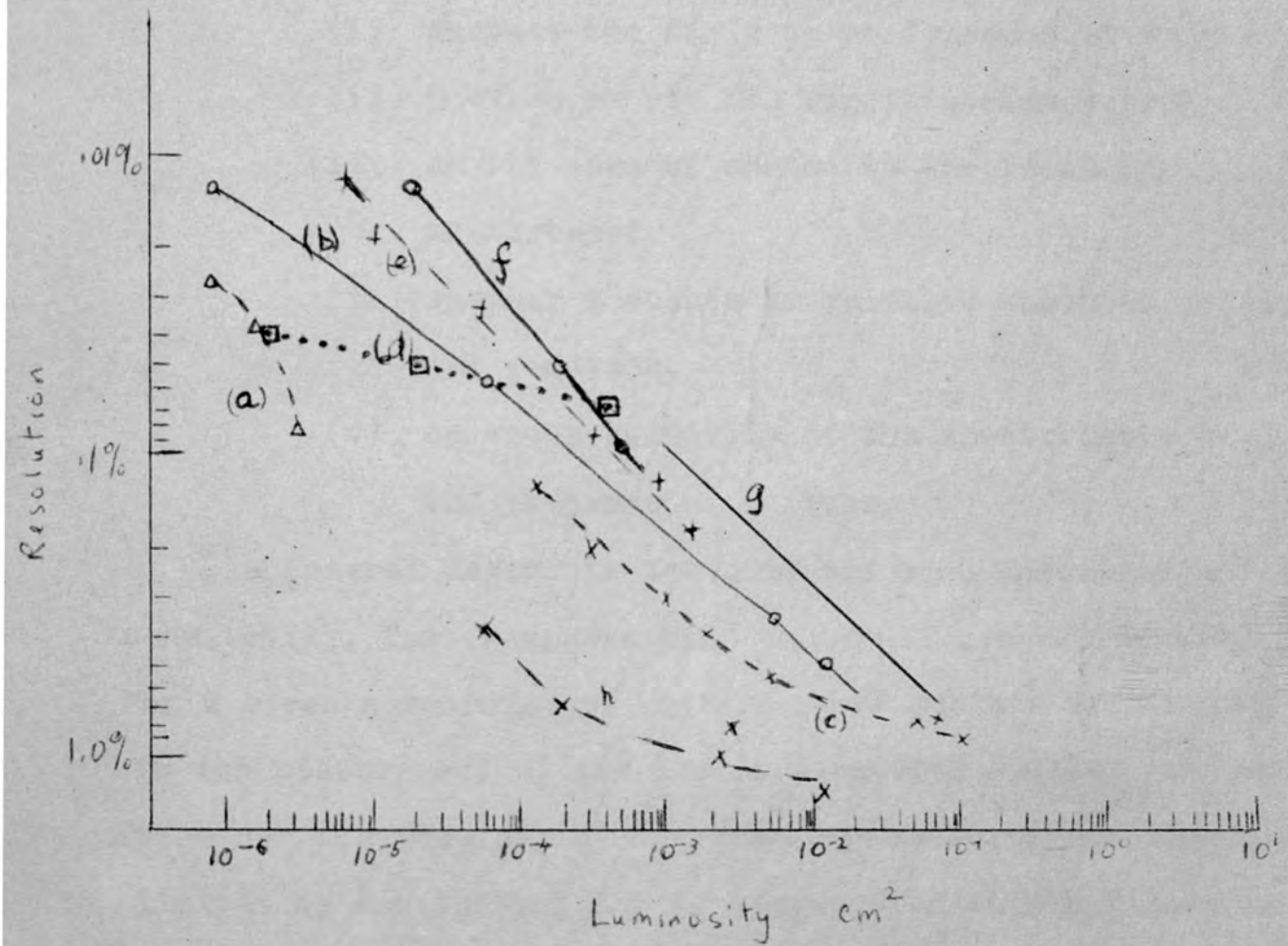

(a)	$\pi\sqrt{2}$, Uppsala	Siegbahn (1956)
(b)	$\pi\sqrt{2}$, Amsterdam	de Vries (1960)
(c)	Sector, Argonne	Freedman (1960)
(d)	Long Lens	Jungerman (1962)
(e)	Prism, Leningrad	Kelman (1964)
(f)	$\pi\sqrt{2}$, Chalk River	Graham (1960)
(g)	$\pi\sqrt{2}$, Colorado	Bartlett (1962)
(h)	Prolate Spheroidal Field	Evans (1968)

2.3. Measurement of the Magnetic Field and Field Stabilization

Various methods are available for the measurement of magnetic fields; the method chosen for a particular spectrometer will depend, amongst other things on

(i) whether the field is homogeneous or shaped

(ii) whether or not the magnet contains iron

(iii) on the ease of access to the field for measurement

(iv) whether absolute or relative momentum values are required.

(v) on the sensitivity of the spectrometer to the presence of a probe.

In general desirable features are high accuracy and sensitivity, fast response time and small probe dimensions. For a given spectrometer the aim is to achieve an accuracy in the measurement of the field, such that neither the resolution nor the accuracy of the momentum measurements should be limited by any instability or imprecision in the field.

In some, but especially in instruments containing iron, a field measuring device is incorporated in a feed-back loop which is used to stabilise the field.

The more important methods of measuring the field will be described briefly, together with the circumstances under which each has been used and the degree of accuracy of which it is capable.

2.3.1. Proton Spin Resonance.

This method depends on the resonant absorption of energy by a system of protons in a magnetic field when a small perturbing field at the correct frequency is applied. The absorption of energy accompanies the re-orientation of the nuclear magnetic moments with respect to the external field; the resonant frequency is proportional to the field, and is normally in the radio frequency region, where techniques are sufficiently developed to allow a high precision measurement to be made. The fields that can be measured by this method are limited to the range 10^2 - 10^4 gauss, corresponding to the frequency range 1 - 100 Mc.p.s. The sample is usually water with the addition of some paramagnetic ions to reduce the relaxation time. The signal is very weak and to obtain a workable signal to noise ratio samples must have a volume of the order of 1.c.c. or more. Thus this method of field measurement is only suitable where the homogeneity of the field is assured; it is, however, extremely precise offering a hundred fold improvement over other traditional techniques.

Jungerman (Jungerman 1962) used this method to measure and control the highly uniform field in his long lens spectrometer to within two parts in 10^5. Resonance could be achieved for fields corresponding to β-ray energies in the range 43 KeV to 2.6 MeV.

2.3.2. The Rotating Coil Generator

(i) Field Measurement. A small coil rotates in the spectrometer field and the E.M. F. developed is balanced against that generated by a similar coil rotating at the end of the same shaft in a uniform reference field. It has been found best (Hedgran 1952) to compare a.c. rather than d.c. voltages. These are then taken off with slip-rings and brushes. Using Be -Cu rings and silver graphite brushes variations in contact resistance have been reduced to less than 0.025 ohms (Petterson 1964). The voltages are developed in anti-phase and the sharpness ofbalance attainable is found to depend critically on the accuracy of the phase adjustment.

Hedgran (Hedgran 1952) used Helmholtz coils to produce the uniform reference field but other workers (Bäckström 1962) have preferred to use a permanent magnet and to compare a fraction of the voltage developed across the coil in this field with that across the coil in the spectrometer field. A Kelvin Varley bridge acts as the potential dividing network. Questions of temperature control and shielding are more easily solved with a permanent magnet.

The reference field must be well separated from the spectrometer field to avoid mutual interference; the long shaft separating the two coils must be very carefully constructed to avoid vibrations. In order to achieve the desired

precision, Hedgran estimated that the maximum permissible torsional misalignment was 0.003^{o} and the coil had to be positioned in the field to within 0.05 cm. He used auxiliary coils to produce a cross field for the final phase adjustment. Such coils can also be used to compensate for the vertical component of the earth's field; the effect of the horizontal component is eliminated by suitable positioning of the system in the meridian.

The net signal which is finally obtained is amplified using a tuned amplifier; in this way spurious noise is filtered out as well as any harmonic signals which result from the inhomogeneity of the field.

Such a device has been used for measuring the field in the 50 cm. double focusing iron spectrometer at Uppsala; the coil is placed at the same distance from the centre of the magnet as the central orbit. Various improvements introduced over the years have permitted a sensitivity of 5 - 10 in 10^{6} to be obtained. (Petterson 1964). The field in the Prolate Spherical Field Spectrometer at Bedford College is also measured by this method as described in Chapter 3.

(ii) Field Stabilization. Feed-back from the system at Uppsala is used to stabilize the field. The complete system is shown schematically in Figure 2.4. The required

Figure 2.4. Field Controlled System for Automatic Operation.

(By Courtesy of the Institute of Physics, Uppsala.)

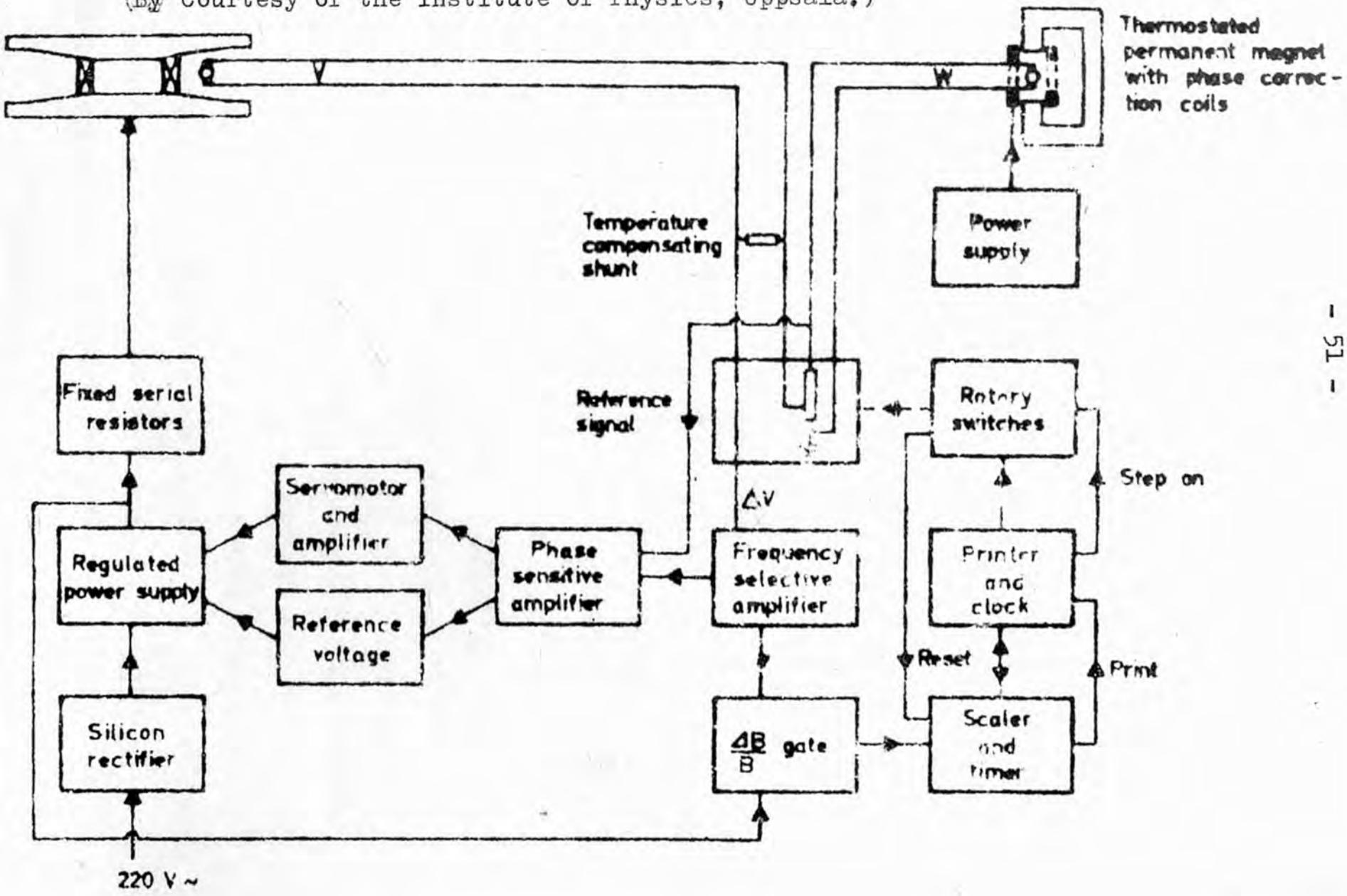

field is set by means of the Kelvin Varley bridge mentioned above. Any net off balance error signal, after filtering and amplification is fed to a phase sensitive detector; this instrument compares the phase of the signal with the phase of a reference e.m.f. derived directly from one of the rotating coils. The output from the detector gives the sign as well as the magnitude of the error and indicates in which direction and by how much the field must be corrected. It acts on the current supply through both a fast and a slow channel. The value of the current depends on the value of a reference voltage within the current supply (see Section 2.4.1. below); this voltage is derived from mercury cells whose potential is dropped across an infinite resolution film helipot. In the fast channel, instantaneous correction to the current is made, electrically, by adding to or subtracting from, the voltage across the cells; in the slow channel the signal is further amplified and then used to drive a servomotor which turns the helipot in the required sense. In this way any deviations of the field from its pre-set value are continuously compensated. The correction is well damped and the system has good momentum stability (2 parts in 10^5) over long intervals.

A similar system has been used by Baird et al (Baird 1962) at Vanderbilt University Tennessee in conjunction with an iron-free double-focusing spectrometer. They operated at

resolutions of 1% and were able to determine the momentum to an accuracy of within 2 parts in 10^4. It is somewhat doubtful, however, whether the introduction of such a system permits any significant improvement in accuracy in an iron-free instrument for which the current-field proportionality is good.

2.3.3. (a) Peaking Strip

In this method use is made of the high permeability of certain ferro-magnetic alloys which have almost rectangular hysterisis loops. An a.c. current is passed through a small solenoid wound round a glass tube into which a strip of the alloy has been sealed. The direction of magnetisation of the strip changes rather abruptly twice per cycle (see figure 2.5) and an e.m.f. is induced in a second solenoid wound close to the centre of the strip, each time the direction changes. The induced voltage peaks are displayed on an oscilloscope screen. In the presence of an external d.c. field the peaks will be displaced. A third coil can be used to generate a d.c. field which will oppose the spectrometer field at the strip. The current which must be passed through this latter coil to maintain the peaks in their null positions on the screen is a measure of the field in the spectrometer. (Symonds 1955).

Bartlett et al (Bartlett 1962) at Colorado have used

Fig.2.5. Principle of Operation of Peaking Strip. Demonstrating the Production of Voltage Pulses on Traversing the B H Loop of a High Permeability Alloy.

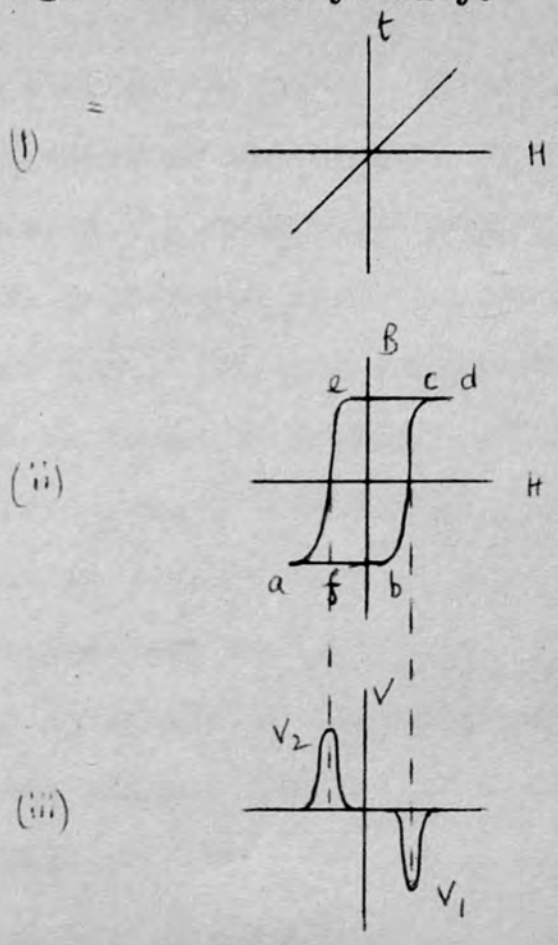

A strip of the alloy is placed in a uniform field (H); a search coil wound close to the strip at its centre will respond to any change in flux density (B) with a voltage $V \propto \frac{dB}{dt}$.

Let the magnetic field increase linearly with time (i); as it increases from a to b (ii) the strip remains saturated, $\Delta B = 0$. Between b and c the flux density changes rapidly from - B to + B and a voltage peak V_1 is induced in the coil (iii).

Similarly on traversing the loop in the opposite direction d,c e,f,a a voltage peak V_2 of opposite polarity is obtained.

this method to measure the field in their 20 cm double focusing iron spectrometer. They claimed to be able to control the field to a few parts in 10^4, and a change of 10^{-2} gauss could be detected. More recently (Bartlett 1964) they claimed an improvement by a factor of a hundred using a commercially available probe and a d.c. milli-ammeter which registered continuously any cut of balance signal. This signal is used to control the current through the solenoid so that continuous cancellation of the spectrometer field to withn 10^{-4} gauss is maintained. A precision potentiometer is used to measure the solenoid current which is proportional to the field.

A fully automatic system incorporating the peaking strip is being planned for use at Uppsala and at Colorado (Siegbahn 1965).

(b) Flux-gate Magnetometer

This method is a variation of the above in that it also depends on the use of high permeability μ-metal. It was developed by Serson (Serson 1957) in connection with surveys during the Geophysical Year. The method was used by Graham et al (Graham 1960) to measure the field form of the 100 cm air cored β - spectrometer at Chalk River.

Two parallel strips of μ-metal are each surrounded by oppositely wound primary coils. A secondary winding surrounds them both. This coil serves both to compensate for the external field and to pick up any induced signal. An a.c. current of 660 c.p.s. passed through the primaries causes the μ-metal to saturate and unsaturate 1320 times per second. Thus the effective permeability of the core of the secondary coil is alternating and in the presence of a d.c. field the flux linked by the secondary will alter thus causing a signal to be picked up; the magnitude and phase of the signal indicate the magnitude and direction of the residual d.c. field. The field in the spectrometer is measured in terms of the current which must be passed through the solenoid for a null signal to be obtained. This current was measured to within 1 part in 10^3 by Graham and his collaborators.

(c) Kelman employed a similar magnetometer as part of the field stabilization system of the Prism Spectrometer at Leningrad. The requirements here are complicated by the fact that there are three magnetic components in the spectrometer, whose fields, though different, must have a definite relation to one another. One "main" current, from a stabilized power supply feeds the lenses and the prism coils and also provides a reference field; this reference field is made to compensate the spectrometer field

exactly at the magnetometer probe. Any residual field gives rise to an error signal which, after amplification and phase detection will correct the current giving rise to the prism field. (Kelman 1964). Kelman claims that during measurement of a line the field instability did not exceed 0.003%.

2.3.4. The Hall Effect

A potential difference is developed across certain current-carrying conductors when placed in a magnetic field; the magnitude of the p.d. is a measure of the magnitude of the field. The effect is rather temperature dependent, and the accuracy of about 1 in 10^3 which is obtainable when it is used as a field measuring device does not compare favourably with that attainable by other methods. It has, however, been used by Bartlett to measure the variation of the spectrometer field with radius, (Bartlett 1962). It was also used to measure the field shape in the spectrometer at Bedford College (Evans 1958).

2.4. Automatic Operation

In recent years many spectrometers have been automated; this permits considerable saving in time and man-power for much of the routine work. The programming facilities vary, but the basic cycle of operations is always the following.

Particles are counted for a pre-set interval (either of time or of counts), at the end of which the relevant information is recorded; the spectrometer field is increased by a constant pre-set amount and once the field has stabilized at the new value the counting recommences and the cycle is repeated.

In the instruments for which the field is linearly dependent on the current to a sufficiently high degree of accuracy, the field may be current-controlled. In others direct control over the field is necessary: feed-back from the field is then used to regulate the current.

2.4.1. Current Control

This is adequate for most iron free instruments and in many cases it permits sufficiently accurate relative measurements of electron momentum with instruments containing iron. To ensure reproducible results such instruments must always be operated on the same part of the hysterisis cycle.

The Chalk River iron free spectrometer is an example of an instrument whose automatic operation depends simply on current control. The current generator is stabilized to within less than 1 part in 10^5 by means of a feed-back loop; the current flows through a standard manganin resistor in series with the field coils and the voltage across this

resistor is compared with a reference voltage; the difference is amplified and fed back through series valves to stabilize the current at a value determined by the reference voltage. This spectrometer is operated continuously and has very versatile programming facilities. A complete run would consist of 1000 equally spaced momentum settings, but runs can be started and stopped at pre-set values and the change in momentum per step can be varied over a wide range. After the index position, which is a measure of the momentum value, has been printed the step command is sent to the current control unit. The increments are accurate to within less than 1% and the automated spectrometer can be satisfactorily used down to a resolution of 0.1%; below this manual monitoring is necessary.

Accurate compensation for the earth's field is necessary in order to obtain the best results from this spectrometer; (see 2.2.(a)) and for use at the very best resolutions (0.01%) it is planned to compensate automatically for diurnal fluctuations in the earth's magnetic field, using a magnetometer in a neighbouring building to provide the correcting signal.

2.4.2. Field Control

The system in use with the double focusing iron spectrometer at Uppsala is typical of a field controlled automatic system.

In this case it is the value of the field, determined by the Kelvin Varley Bridge (see figure 2.4) which is pre-set and which is changed by fixed increments between readings. The momentum of the focused electrons is proportional to the bridge setting to a high degree of accuracy. The current adjusts automatically to the necessary value via the field stabilization loop (see Section 2.3.2.ii).

Once the field has stabilized at the pre-set value to within a margin set by the $\Delta B / B$ gate (see diagram 2.4) the scaler is triggered and it then counts for a pre-set time interval. The stop pulse of the timer triggers the printer; from the printer a trigger pulse is fed to Ledex Rotary relays which are used to increase the setting of the Kelvin Varley bridge and thus also the value of the spectrometer field, by a pre-set constant amount. The time required for increasing the field between readings has been reduced from 20 sec to less than 2 sec and thus short lived isotopes can more easily be studied. Various programming facilities are available; however, great elaboration was

not thought to be justified in view of the labour of construction and maintenance involved.

2.5. Particle Detectors

A magnetic β^- - spectrometer requires the use of an auxiliary particle detector. Properties to be looked for in particle detectors are high efficiency, small dead time, fast response, the ability to detect particles over a large energy range, as well as low background counting rate.

2.5.1. Scintillation Detectors. The scintillation counter consisting of phosphor and photomultiplier, is widely used in conjunction with magnetic spectrometers. The short output pulses, and in particular, their fast rise times, make this detector most suitable for fast coincidence work; these features also permit high counting rates. The ability of the scintillation counter to detect low energy particles is limited by the signal : noise ratio. The noise is largely due to thermionic emission in the photomultiplier and this is minimized by the design of the tube. It can be further reduced by cooling the photomultiplier below room temperature (see chapter 4); the photosensitivity at low temperature may be maintained by special design of the photocathode. (Birks 1964). The performance of the photomultiplier is affected by the presence of magnetic fields. The

photomultiplier is often placed outside the field and the scintillation led to it from the phosphor along a perspex light guide. Stray fields up to 25 gauss may be tolerated if the tube is surrounded by one or more μ-metal shields. For the very best resolutions, however, (0.01%) this shielding may cause significant distortion of the spectrometer field (Graham 1960) and other detectors are preferred.

2.5.2. Gas Counters as Detectors.

These have the advantage of being unaffected by magnetic fields; Geiger-Müller tubes are frequently used as detectors with magnetic spectrometers, but gas flow proportional counters are also so employed. With thin film end windows they can be used to detect β-particles down to energies of 20 KeV or lower.

The output pulses are much slower than those from scintillation counters, rendering G-M detectors unsuitable for fast coincidence studies. Recently a fast gas counter has been reported (Krusche 1965) consisting of two thin sheets of Ni foil with about 2 m.m. thickness of gas between them. A resolving time of 0.6 ns has been obtained for a coincidence circuit using such counters, but there is no indication of their having been used as detectors in conjunction with magnetic spectrometers.

Since energy selection takes place before detection the counting rate is not high enough for the dead time of G-M tubes to constitute a serious handicap. The high background rate associated with their large sensitive volume is a more significant disadvantage.

2.5.3. Semiconductor Detectors offer several advantages; fast response time (10 ns), insensitivity to magnetic fields, and compact size, with a correspondingly low background rate. Their insensitivity to γ-rays makes them suitable for application where high energy reactions are being studied; their small size has also led to their use in arrays, especially when, as is the case with the 180° spectrometer, β-rays of different energy are focused simultaneously.

Considering the many advantages associated with these detectors it is surprising that they are not as yet more widely used as detectors in magnetic spectrometers. (c.f. Table 2.1).

2.5.4. Photographic Detection. This method of detection is still used in conjunction with the 180° spectrometer as it enables simultaneous study of a range of the spectrum over long periods. However, it has largely been superseded for intensity measurements owing to the difficulty of intepreting the data accurately.

CHAPTER 3

Automatic Operation of the Prolate Spheroidal Field Spectrometer

3.1. Introductory

3.1.1. Description of the Spectrometer

The Prolate Spheroidal Field β - Spectrometer was mentioned in Chapter 2 as an example of a lens spectrometer in which the field has been shaped so as to give rise to an intermediate ring focus and reduce the spherical aberration. The slit and baffle system is shown at the left hand side in figure 3.1. The properties of the spectrometer and details of its construction have been described by Evans et al (Evans 1958) and by Freeman (Freeman 1960); subsequent modifications are noted by Michelson (Michelson 1961). The focused electrons emerge at 45^{o} and their trajectories reach a maximum distance of 38 cm. from the axis; after passing through the ring slit they are sharply reflected by the strong field gradient such that both source and detector lie to the same side of the slit. The field is shaped using iron, the coils being wound inside the cylindrical iron casing. This should reduce the flux leakage between the spectrometer and its surroundings. There was evidence, however, (section 3.4.) of a stray field due to the

Figure 3.1. Sectional Diagram of Double β-Spectrometer.

(By Courtesy of Dr. D. Michelson, Brunel College.)

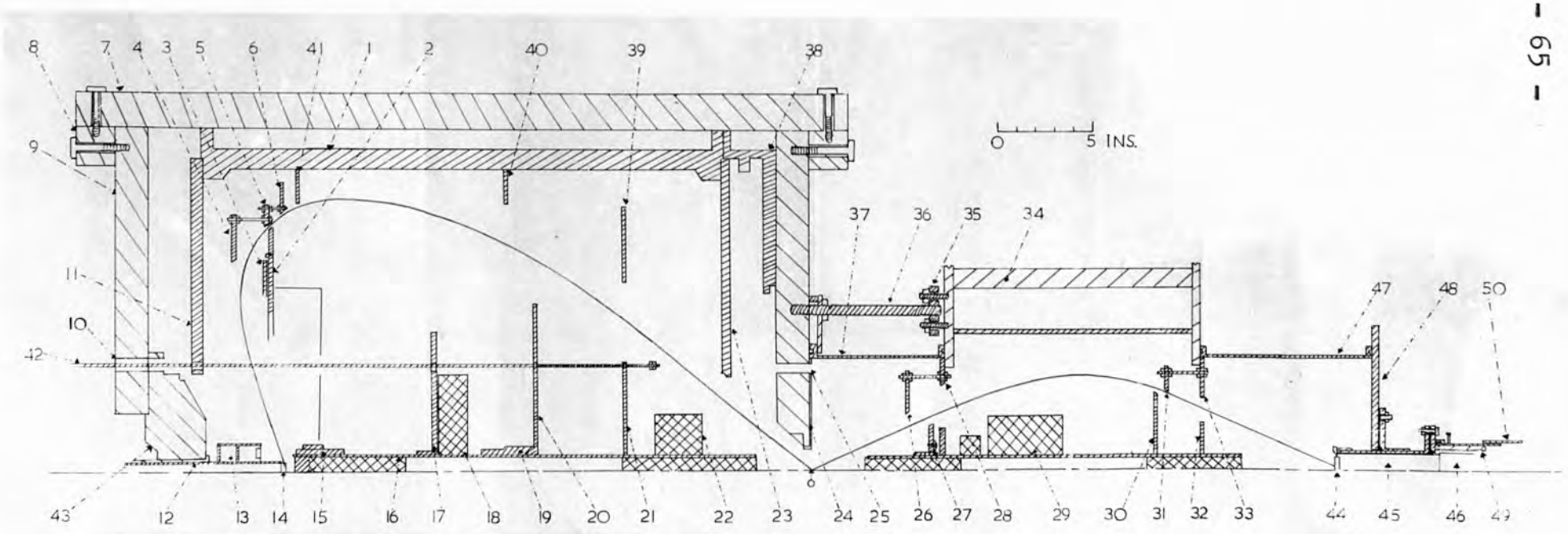

Figure 3.1. Sectional Diagram of Large and Small Spectrometers.

Key to Important Features.

1. Aluminium Tank.
2. Plate of Slit Assembly.
4, 5, 6. Back, Middle and Front Rings respectively of Slit.
7. Iron Bar.
9. Iron Plate.
11, 38. Aluminium Plate.
12. Brass Tube surrounding Light Pipe.
14. Crystal of Large Spectrometer.
18, 22, 29. Lead Blocks.
20. Ring of Angle Baffle.
25. Pumping Hole.
26. Angle Defining Baffle of Small Spectrometer.
30. Moving Disc of Ring Slit.
32, 33. Fixed Sections of Ring Slit.
37. Brass cylinder - has entry to pumping line and gate for introduction of source.
44. Crystal of Small Spectrometer (c.f.Fig.4.4)
45. Light Guide of Small Spectrometer (c.f. Fig. 4.4)

46. Photomultiplier of Small Spectrometer
    (c.f. Fig. 4.4)
47. Brass Cylinder.
48. Brass End Plate.

spectrometer at the neighbouring Helmholtz coils.

Low flux leakage is especially desirable for $\beta - \beta$ coincidence measurements, when, as in our case, a second magnetic spectrometer is joined to the first. Otherwise the two fields will not be able to be varied independently and field-current linearity will no longer obtain. The fact that the source is shielded from the main field, as has been demonstrated experimentally (Evans 1958) is also a useful feature for coincidence studies between electrons emitted in opposite directions.

3.1.2. Projected Automation and Required Precision

It was decided to follow the practice of other laboratories in constructing an automatic system for the spectrometer; this would avoid the time and tedium involved in counting infrequent coincidences. The essential features of such a system have been described in Chapter 2. The automatic system should be such as to make best possible use of the spectrometer characteristics.

(a) Accuracy. A rough estimate of the accuracy required of the automatic system may be made. The limit to the resolving power of the spectrometer is about 0.5% though in practice for coincidence studies it will be operated at better transmission and

correspondingly poorer resolution. Supposing that the position of a line can be estimated to within 1/10 of the full width at half maximum height; then the resolution limits the precision obtainable for the position of a line to about 0.5 x 1/10 = .05% or 1 in 2000. The magnetic rigidity at any point in an automatic run should then be determined to the same degree of accuracy. A lesser precision would probably suffice for plotting a continuous β - spectrum which is a more slowly varying function of momentum.

(b) Momentum Increment. The minimum momentum increment that would be needed to determine the position of a line with the above stated accuracy can also be estimated. If ten points are needed to define the upper half of the line then the increments in momentum should be about 1/10 x .5% of the mean momentum, which for the Th F line, i.e. for electrons of 138 KeV, is about 69 gauss - cm (about 1 mA of current). Larger increments will also be necessary for operation at higher resolutions and also for the rough scanning of a spectrum.

3.1.3. Choice of System

The factors determining the choice between a current controlled and a field-controlled system have been discussed

in Chapter 2. Despite the presence of iron in the spectrometer, previous operators (Evans 1958,* Freeman 1960) have found it sufficiently accurate to assume a linear relationship between current and momentum provided that the spectrometer was always operated on the same part of the hysterisis loop. Thus current-controlled automatic operation should be feasible at least as a first attempt. Certain advantages, notably the avoidance of hysterisis effects and ultimately a better field stability, should accrue from the introduction of a field controlled system, but it is not immediately clear that the resolution obtainable with the spectrometer justifies these refinements.

3.2. Construction and Operation of Automatic System

3.2.1. Sequence of Operations

The logical sequence of events in the operation of the automatic system is shown schematically in figure 3.2 and is as follows. The commercial pieces of equipment are referred to by letters and are listed in Appendix I.

i. The controls are set for automatic operation; the current range, current increment between readings, and counting interval are selected.

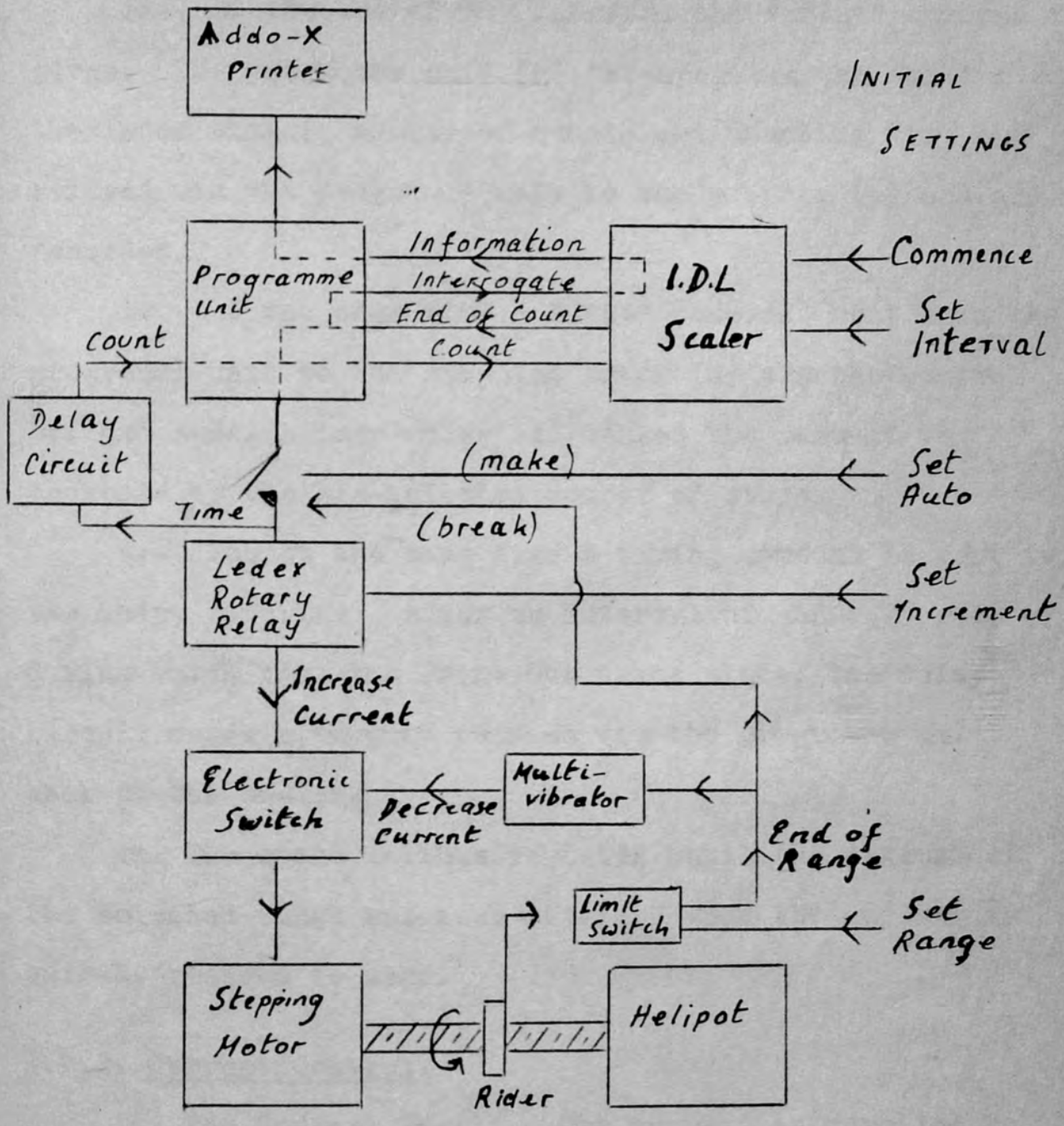

Figure 3.2. Sequence of Automatic Operations.

ii. The "count" command is given and the scaler (a) counts for the pre-set interval of time or number of counts.

iii. At the end of the interval the "print" command is given. The programme unit (b) interrogates the scaler; the index number, number of counts and counting time are relayed via the programme unit to the printer (c) and are recorded.

iv. At the same time a "step" command, sent from the programme unit to the stepping motor (d) via the control box and ledex rotary relay (e) causes the current to increase by the pre-selected number of steps.

v. Also at the same time a timing command is sent to the delay circuit; after an interval of about 25 sec during which time the Print Out takes place, the delay circuit sends a "count" command via the programme unit back to the scaler.

vi. The cycle is thus repeated until the maximum of the selected range has been attained when the current is quickly reduced to zero.

3.2.2. Current Control

(a) The Current Supply. The current is supplied by the Newport Instrument Supply (f) of which a schematic diagram is given in figure 3.3. A motor fed by 3-phase Mains supply turns a generator coil which

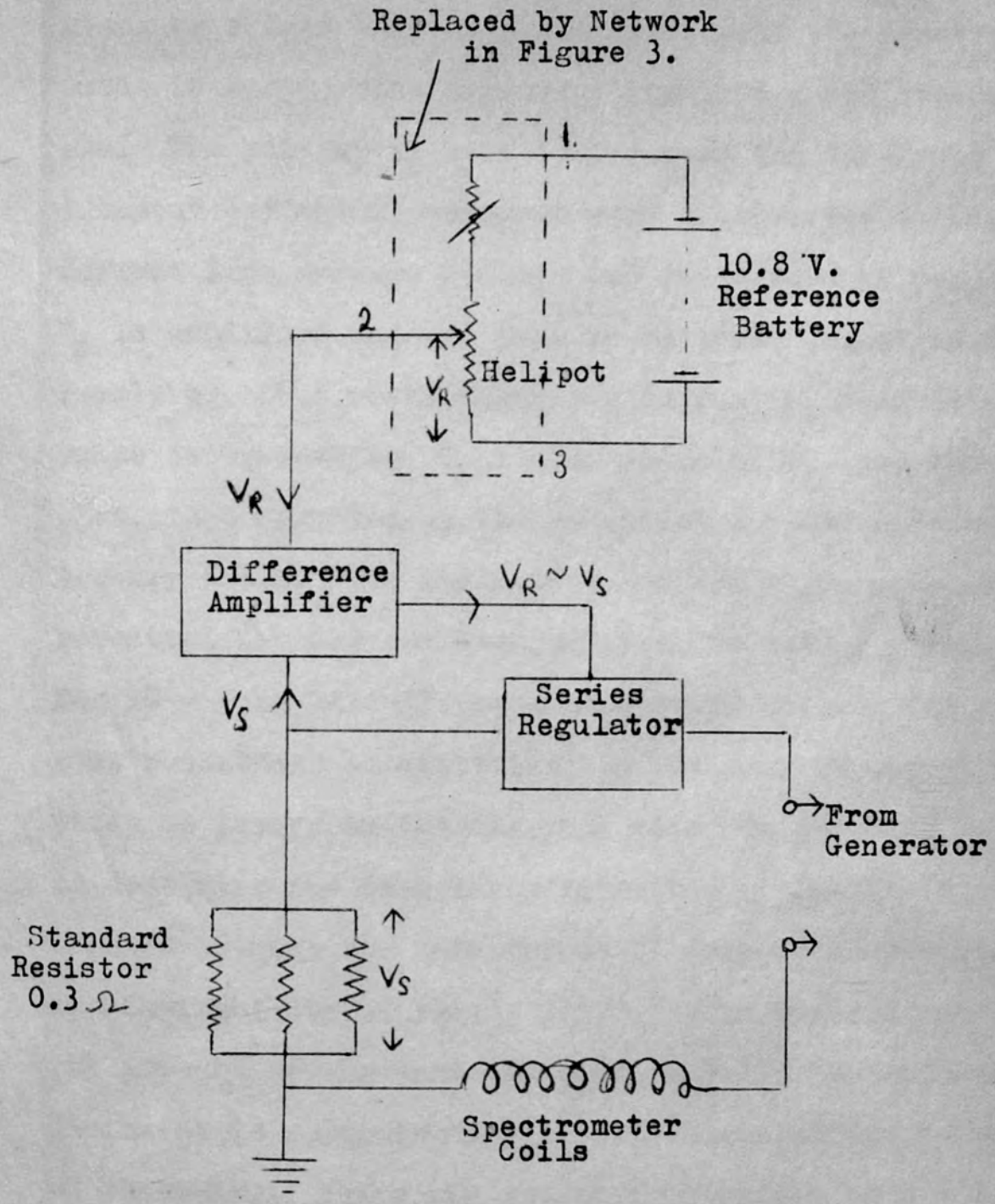

Figure 3.3. Schematic Diagram of Current Supply Before Modification.

provides a low ripple d.c. voltage; this is stabilized by means of a feed back loop and applied to the spectrometer coils in series with a current regulator and standard resistors. The voltage V_S developed across the latter by the spectrometer current is compared with a reference voltage V_R derived from mercury cells. Any difference between V_R and V_S is amplified and fed back as an error signal to the series regulator, thus maintaining the current i_s constant at a value determined by V_R . The value of V_R, and thus of i_S also, is controlled by the potential divider across the mercury cells. The resistance network which acts as potential divider has been modified to suit our requirements. The 10 - turn helical potentiometer or helipot (g) of 10 K ohms resistance is maintained in the network and it is this which is turned by the stepping motor to increase the current. In designing the resistance network a compromise had to be reached between the need for small current increments and the desirability of having fairly large current ranges. In the present arrangement (see figure 3.11) the minimum current increment is approximately 3.7 mA corresponding to two steps of the motor. There are two current ranges of 0 - 3.7 amps and 3.5 - 7 amps with a facility for switching between them without any abrupt change in the current. The required range is selected by Wafer Switch W 2 and a 10 K potentiometer,

X, is used for the transition from one range to the next.

A stability of 1 in 10^5 is claimed for the current generator over periods of half an hour; in practice the current was found to drift to the extent of about 1 in 5000 in half an hour even after the generator had been running for several hours.

(b) Stepping Motor and Electronic Switch. The stepping motor consists of one rotor and two stators; the rotor is a permanent magnet with twelve pairs of poles distributed on the circumference. The stators are made of soft iron supplied with energising coils. Each consists of twelve pairs of poles distributed around the rotor (Figure 3.4a), the polarity of a particular pole being determined by the direction of the d.c. current in the coil. There are thus 2 x 2 possible combinations for the resultant stator field, with 12 x 2 x 2 = 48 positions for the rotor. The rotor takes one step each time the current in one of the stator coils is reversed. To simplify switching, each stator coil is divided into two equal windings each of which may be energised in turn. By adopting a suitable switching order the motor steps always either in the clockwise or in the anti-clockwise direction.

Figure 3.4. Principle of Operation of Stepping Motor.

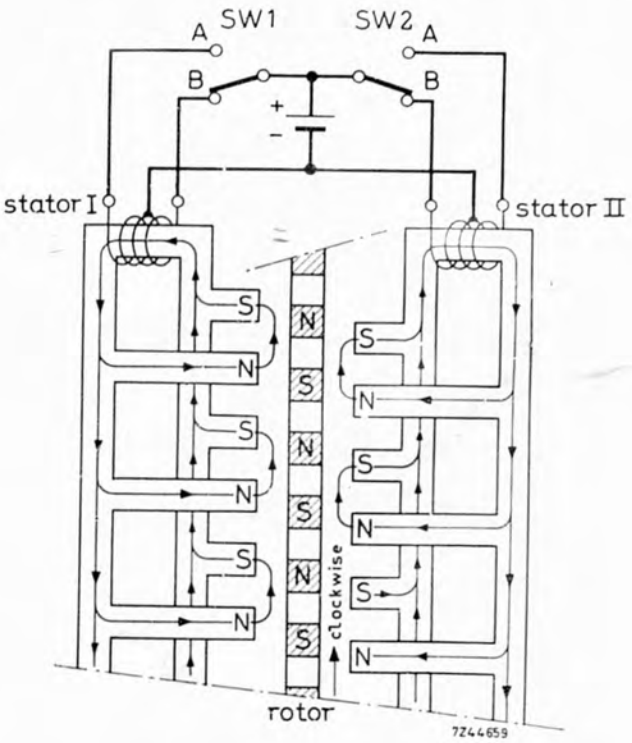

(a) Expanded Diagram showing Distribution of Poles around Rotor.

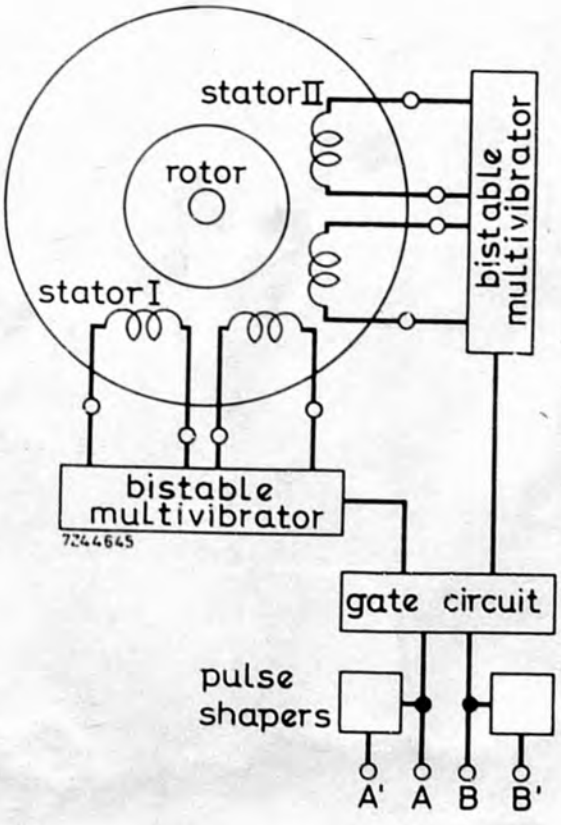

(b) Schematic Diagram showing Method for Electronic Switching.

(By Courtesy of Impex Electrical Ltd.)

The switching may be done manually, or mechanically or, as in our case, electronically, using the specially designed electronic switch (h) *. The windings are incorporated in the collector circuits of two pairs of transistors. These function as bistable multivibrators such that the direction of magnetisation of one of the stators is reversed each time a pulse is applied. Suitably biased diodes control the switching sequence by selecting the multivibrator to which a given input pulse will be fed and thus the stator whose magnetisation is to be reversed. Two inputs, A and B, are provided corresponding to different switching sequences and hence different directions of rotation for the motor. Figure 3.4 (b) shows schematically how the switch operates on the motor. Positive pulses of not greater than 10 V magnitude and 50 μs rise-time are required to trigger the multivibrator, but pulse shapers are included in the switch, which will shape negative pulses to the above requirements.

The angular step size for the motor is specified as $7^{\circ}30'$. This has been geared down in the ratio 25:6 giving a total of 48 x 25/6 = 200 steps for one complete revolution of the helipot or 2000 steps in all. The angle of rotation of the helipot per step

* See Appendix A.1

is $1^{o}48"$. In practice the magnitude of the step was found to alternate, whereas the sum of two successive steps was much more nearly constant. Successive current increments varied by as much as 30%. This was shown to be a property of the motor by subsequent measurements of the angle of rotation under different load conditions. It may well be attributed to a lack of symmetry between the two stators. The effect has been largely overcome by causing the motor to take even numbers of steps for each current increment as described below.

3.2.3. Mechanical Construction

The pinion of the stepping motor fits directly into the specially constructed gear box (i) * which in addition to reducing the size of the step, gives a mechanical advantage.> 4. The shaft of the gear box is fitted with a safety clutch and toothed gear wheel to the shaft of the helipot. A Beckman dial reading to 1/100th of a turn is attached to the opposite end of the helipot. Figure 3.5 (a) shows the way in which the components are assembled.

(a) The Safety Clutch. The clutch slips whenever the motor encounters too great a retarding torque, thus disengaging the motor from the potentiometer and preventing overloading the motor or damaging the potentiometer.

Two designs were tried: the performance of the first, which depended on the friction between a flat rubber surface pressed firmly against the flat brass surface of the toothed gear-wheel under the action of a helical spring (see Figure 3.5a), was found to be unpredictable as it had a tendency to slip in the normal course of running.

In the second design small ball bearings are engaged in shallow sockets, the bearings being held in place by means of light springs fitted into two slots (see Figure 3.5(b)). The compression of the springs, which can be adjusted by means of the screw, determines the torque under which the clutch will slip. This "slipping" torque is larger and more constant, and the performance of the clutch in general more consistent than was the case for the friction clutch; it was this design, therefore, which was adopted for use.

(b) Worm Drive and Limit Switches. The toothed gear wheel is used to drive a small rider along a screw thread with a pitch of 10 turns per inch. (Figure 3.6). The gears are in the ratio 2:1 so that the total travel of the rider for 10 turns of the helipot is 2" . The rider is driven against micro-switches

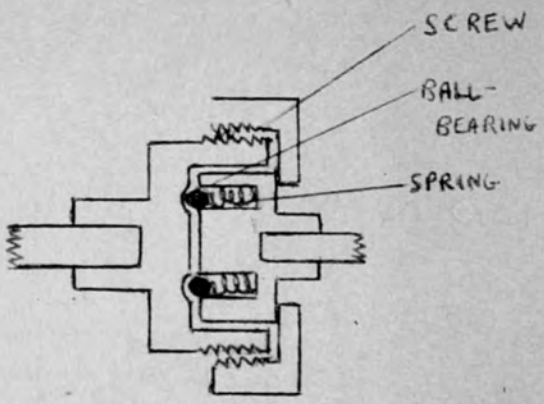

Figure 3.5 (b) Ball and Socket Clutch.

Figure 3.5 (a). Mechanical Arrangement for increasing the current automatically.

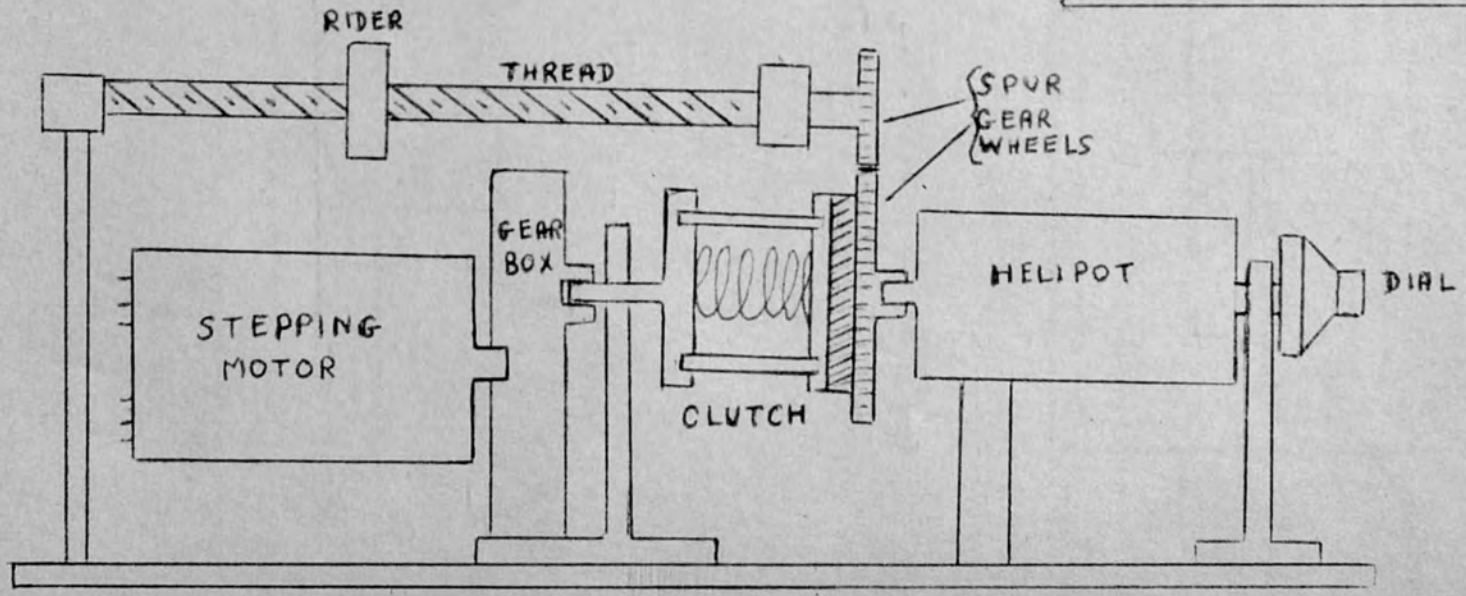

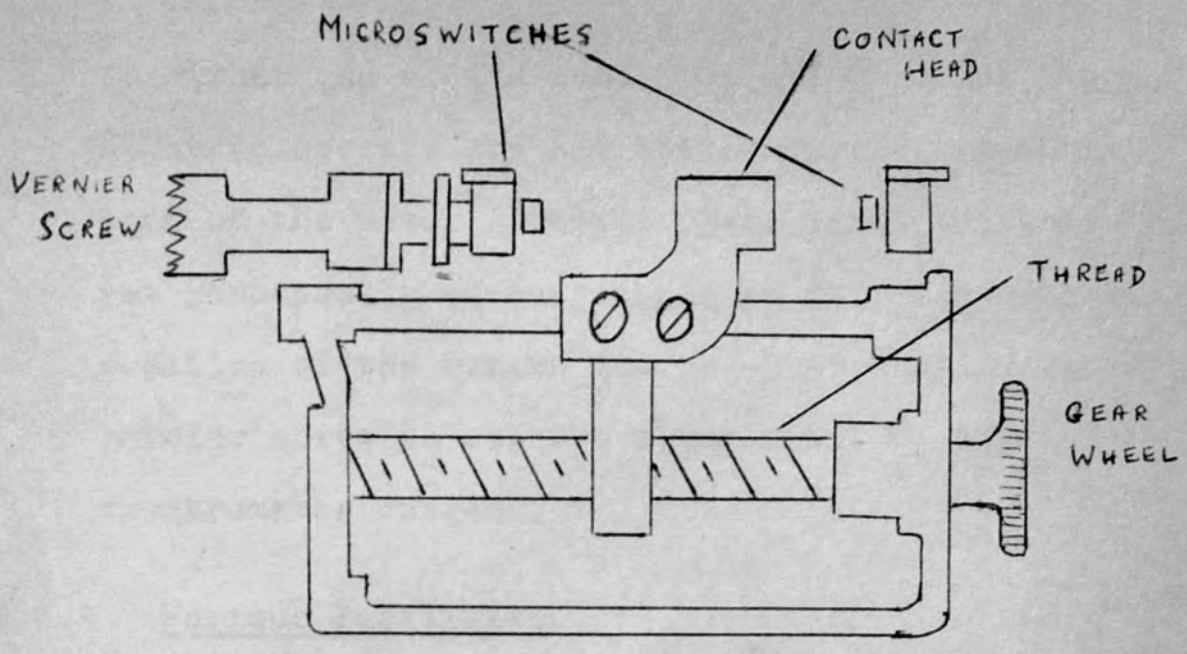

(a) Plan

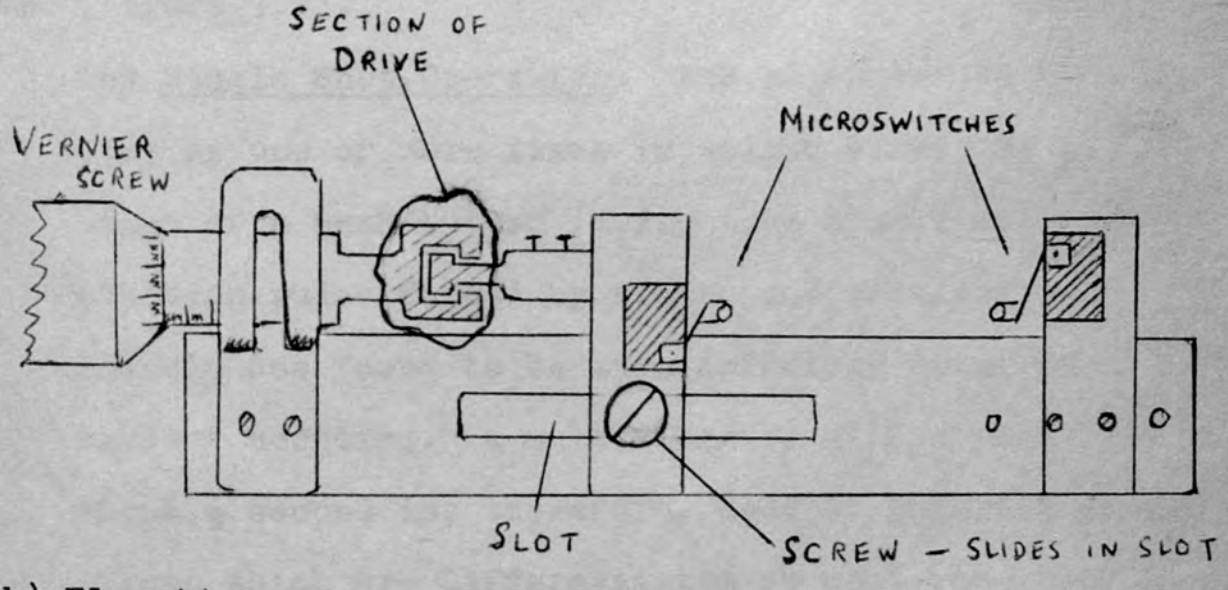

(b) Elevation

Figure 3.6. Worm Drive and Limit Switches.

at either end of its run. The switches are very light to operate and add little to the frictional load of the motor. One of these limit switches is set permanently to correspond to zero current; the position of the others can be altered by means of a vernier screw to set the upper limit to the spectrometer current.

3.2.4. Various Facilities.

Besides the automatic mode of operation, it is possible to increase the current either by the "single Shot" or the "Continuous" method. The wafer switch W.I. permits selection between the different modes of operation (figure 3.7).

(a) Single Shot Operation: the motor can be made to step up one or more times in either direction by means of a push button (S_1). The simple step-function pulse formed by making and breaking a circuit was found to be unsatisfactory owing to contact bouncing. A multivibrator with a period of about $\frac{1}{2}$ second is, therefore, used to generate square pulses which are differentiated to meet the input requirements of the electronic switch. (Section 3.2.2.). The number of steps is controlled by the length of time for which the push button is kept down. The

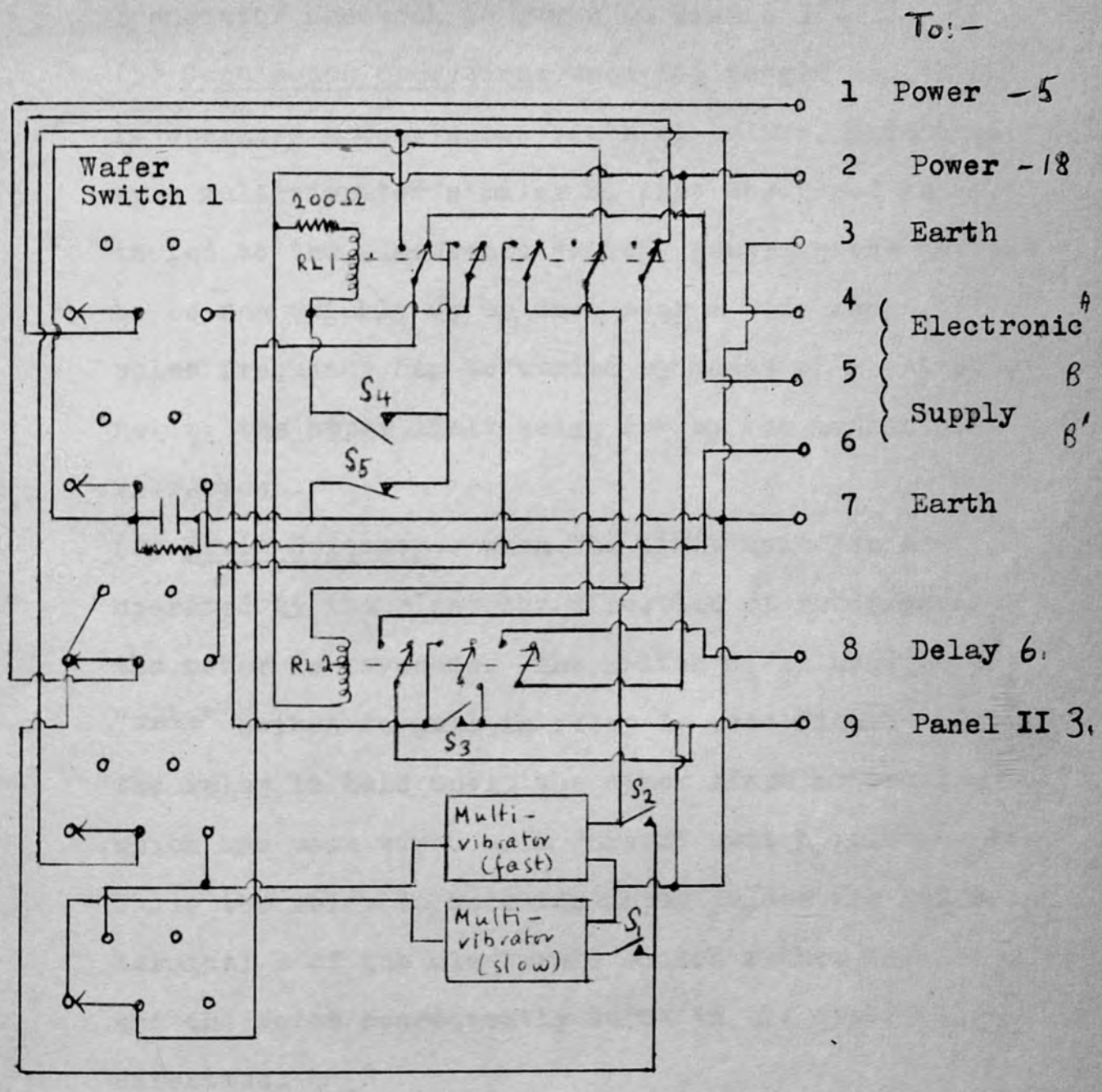

Figure 3.7. Electrical Arrangement for Automatic Operation. Panel I.

circuit, which is based on one given in The Mullard Transistor Handbook is given in Figure 3.8.

(b) Continuous Operation: when the toggle switch S_2 is operated a continuous train of pulses, generated by a multivibrator similar to that described above, is fed to the electronic switch, enabling the current to be run quickly up or down over a wide range. The pulse frequency can be varied by means of a potentiometer, the upper limit being set by the mechanical vibrations.

(c) Limit Switches: when the limit switches are operated by the rider the direction of rotation of the motor is reversed. The switch S_4 is used as a "make" switch to pull in relay 1. (see Figure 3.7); the relay is held until the other limit switch S_5, which has been wired as a "break" switch releases it. While the relay is held the input pulses are fed to terminal B of the electronic switch rather than to A and the motor consequently turns in the opposite direction.

3.2.5. Details of Automatic Operation

After selecting the automatic mode with the wafer switch W 1 the push button S_3 is depressed; this closes Relay 2 which causes the input signals from the Programme

Fig. 3.8. Multivibrator for Operation of Electronic Switch.

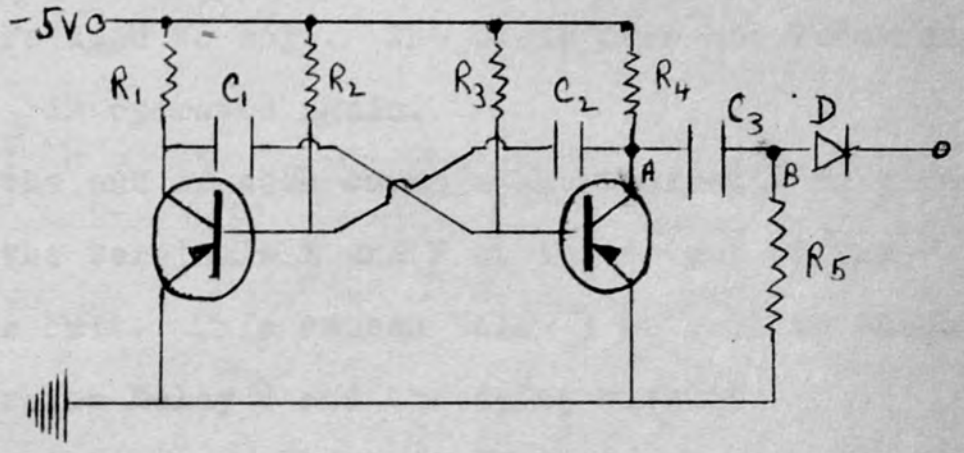

Pulse Shape

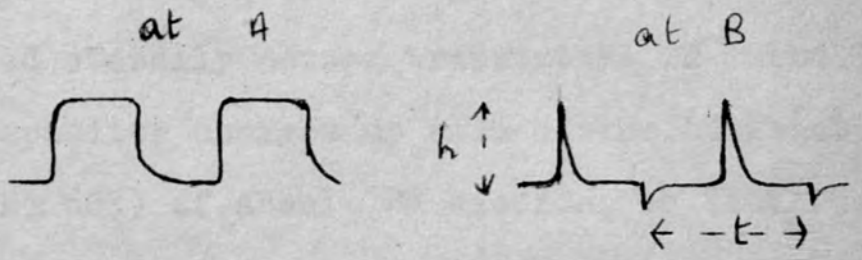

Component Values

	R_1	R_2	R_3	R_4	R_5	C_1	C_2	C_3	D
M.V.1 (Fast)	1 K	11 K	330 Ω +10K*	1 K	4.7k	8 μF	8 μF	.5 μF	OA5
MV2 (Slow)	1 K	12K	12K	670 Ω	1 M	100 μF	100 μF	.05 μF	OA5

* Potentiometer

Circuit Characteristics

	Pulse height	Period t sec	Rise-time
M.V.1	1.8 v	.06	.2 μs
M.V.2	4.5 v	.35	.2 μs

Unit to be fed to the motor. This relay is held until the upper limit switch is operated; thereupon, the fast multivibrator feeds pulses to the switch and the current is quickly reduced to zero. The cycle does not recommence unless S_3 is operated again.

At the end of each count a short circuit is given between the terminals E and F at the output of the Programme Unit. This causes Relay 3 to pull in which in turn operates Relay 4 and the delay circuit.

(a) Delay Circuit (Figure 3.9). A holding contact maintains Relay 4 closed and 12 volts are thus applied steadily across transistors TR 1 and TR 2; the capacitor charges up with a time constant (250μF x 60K) of about 20 seconds, so that the base of T1 is driven increasingly negative. Thus the current drawn from the emitter of T2 increases until it is sufficient to activate the coil of Relay 5. When this is pulled in a short circuit signal is sent to terminals A and G of the programme unit which causesthe scaler to recommence counting. Simultaneously the holding contact of RL 4 is released but the capacitor placed across the coil prevents the power to the transistors being cut off until the count command has been transmitted to the scaler.

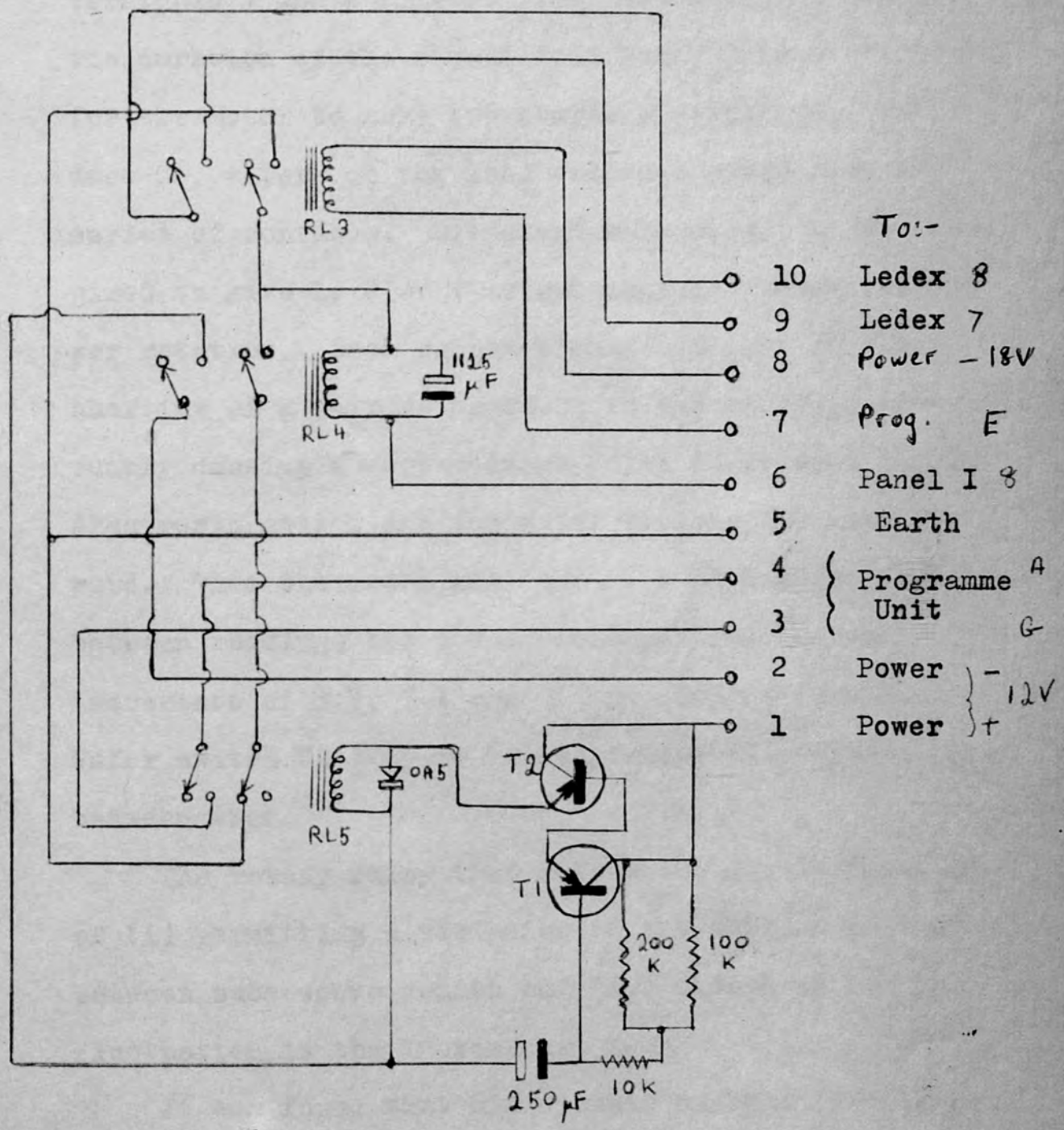

Figure 3.9. Electrical Arrangement for Automatic Operation Delay Circuit.

(b) The Ledex Rotary Relay (e)* is also operated when Relay 3 is pulled in. The commutator is wired so that the switch makes 1 complete revolution every time the terminals 7 and 8 (Figure 3.10) are shorted. In fact the duration of the signal from Relay 3 is sufficient for the motor to make two complete rotations; as it does so, wipers on the load switches sweep over a series of contacts. Different wafers, α, β, γ, are wired to give 1, 2 or 4 output signals respectively per rotation. Each output signal consists in the shorting of a pair of contacts in the external circuitry causing a step-voltage pulse to be sent to the electronic switch and the motor to take one step forward. Thus the motor may take 2, 4 or 8 steps forward between readings and these correspond to current increments of 3.7, 7.4 and 15 mA approximately. Wafer switch W2 (Figure 3.11) permits selection between them.

The rotary relay thus serves the double function of (i) permitting a variation in the current increment between successive counts and (ii) smoothing out the fluctuation in the increment.

It was found that microphonic signals from the commutating switch of the Ledex relay and from the

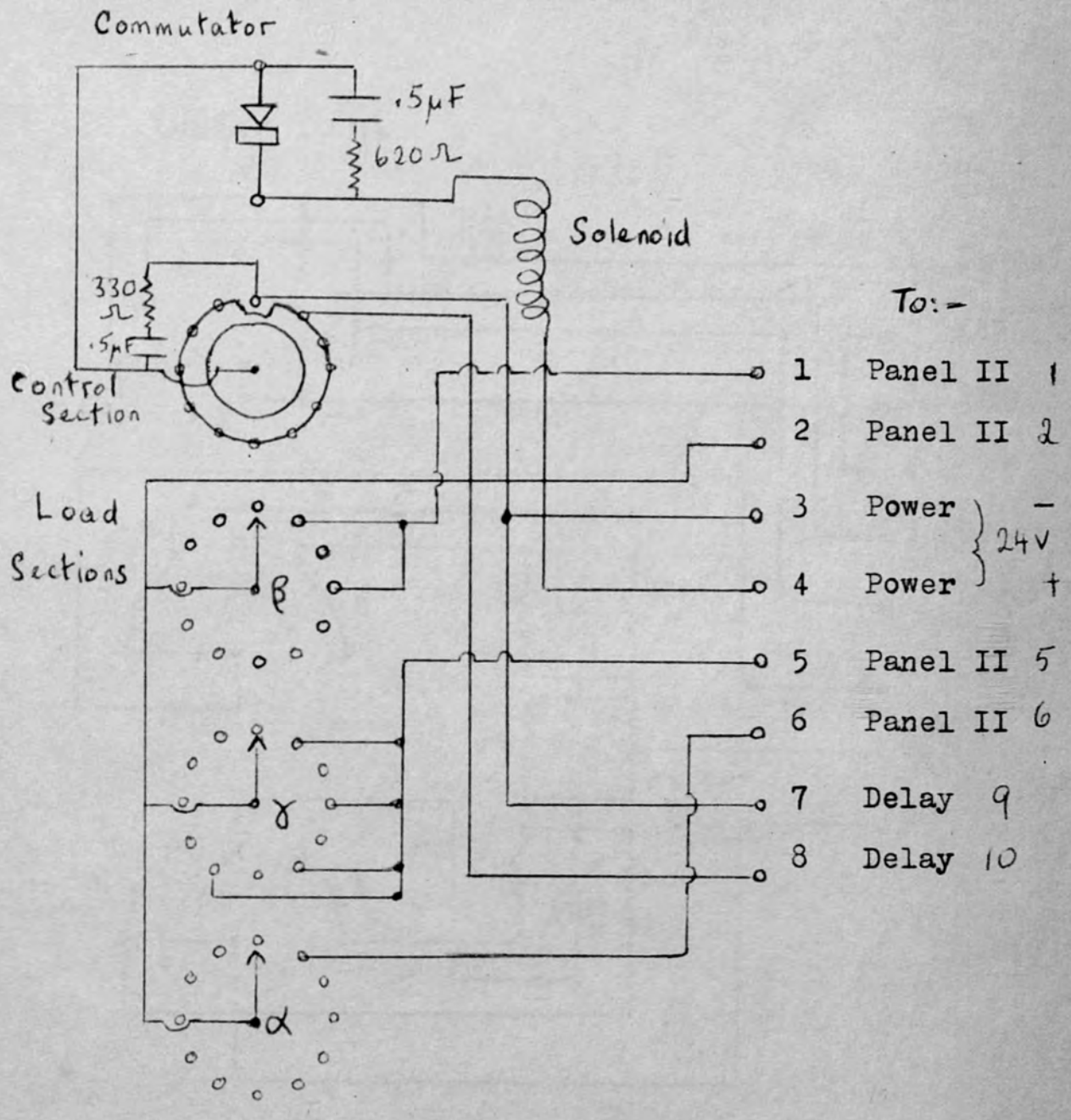

Figure 3.10. Electrical Arrangement for Automatic Operation Ledex Rotary Switch.

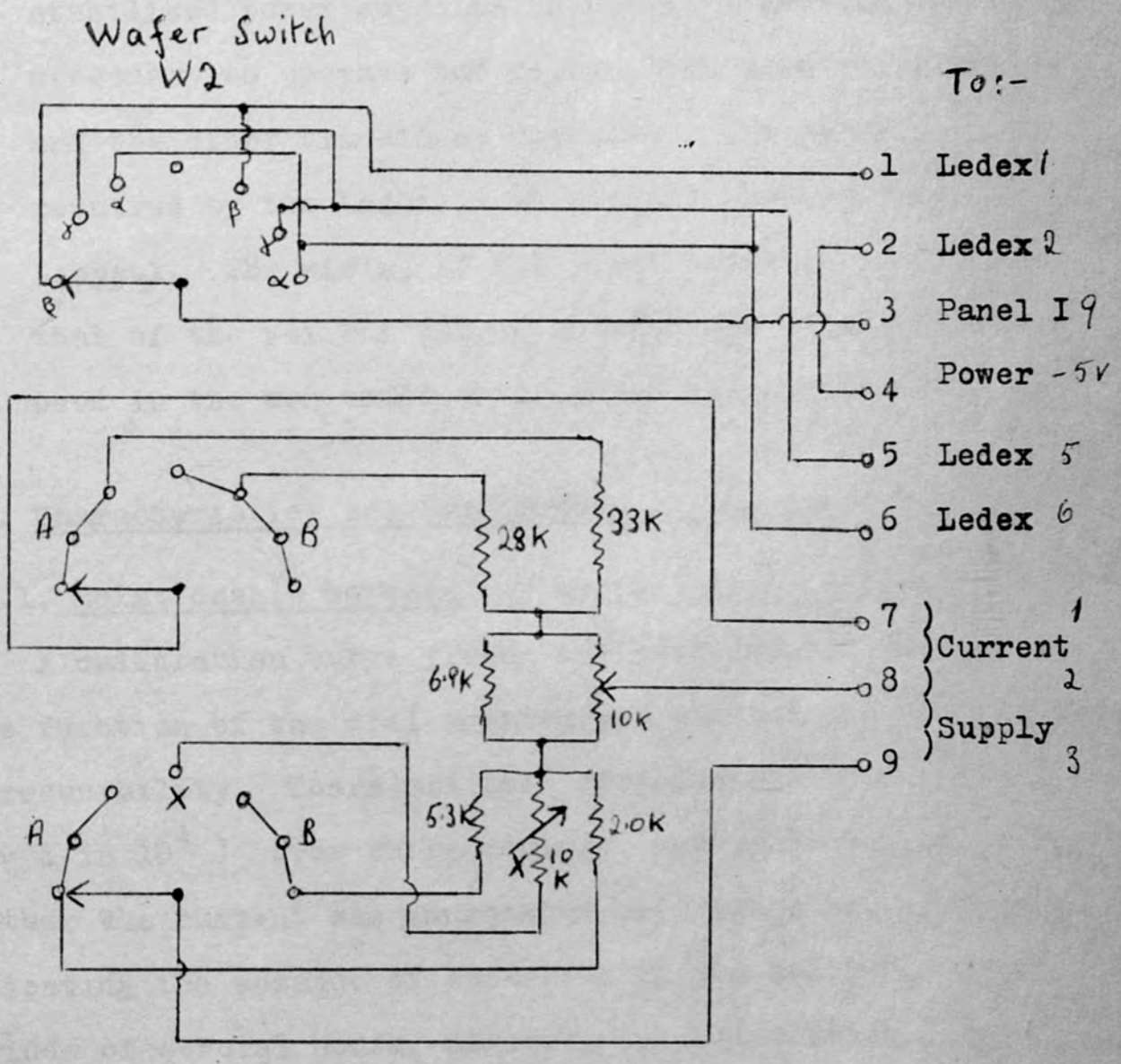

Figure 3.11. Panel II - Including Resistance Network Introduced into Newport Power Supply (Figure 3.3).

coils of the various other relays caused the motor to step on spasmodically. R. C. damping networks were included to overcome these effects.

(c) Power Supplies and Inter Connections. Two commercial stabilised power supplies (j and k *) provide the power necessary to operate the relays, the electronic switch and the other transistor circuits. The power required by the Ledex is at present obtained from a Labpack. The wiring of the power supplies as well as that of the various plugs, sockets and edge-connectors used in the construction is given in Appendix II.

3.3. Characteristics and Performance of the Automatic System

3.3.1. Relationship between current and dial setting

A calibration curve giving the spectrometer current as a function of the dial setting was plotted and checked for reproducibility. There was good reproducibility ($\sim$ 1 in 10^4) over short periods, independently of whether the current was increasing or decreasing, thus indicating the absence of back-lash in the helipot. Over periods of several hours, however, the calibration line was displaced by as much as a few per cent; this is to be

expected on the basis of the drift in current noted in 3.2.2. above. Thus if the dial setting is to be used as more than a rough guide to the spectrometer current, it should be recalibrated fairly frequently, at at least one point.

One might expect the current to increase linearly as the helipot is turned and the dial reading increases; in fact there is a slight departure from linearity which is shown in figure 3.12, where the increase in current Δ i corresponding to one complete rotation of the helipot is plotted against the number of the revolution. The steady increase in Δ i suggests a non-infinite impedance in the circuit leading to the potentiometer slider resulting in a slight drain of current from the mercury cells. The trend was found to be reproducible.

3.3.2. Size of Increment

(i) Systematic Variations. The current increment corresponds to 2, 4 or 8 steps taken by the motor i.e. 1, 2 or 4 hundredths of a turn on the helipot, respectively. Thus, on the basis of what has been said above, the current increment corresponding to two steps by the motor will vary from 3.65 mA at the low end of the range to 3.77 mA at the high end. In the investigations of a restricted portion of a spectrum the constant used for converting from number of

Figure 3.12. Variation of Current Increment with Helipot Setting.

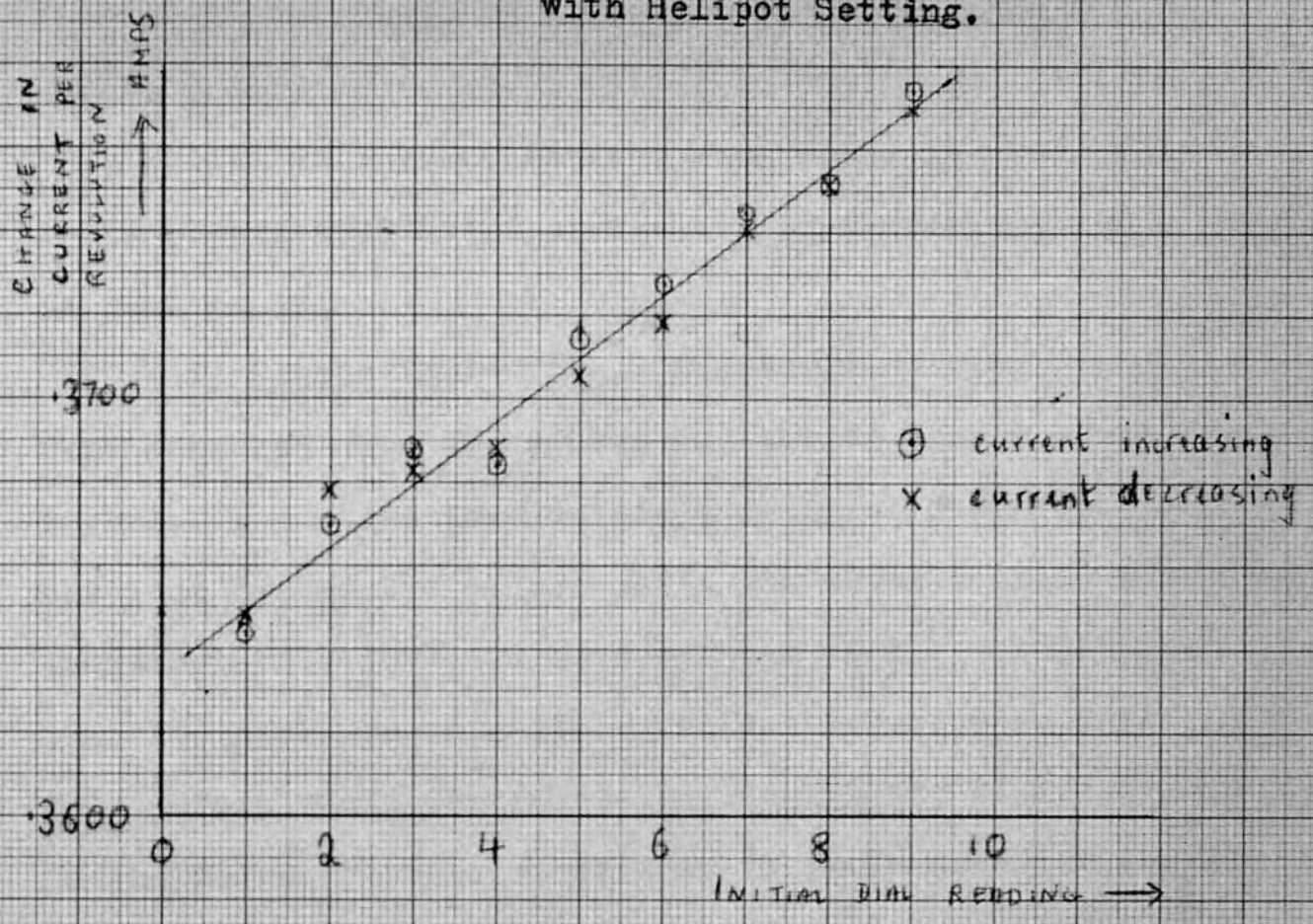

Figure 3.13. Distribution of Current Increments.

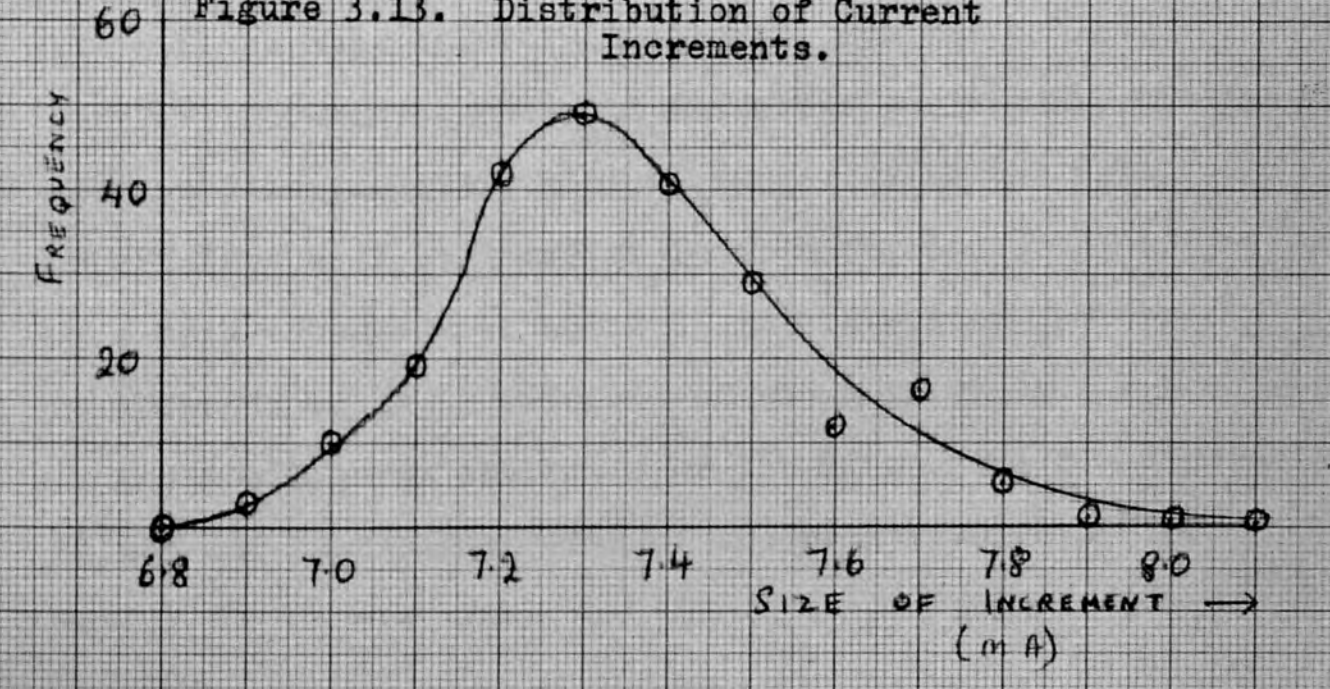

increments to change in current or momentum should be chosen according to the position in the range. If, in a more extensive investigation a mean value is used, this could be expected to give rise to a systematic error of as much as 1%.

(ii) Random Variations. Successive current increments were measured when the system was set to take 4 steps per signal. The steps were within a restricted current range so that the systematic effect noted above was small. A mean increment of 7.35 $\pm$ .20 mA was found as the result of more than 200 such measurements. The distribution is given in Fig. 3.13. This would contribute an uncertainty of about .01% in the value of the current when it is focused for the F line of Thorium B, and this is well within the required limits. It may be assumed that the uncertainty in the momentum will be approximately the same. For the smaller current increments, those of two steps per signal, the uncertainty is probably twice as large. Also the relative uncertainty will be lower at lower energies.

This variation of about 3% in a 4 - step increment corresponds to an uncertainty of about 1/100 x 4 x 1'48" = 12" in the position of the rotor of the motor. Such a figure is not unreasonable in view of the construction of the motor.

3.3.3. Spectrum Lines Plotted Automatically.

For these tests and those reported in the subsequent section a source of Th B+ C + C' deposited on a brass button was used; the low current range was used exclusively but this included many well determined conversion lines.

The F line of 138 KeV energy was plotted automatically at different resolutions. The resolution was reduced by narrowing the ring slit. For the slit setting of 60 the current increased by 4 steps between counts; for the other settings by 2 steps. The family of curves so obtained is shown in Figure 3.14 with the index number displaced for each curve so that the peaks should coincide. Reasonable line shapes are maintained down to the best resolutions.

Figure 3.15 compares the points obtained when the line is plotted automatically and that when it is plotted in terms of current. The scales of current and index number have been superimposed and have been expanded, c.f. Figure 3.14, so as to exaggerate any discrepancies. Such discrepancies exist but amount to only a fraction of the current increment.

3.3.4. Relationship of Magnetic Rigidity to Current and Index Number.

The part of the spectrum of Th B + C + C' included in the low energy range was plotted automatically at a

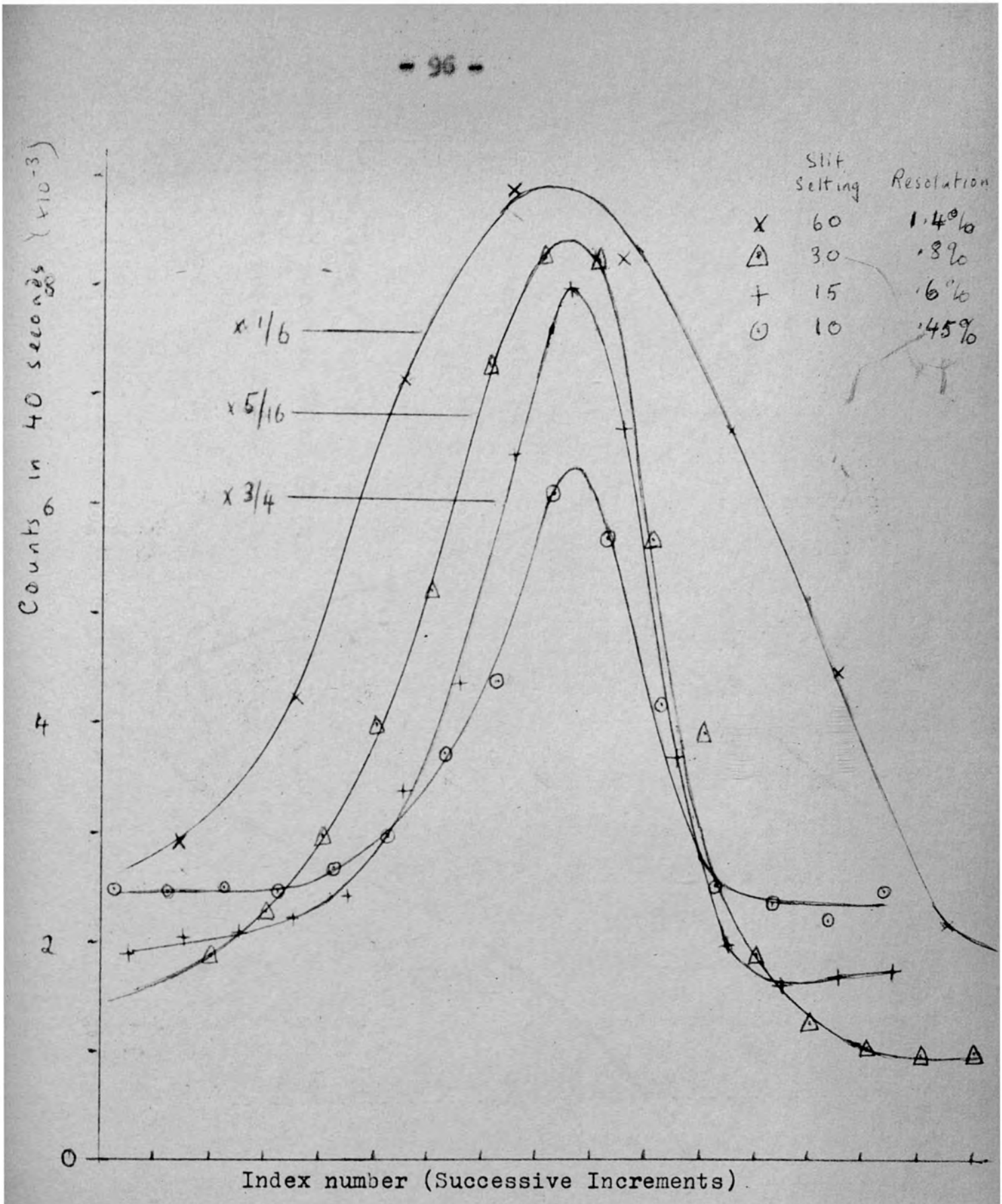

Figure 3.14. F Line Plotted Automatically at Different Resolutions.

Figure 3.15. Comparison of Plot of F Conversion Line Plotted
(a) automatically and (b) by current measurement.

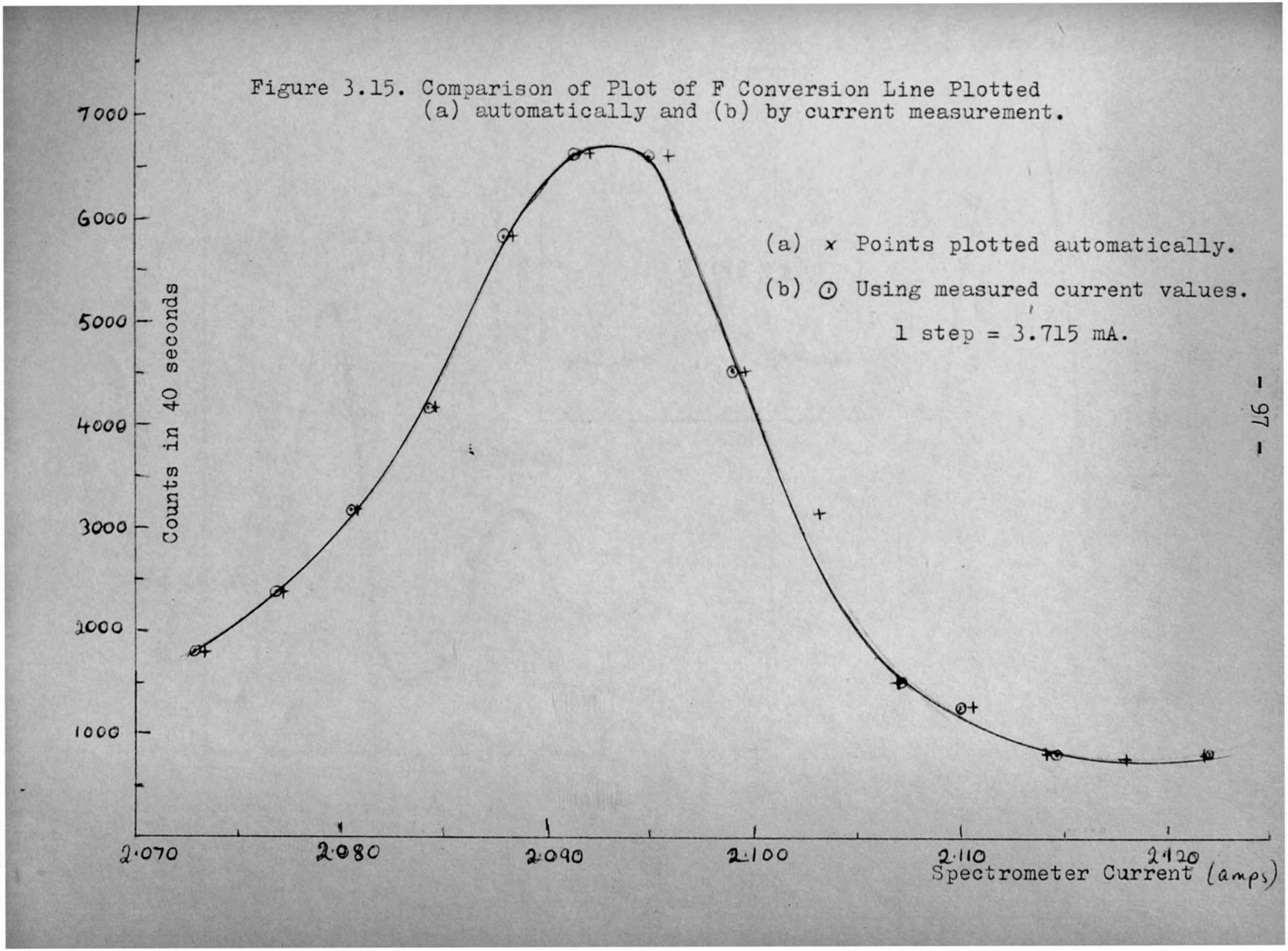

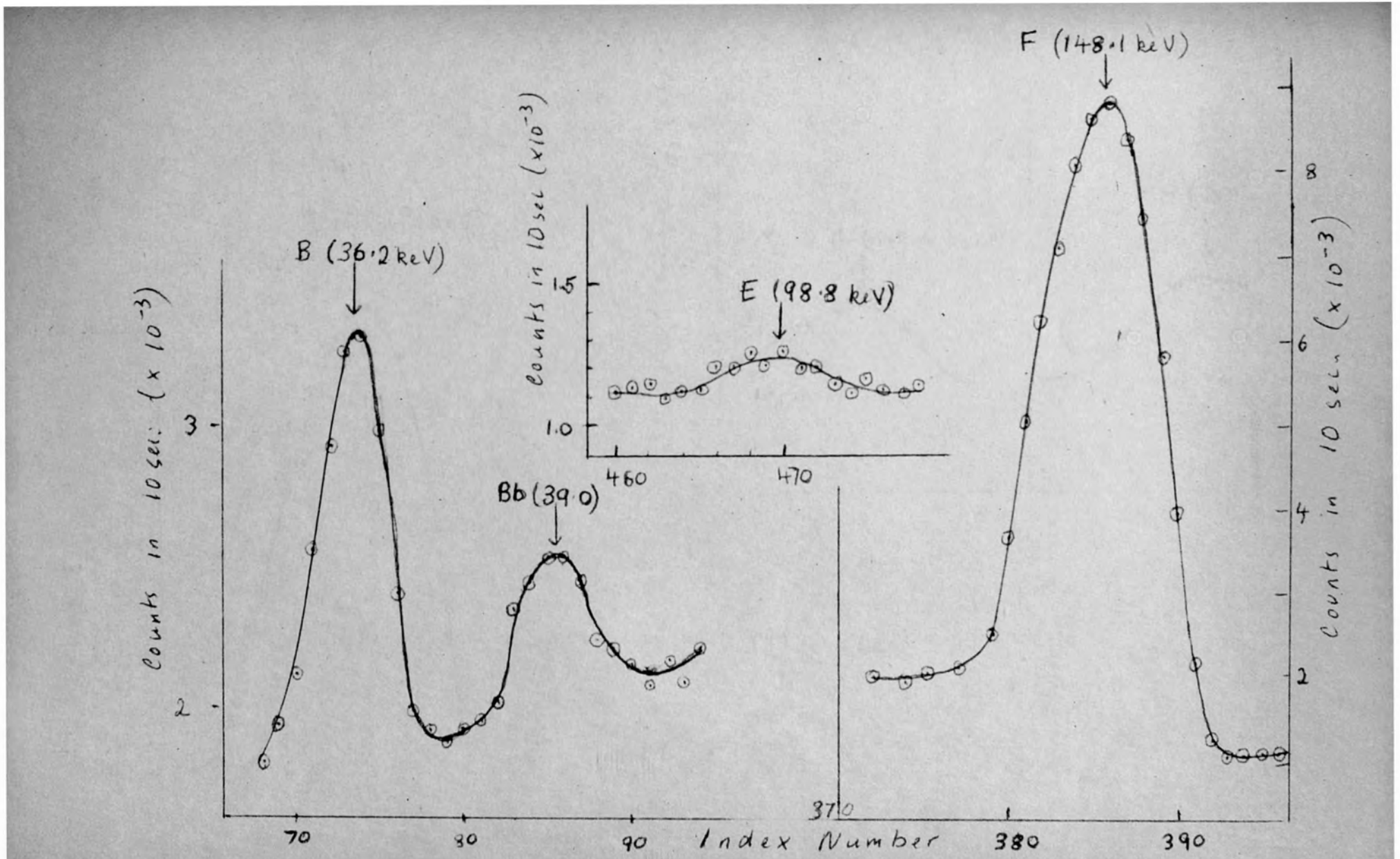

Figure 3.16 (a) Conversion Lines of Th. B. + C + C' Plotted Automaticslly.

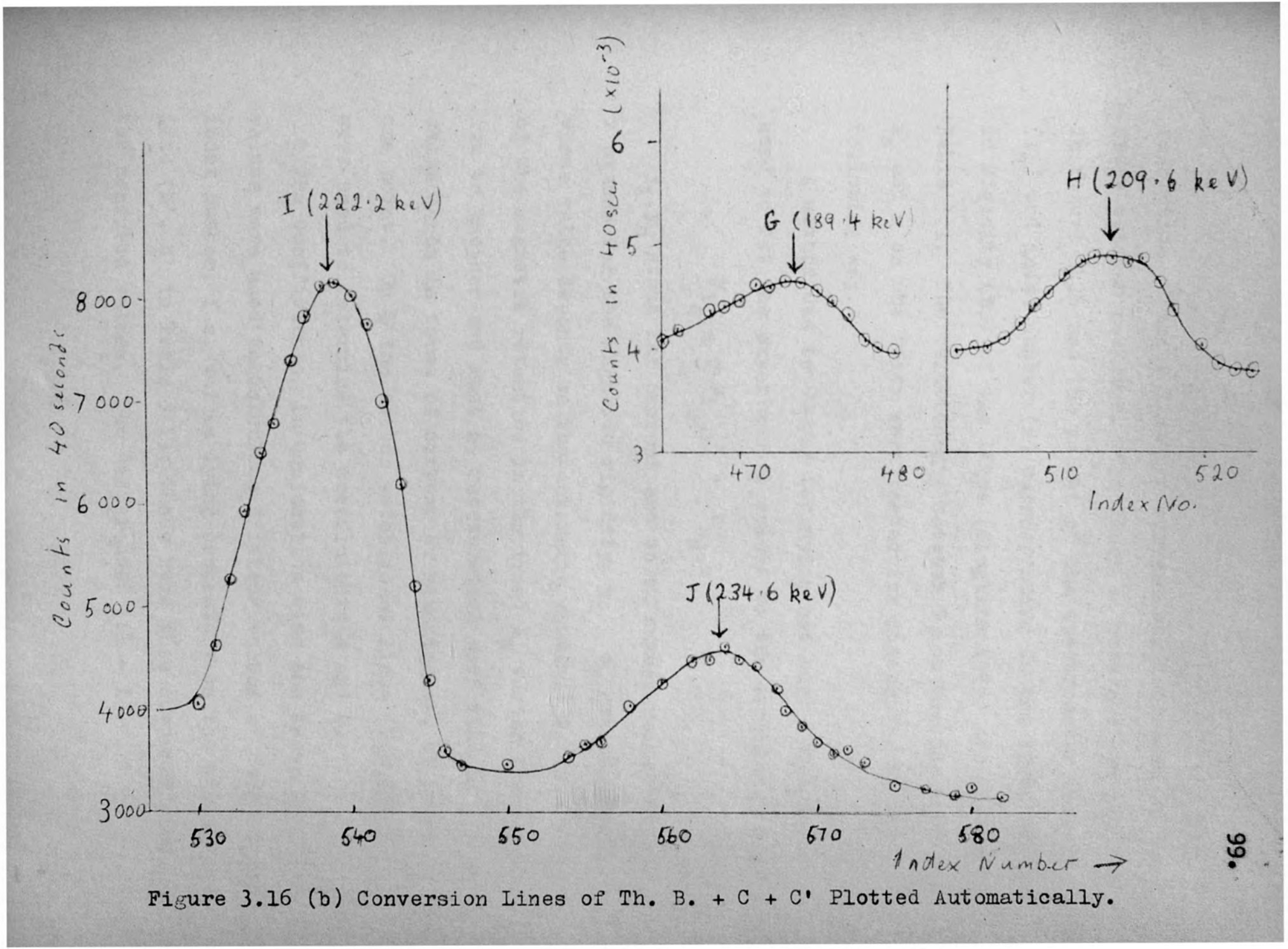

Figure 3.16 (b) Conversion Lines of Th. B. + C + C' Plotted Automatically.

resolution of about 1.3% the current was increased by two steps between readings. The lines so obtained are plotted in figure 3.16 and the values of the spectrometer current (i_s) and index number (n) corresponding to the known magnetic rigidity ($B\rho$) of the lines (Siegbahn 1965) are listed in Table 3.1. The relationship between $B\rho$ on the one hand and i_s and n on the other were tested for linearity, in the following way.

A method due to Cauchy (Champion and Davy 1941) was used to fit the experimental values to the straight lines;

$$y_{i_s,n} = a_{i_s,n} x + b_{i_s,n}$$

y_i, y_n stand for current and index number respectively, x stands for the magnetic rigidity, a_{i_s}, a_n are constants whose value depends on the automatic system; b_i is a measure of the magnetic retention in the iron; b_n varies from one run to another and must be redetermined each time by calibration in terms of current or momentum at, at least one point. Only the better established lines (B,E,F,I,J) were used to determine the coefficients a and b.

The coefficients, in conjunction with the known $B\rho$ values were used to calculate "fitted" values of current and index number, i.e. values lying accurately on the straight line (i', n' in Table 3.1); these were then compared with the measured values. The differences (i' - i),

TABLE 3.1

Analysis of relationship of magnetic rigidity to current and to index number.

Line	B gauss-cm	Index No.n	Error δn	"Fitted" Index No. n'	n'-n	Spectrometer current i_s -amp	Error δi_s mA	"Fitted" current i'_s-Amps	$i'_s - i_s$ mA
B	652.4	73.7	0.3	74.9	+ 1.2	.9440	1.1	.9441	+ .2
B	678.6	85.6	0,6	85.9	+ .3	.9861	2.2	.9849	- 1.2
E	1109.9	268	1.5	267.8	- 1.2	1.6564	5.5	1.6561	- 03
F	1388.4	385.8	0.5	385.3	- .5	2.0873	1.9	2.0895	+ 2.2
G	1597.5	473.0	1.5	473.4	+ .4	2.4105	5.5	2.4150	+ 4.5
H	1694.7	514.2	1.0	514.4	+ .2	2.5631	3.7	2.5662	+ 3.1
I	1754.0	539.4	1.0	539.4	0	2.6603	3.7	2.6585	- 1.8
J	1811.1	564.0	1.2	563.5	- .5	2.7483	4.4	2.7474	- 0.9

a_i = 1.5563 amps/gauss-cm $\quad b_i$ = - .0712 amps

a_n = .4217 per gauss-cm $\quad b_n$ = - 200.3

$(n' - n)$ between the measured and "fitted" values are listed in the table and are seen to be of the same order as the estimated uncertainties ($\delta i, \delta n$) in determining the position of the peaks of the lines.

If the departure from a strictly linear relationship were due to the automatic system one would expect $n' - n > \delta n$. If, on the contrary, it were inherent to the spectrometer at the given resolution then one would get $\delta n > (n' - n)$. Since $n' - n \sim \delta n$ the source of the irregularity is not evident.

However, the fact that $(i' - i)$ is also of the same order as δi suggests that the fault lies at least partially with the spectrometer. Further runs at better resolution would be necessary to verify this.

The non-linearity is such as to limit the precision with which the magnetic rigidity at a particular point can be determined from the value of the index number at that point, to about 2 in 1000. The accuracy is also limited in that the values of a_i, a_n are not perfectly reproducible; the overall precision that can be expected of the system is about 5 in 1000.

3.3.5. Evaluation of the Automatic System

The estimated precision of the present automatic

system is an order of magnitude less than that initially prescribed (section 3.1.2).

While the present system is useful for routine or preliminary investigations, for the investigation of continuous spectra or the approximate location of conversion lines, greater momentum precision is necessary if the spectrometer characteristics are to be fully exploited.

The programming facilities of the present system are limited; the compromise value of 3.7 mA for the minimum current increment does not meet the requirement as set out in section 3.3.1. The step size cannot be reduced without simultaneously reducing the current range for a given setting and this interdependence is clearly undesirable. The only alternative, gearing down the motor still further, would make the angular step size excessively small.

An alternative current-controlled system has been proposed. The helipot would be replaced by a Kelvin Varley chain of resistors and the stepping motor by a set of rotary relay switches. There would then be a well-

-determined and discontinuous change in resistance, and so in current, between counts, thus avoiding the uncertainty inherent in the use of a stepping motor and the steadily varying resistance of a helipot. Smaller current increments would be possible and there would be greater possibility of introducing different programming facilities.

If, with such a system, the stability and precision still do not meet the operating requirements then the introduction of a field-controlled system must be envisaged.

3.4. Measurement of the Magnetic Field

3.4.1. The advantages to be gained by using a field-controlled system are the elimination of non-linear effects due to magnetic retention or saturation in the iron and an improvement in the field stability. In order to benefit from these advantages the field measuring system used in the feed-back loop should be capable of an accuracy not less than a few parts in 10^4. To this end an improvement in the existing system was undertaken.

The field is measured by the rotating coil method; details of the construction have been given by Evans (Evans 1958*) and by Michelson (Michelson 1961). A pair of Helmholtz coils provide the reference field; the current through these coils at the balance point is proportional to

the field in the spectrometer. The balance is detected by feeding the difference signal from the rotating coils to an amplifier tuned to their frequency of rotation (25 c.p.s.) and then displaying the output signal on an oscilloscope. The system is shown diagramatically in Figure 3.17. The phase of the reference signal can be adjusted relative to that of the signal from the spectrometer field, by means of levelling screws with which the Helmholtz coils are provided.

Previously the accuracy was limited to about 1 in 10^3 by the noise. It was hoped to better this by using an improved tuned amplifier.

3.4.2. The Tuned Amplifier.

Besides the signal at 25 c.p.s. the e.m.f. picked up by the brushes inevitably contains harmonic components due to the field-gradient in the spectrometer as well as noise, and mains pick-up at 50 cycles per second. The latter is especially troublesome and a relevant characteristic for describing the performance of the amplifier is thus the ratio

$$\alpha = \frac{\text{voltage gain at 25 c.p.s.}}{\text{voltage gain at 50 c.p.s.}}$$

The transistorized amplifier described by Bertoya (Bertoya 1963) in which the tuning is done by a twin-T filter appeared to be suitable for this very low frequency

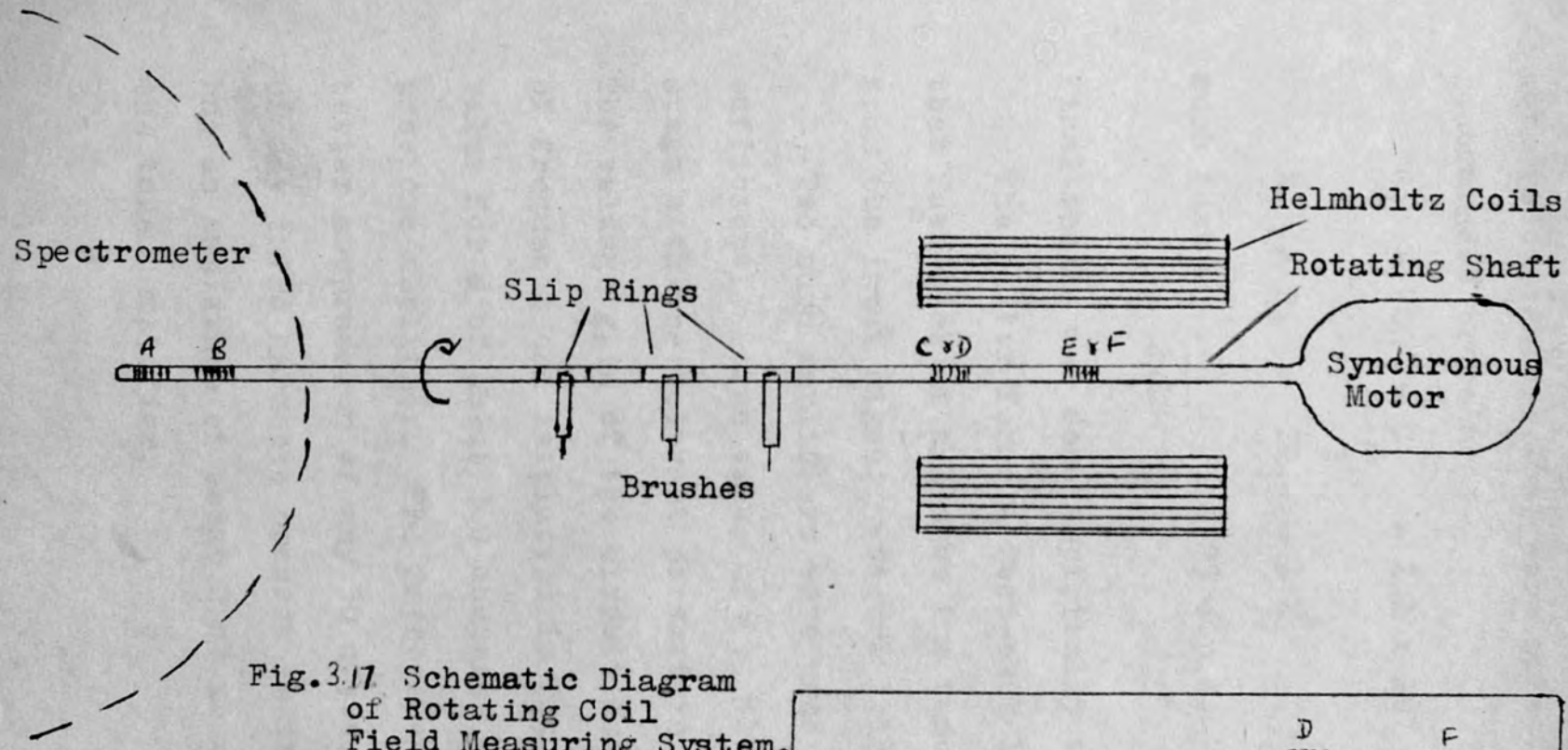

Fig. 3.17 Schematic Diagram of Rotating Coil Field Measuring System.

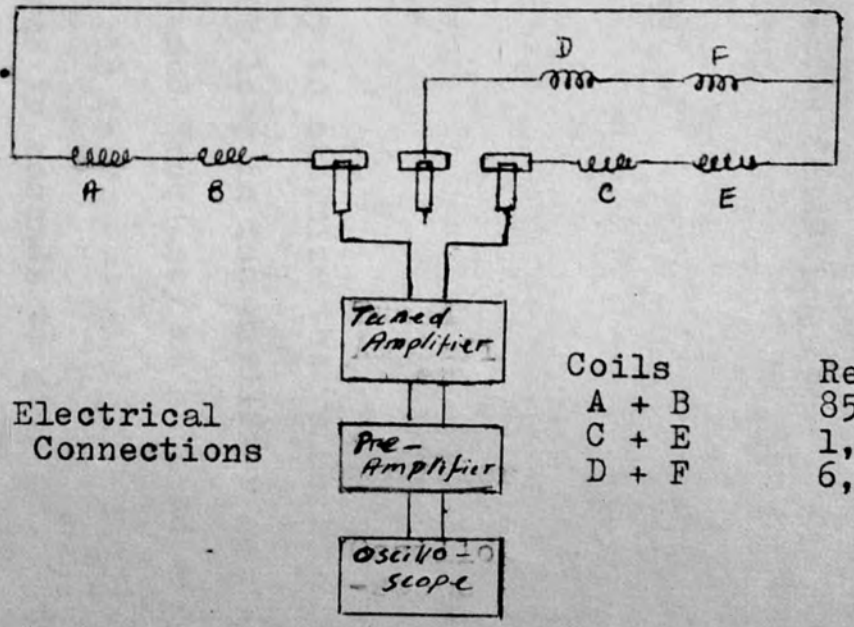

Electrical Connections

Coils	Resistance
A + B	850
C + E	1,000
D + F	6,500

application. Values for the components of the Twin-T network (see figure 3.18a) were selected following the recommended procedure:

$$C_1 = C_2 = \frac{C_3}{2} = 2.1 \times 10^2 \ \mu F$$

$$R_1 = R_2 = 2R_3 = 3 \ K$$

such that $\omega_f = \frac{1}{2\pi RC} = 25$ c.p.s.

Final tuning was done empirically to optimize the value of α.

The filter forms a feed-back loop in the amplifier so that feed-back at all save the tuned frequency is subtracted from the input signal. (figure 3,18 (b)).

Two such amplifiers were used in cascade to give a sufficiently large value of α; the circuit diagram of one stage with the relevant parameters is given in figure 3.19. The voltage gain of the circuit was measured as a function of frequency and is plotted in fig. 3.20. This gives a value for α of about 360 compared with about 28 for the previous amplifier. The improvement is chiefly due to the better suppression of any 50 c.p.s. component; less than .2 of any third harmonic present is transmitted. The noise has an amplitude of about 2 mV measured at the output of the tuned amplifier.

$R_1 = R_2 = 3K$

$C_1 = C_2 = 2.1 \times 10^2 \mu F$

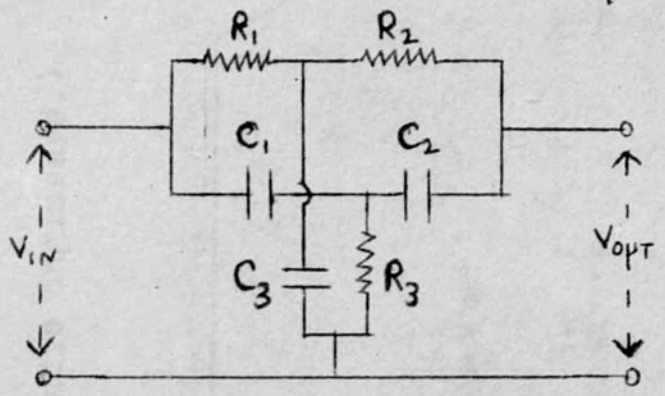

Figure 3.18 (a). Twin - T Filter Network.

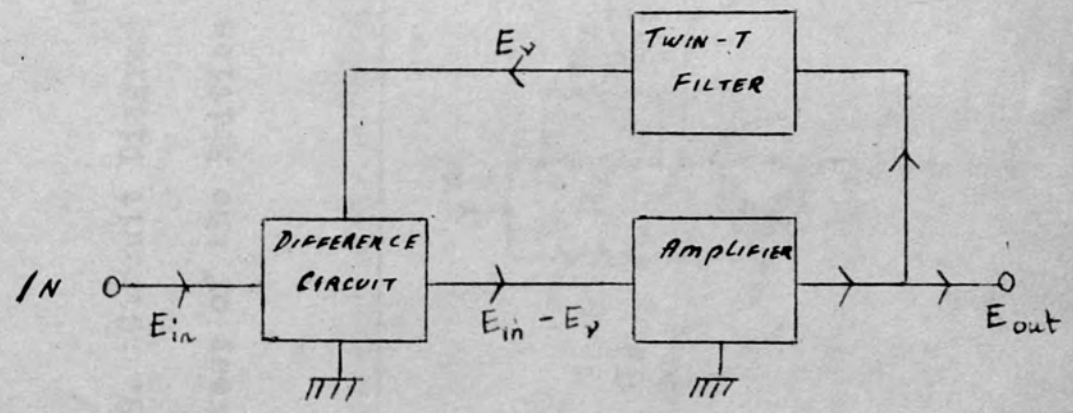

Figure 3.18 (b). Principle of Twin-T Selective Amplifier.

Figure 3.19. Circuit Diagram of Twin-T Selective Amplifier.

(By Courtesy of the British Institute of Radio Engineers.)

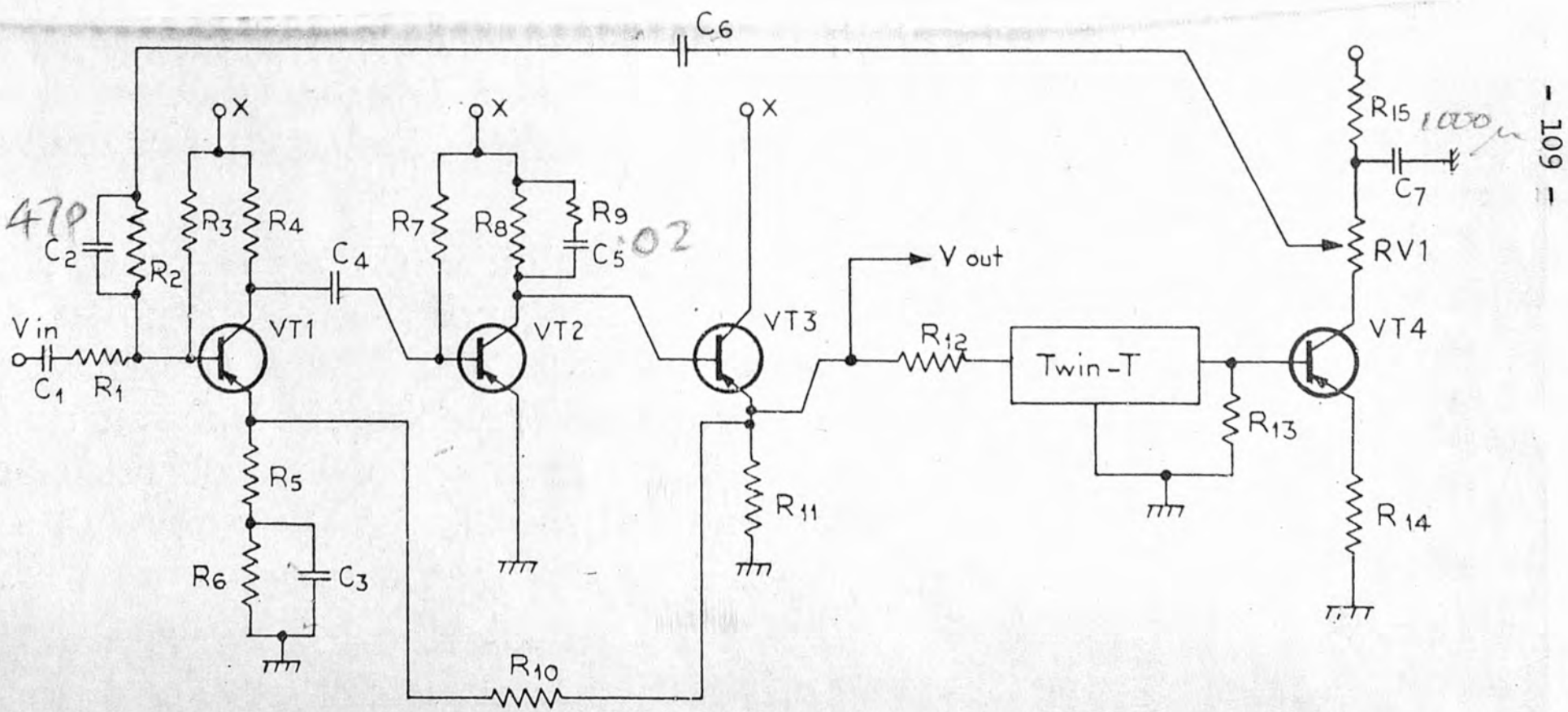

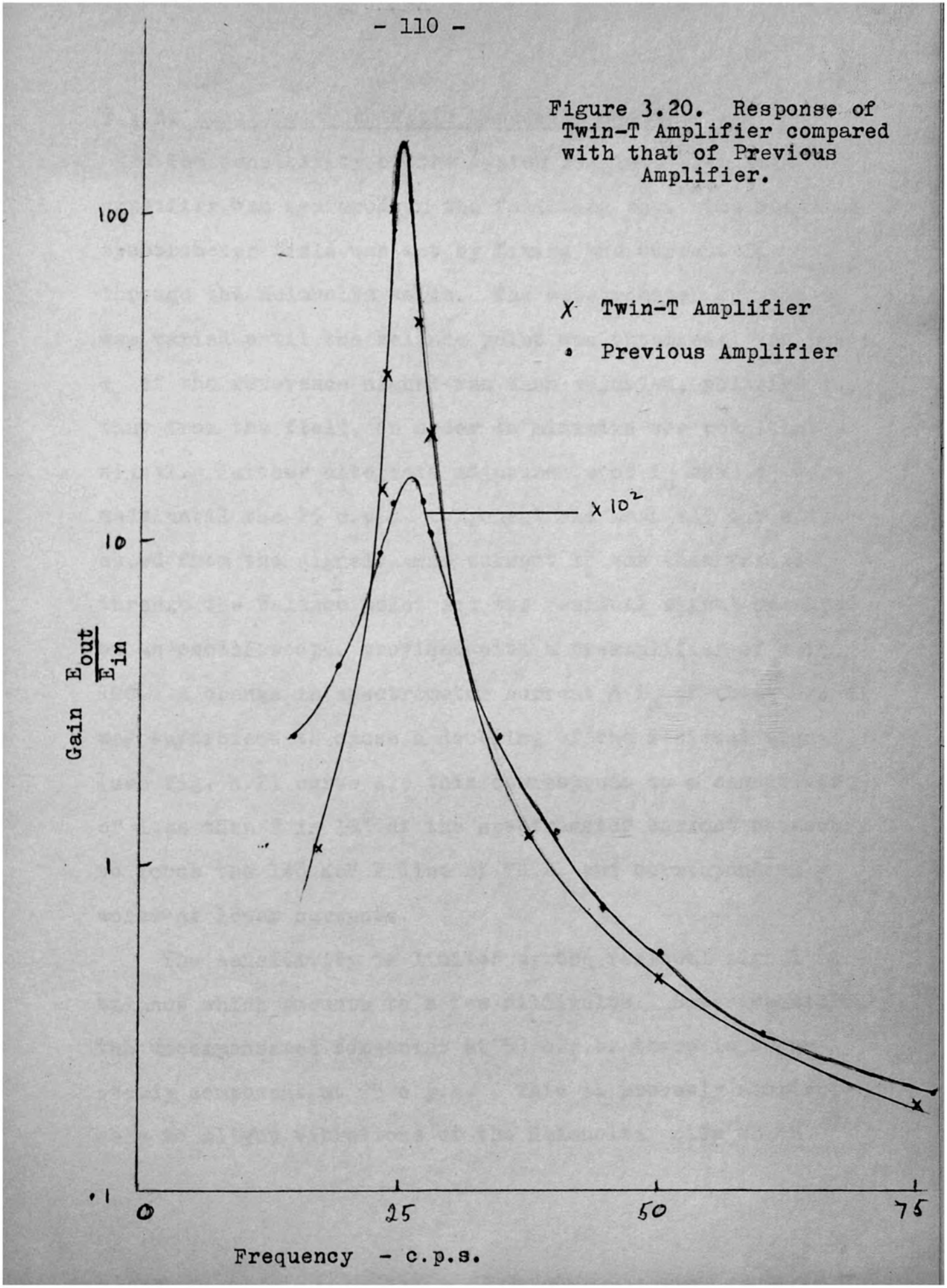

Figure 3.20. Response of Twin-T Amplifier compared with that of Previous Amplifier.

3.4.3. Sensitivity of Field Measuring System

The sensitivity of the system complete with Twin-T amplifier was measured in the following way. The required spectrometer field was set by fixing the current i_H through the Helmholtz coils. The spectrometer current i_s was varied until the balance point was obtained; the phase ϕ of the reference signal was then adjusted, relative to that from the field, in order to minimize the resultant signal. Further alternate adjustments of i_s and ϕ were made until the 25 c.p.s. component had been all but eliminated from the signal. The current i_s was then varied through the balance point and the residual signal measured on an oscilloscope, provided with a preamplifier of gain 100. A change in spectrometer current Δi_s of about 0.3 mA was sufficient to cause a doubling of the residual signal (see fig. 3.21 curve A); this corresponds to a sensitivity of less than 2 in 10^4 at the spectrometer current necessary to focus the 148 KeV F line of Th.B. and correspondingly worse at lower currents.

The sensitivity is limited by the residual signal at balance which amounts to a few millivolts. Superimposed on the uncompensated component at 50 c.p.s. there is an unsteady component at 25 c.p.s. This is probably attributable to slight vibrations of the Helmholtz coils which

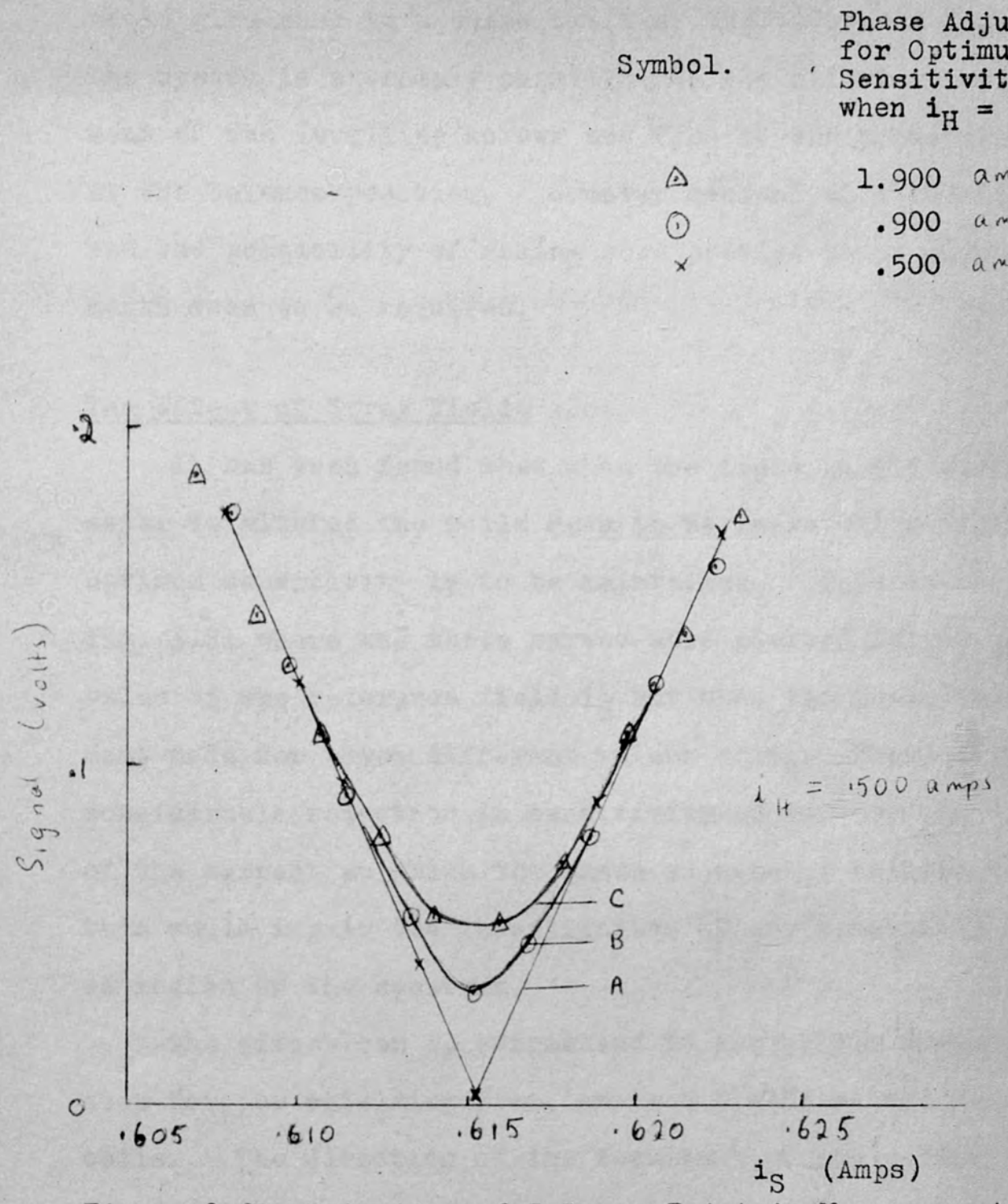

Figure 3.21. Detection of Balance Point in Measurement of Magnetic Field, showing Loss in Sensitivity as Phase Setting is Altered.

would give rise to a phase shift of the reference E.M.F. The system is extremely sensitive to the slightest adjustment of the levelling screws and thus of the phase when at the balance-position. Greater mechanical stability and the possibility of making more precise phase adjustments seem to be required.

The Effect of Stray Fields

It has been found that when the field in the spectrometer is altered the coils have to be re-levelled if the optimum sensitivity is to be maintained. This is shown in fig. 3.21 where the three curves were plotted for the same value of the reference field i_H but with the phase adjustment made for three different values of i_H. There is thus considerable reduction in sensitivity at any but the value of the current at which the phase adjustment is made and this would impair the investigation of any reasonably extended region of the spectrum.

The effect can be attributed to incomplete compensation for, or shielding from, ambient fields at the Helmholtz coils. The direction of the resultant of the reference field with any stray field will vary as either or both of the components are altered. Not only does this lead to loss in sensitivity but also it is the resultant field

rather than that due to the Helmholtz coils which will be proportional to the spectrometer field. Simple tests revealed the presence of an uncompensated stray field even in the absence of any current in the spectrometer and that this increased if the current increased above zero. This indicates the need for more careful shielding of the reference field as well as better compensation for the earth's field. These requirements could most easily be met if the Helmholtz coils were to be replaced by a permanent magnet as has been done at Uppsala. (See Section 2.3.2). There the system has been developed to the point at which it is capable of an accuracy of 5 in 10^6; while such a figure is not required in the present case, further improvements along the suggested lines will be necessary before a sufficiently accurate and reliable feed-back loop from the field can be constructed.

CHAPTER 4

Modification to the Detector of the Small Spectrometer

4.1. Introductory.

4.1.1. The Small Spectrometer.

A smaller iron-clad lens spectrometer is joined to the prolate spheroidal field spectrometer for β-β coincidence studies (Michelson 1961). It is shown at the right hand side in figure 3.1. The current is supplied by large capacity accumulators (15 cells A.E.I. Type BB 35), which are simultaneously charged from 240 volt d.c. mains supply. The circuit diagram is given in figure 4.1.

The particles are detected by a plastic scintillation phosphor and photomultiplier; the photomultiplier is placed outside the field and the scintillation is conducted to the photo cathode along a light guide. A lower limit to the energy of electrons which can be detected is set by the amplitude and intensity of the signal relative to that of the photomultiplier noise. Ways must be sought for increasing the one and reducing the other.

4.1.2. Factors affecting Signal Pulse Height.

The chief factors affecting the amplitude of the final electron pulse arriving at the anode of the photomultiplier

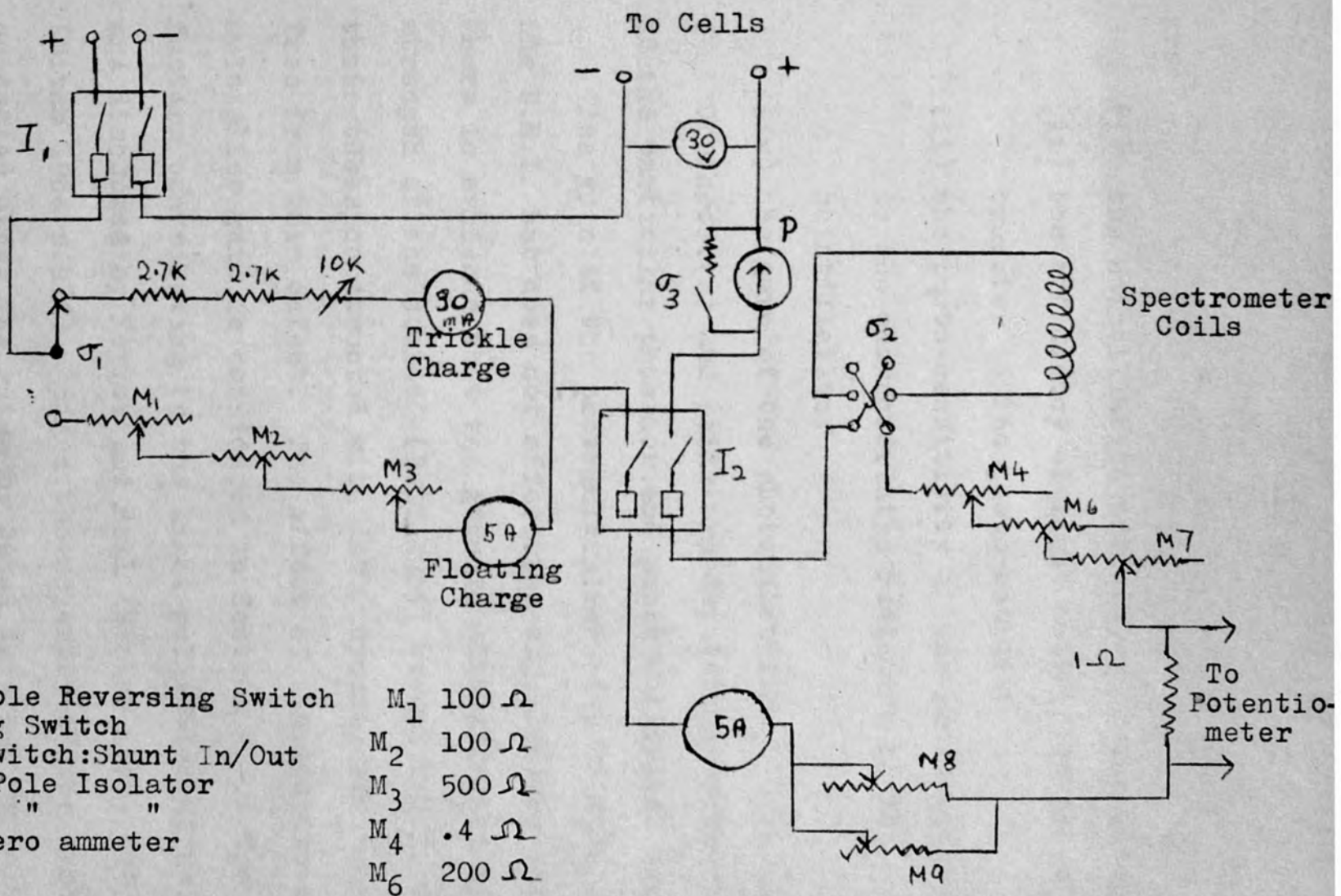

σ_1	Single Pole Reversing Switch	M_1	100 Ω
σ_2	Reversing Switch	M_2	100 Ω
σ_3	Toggle Switch: Shunt In/Out	M_3	500 Ω
I_1	Fused 2 Pole Isolator	M_4	.4 Ω
I_2	" " "	M_6	200 Ω
P	Centre Zero ammeter	M_7	140 Ω
		M_8	3 Ω
		M_9	.4 Ω

Fig. 4.1. Current Supply for Small Spectrometer.

are

(i) the scintillation efficiency of the phosphor;

(ii) the efficiency of light collection and of transfer to the photo-cathode;

(iii) the photo-sensitivity of the photo-cathode to the characteristic radiation of the scintillation;

(iv) the gain of the photomultiplier.

Of these (i) and (iii) are determined by the properties of the particular phosphor and photo multiplier used.

The gain of the photomultiplier (iv) is determined by the E.H.T. but does not affect the signal:noise ratio. There is evidence that the gain is also affected by the strength of the source (Bell 1955), though E.M.I. claim that their tubes, constructed with Cs$b dynodes are relatively free from this defect. The effect of temperature on photo-multiplier gain is considered in Section 4.3. The many factors contributing to the light collection efficiency (iii) are discussed by Neiler and Bell (Neiler 1965) and by Birks (Birks 1964 p.97f). Since the majority of the light is conducted along the guide by total internal reflection at the surface it is important that the guide should be well polished, particular attention being given to the elimination of circumferential scratches.

4.1.3. Noise in the Photomultiplier.

The causes of photomultiplier noise have been discussed by Birks (Birks 1964 p.124). The most intense source at room temperature is thermionic emission from the photo-cathode, though this contributes only low amplitude pulses; their number may be greatly reduced by moderate cooling of the tube.

The larger noise pulses are more difficult to eliminate; their intensity varies widely between different tubes even of the same type and depends on the previous history of a particular tube. The satellite pulses whose number increases as soon as the counting rate increases, are particularly troublesome; they are caused by ion or optical feed-back processes which cause the emission of multi-electron pulses from the photo cathode,

4.1.4. The Phosphor and Light Guide.

The former phosphor was replaced by a new sample of Naton 131: a thin disc 1½" in diameter and 1/8" thick. This was joined to a cylindrical light guide of polyvinyl toluene 1 1/4" in diameter and 5½" long. The E.M.I. Type No.9514A photomultiplier tube was retained.

The light guide was loosely surrounded by shiny aluminium foil, so that some of the light escaping from the sides might be recovered. A very thin reflecting film was placed over

the end of the phosphor. Much of the light from the scintillation is totally reflected at this surface but the film should increase the light collection efficiency by redirecting light which would otherwise escape; it is considered further in the next section.

4.2. The Thin Film Reflector

4.2.1. General Consideration.

The film has to be extremely thin in order to minimize the energy loss of β-rays which traverse it; at the same time it should have high reflecting power. It must be loosely coupled to the phosphor surface in order to maintain optimum conditions for total internal reflection.

The relative merits of different diffuse and specular reflectors have been investigated by Koechlin (Koechlin 1955). Magnesium Oxide with an optimum reflectivity of 96% is among the best, while Aluminium whose reflectivity is 90%, is the best of the specular reflectors.

The feasibility of depositing a layer of MgO by burning Magnesium ribbon in air was investigated, but was rejected owing to the difficulty of depositing a layer of known and uniform thickness on the phosphor surface. Instead a thin layer of Aluminium evaporated on to a VYNS resin film and subsequently placed over the surface of the phosphor was used.

4.2.2. Preparation of Film.

VYNS resin, in solution in cyclohexanone was dropped on a clean water surface and drawn out to form a film according to the procedure recommended by Yaffe (Yaffe 1962); the film was picked off the surface with a wire frame. The film was made as thin as possible consistent with the need for it to withstand the heating and bombardment involved in the deposition of the Aluminium.

Edwards coating Unit (Type No. 12 E 115) was used for the deposition. Short pieces of Aluminium wire were hung in loops from a zig-zag of tungsten wire of $\frac{1}{2}$ mm diameter. A current of about 25 amps was passed through the wire to evaporate the Aluminium. The frame supporting the film was placed 15 cm vertically above the coil and a mask was used to control the time of deposition. The whole system was at a pressure of 10^{-4} mm of mercury. Care had to be taken to adjust the rate and duration of the evaporation so that the bombarding atoms did not damage the film but formed a uniform shiny surface.

4.2.3. Estimation of Film Thickness.

A rough estimate of the thickness and therefore of the stopping power of the film was obtained by a modification of a method used by Enge and Wahlig (Enge 1953). The isotope

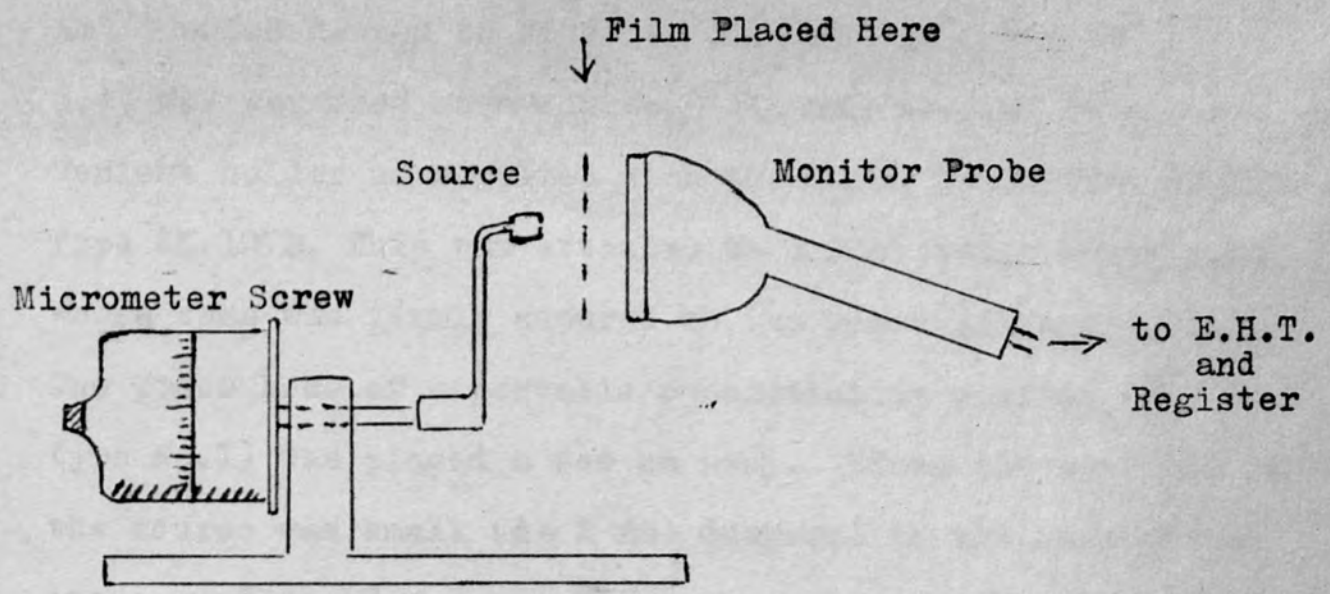

4.2. Diagram of Apparatus used to Estimate Thickness of Reflector Film.

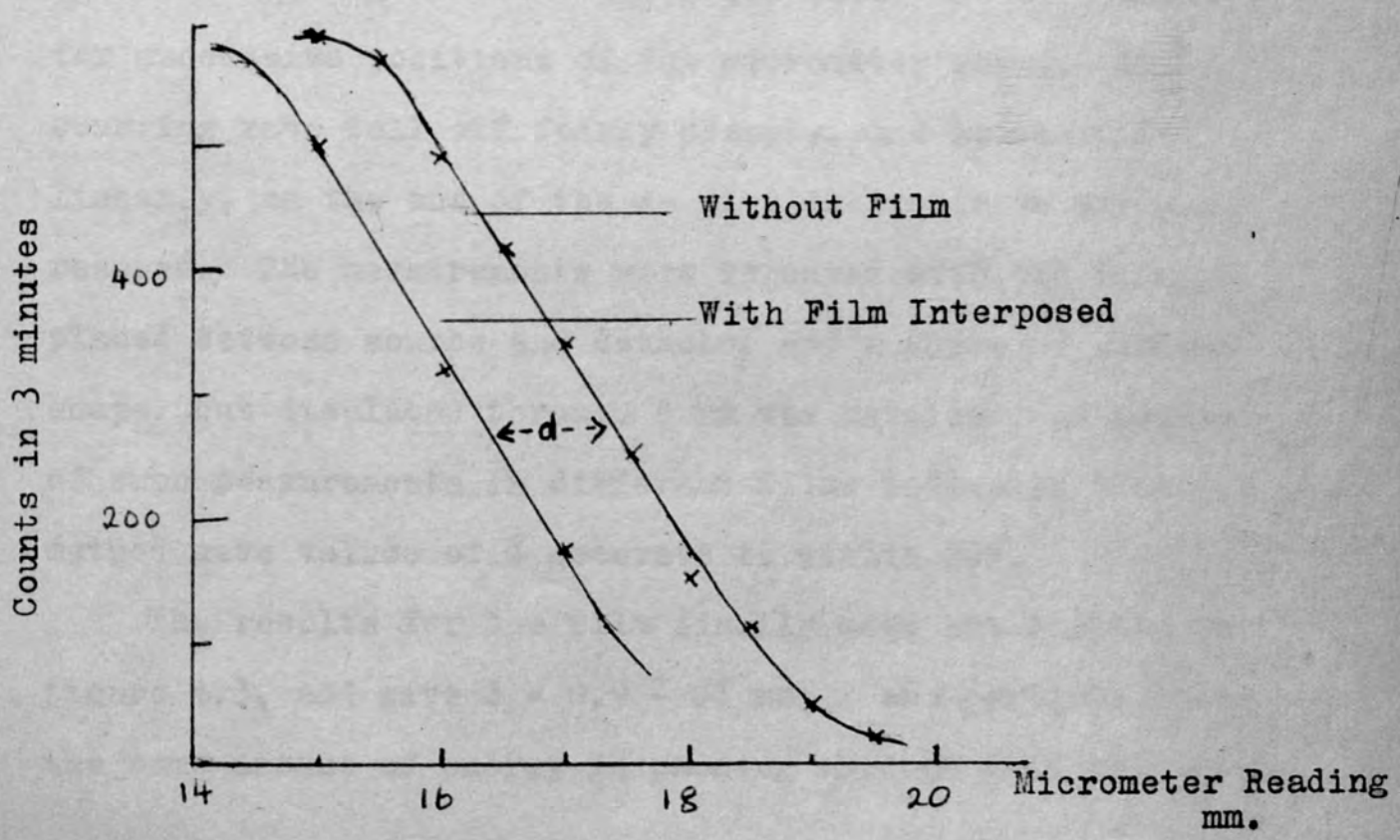

Fig. 4.3. Variation of Counting Rates as Source was Moved Towards Detector.

Am^{241} which decays to Np^{237} by emitting an α-ray of 5.47 MeV was used as a source. It was mounted on a convenient holder as supplied with the Panax Demonstration Kit Type SK.107B. This was attached to a micrometer screw head whose base was firmly secured to the bench (figure 4.2). The probe head of a portable contamination monitor (E.M.T. type No.1) was placed a few cm away. Since the aperture of the source was small ($d \sim 2$ mm) compared to the area of the probe surface (7 x 7 cm) there was only a small change in the solid angle of collection as the source was moved through a distance of 1 cm or so. The monitor had a mechanical register which could count up to about 200 α- particles per minute. Particles were counted for intervals of 3 minutes for successive positions of the micrometer screw. The counting rate fell off fairly sharply, and approximately linearly, as the end of the α- particle range in air was reached. The measurements were repeated with the film placed between source and detector and a curve of similar shape, but displaced through d mm was obtained. A series of such measurements in different films indicated that the method gave values of d accurate to within 20%.

The results for the film finally used are plotted in figure 4.3. and give $d = 0.9 \pm .1$ mm; an α-particle loses the same amount of energy in passing through this thickness

of air as in traversing the film. If the difference in mean atomic weight of the film and of air is sufficiently small so that its effect on their relative stopping power may be ignored for the present approximate calculation, then the surface density of the film in milligrams per square cm can be assumed equal to that of d mm of air. Thus $t = 0.09 \times .0012 = .11 \pm .01$ mg cm^{-2}. This, in conjunction with graphs based on experimental observations, enables the energy loss of electrons of known energy on traversing the film, to be found. For example, electrons giving rise to the 24 keV conversion line of Th.C will lose 1 keV approximately in traversing the film (Evans 1955 p.624); the relative loss decreases as the energy increases.

4.3. Cooling of the Detector Assembly.

4.3.1. Effects reported by various Workers.

Change of temperature tends to affect the behaviour both of the phosphor and of the photomultiplier.

Plastic phosphors in general show an increase in scintillation efficiency as their temperature is reduced to about 100°C below room temperature. The extent of the increase varies according to the composition of the phosphor (Birks 1964 p.338).

The effect of cooling the photomultiplier has been the subject of investigation by several workers; in general, besides the expected decrease in the thermionic noise, it leads to a change in the amplitude of the signal due to particles of a given energy. Matveer et al (Matveer 1962) present an analysis of the different results; there is considerable variation in behaviour even for tubes of the same type. In most cases the temperature coefficient is negative when the wave-length of the incident light $\lambda < 4000$ Å but positive for $\lambda > 5000$ Å. From this dependence of the sign of the temperature coefficient on λ, Matveer deduces that the photo-cathode must be at least partly responsible for the effect. Both Kinard (Kinard 1957) and Laustriat and Coche (Laustriat 1958) maintain on the contrary that the temperature effect is largely due to the dynodes, and support their contention with measurements taken when different parts of the total photomultiplier assembly were cooled separately. The increased sensitivity of the dynode system as the temperature is lowered is probably due to an increase in the mean free path of the secondary electrons which thus lose less of their energy before reaching the surface (Dekker 1958 p.440). The magnitude of the effect varies greatly between tube types and even between different tubes of the same type. Laustriat and Coche report a value of .7% per ^{o}C for the DuMont tube

type 6292; this would give rise to a considerable increase in pulse amplitude if the tubes were cooled to the temperature of solid CO_2. The need for good temperature stability is emphasized. In general slight fluctuations will not effect the behaviour of the system as a detector; for low energy pulses, however, when the discrimination level between noise and signal pulses is finely set, such fluctuations might well be a serious handicap.

4.3.2. Experimental Arrangement.

The photomultiplier of the small spectrometer was cooled by circulating methylated spirits at $-78^{o}C$ through copper piping which surrounded the brass cylinder in which it was housed. (Figure 4.4).

The methylated spirits was circulated by means of a gear pump and was cooled in a reservoir of solid CO_2 in methylated spirits contained in a 5 litre dewar flask. A spiral consisting of 6 turns of copper tubing of $\frac{1}{2}$" diameter served as the heat exchanger. The pump was driven by a d.c. motor and the speed could be altered by adjusting the d.c. voltage applied to the motor in the range of 3-9v. An insulating flange of paxolin separated the cooled portion of the detector from the electronics, thus preventing condensation.

The temperature of the liquid emerging from the system

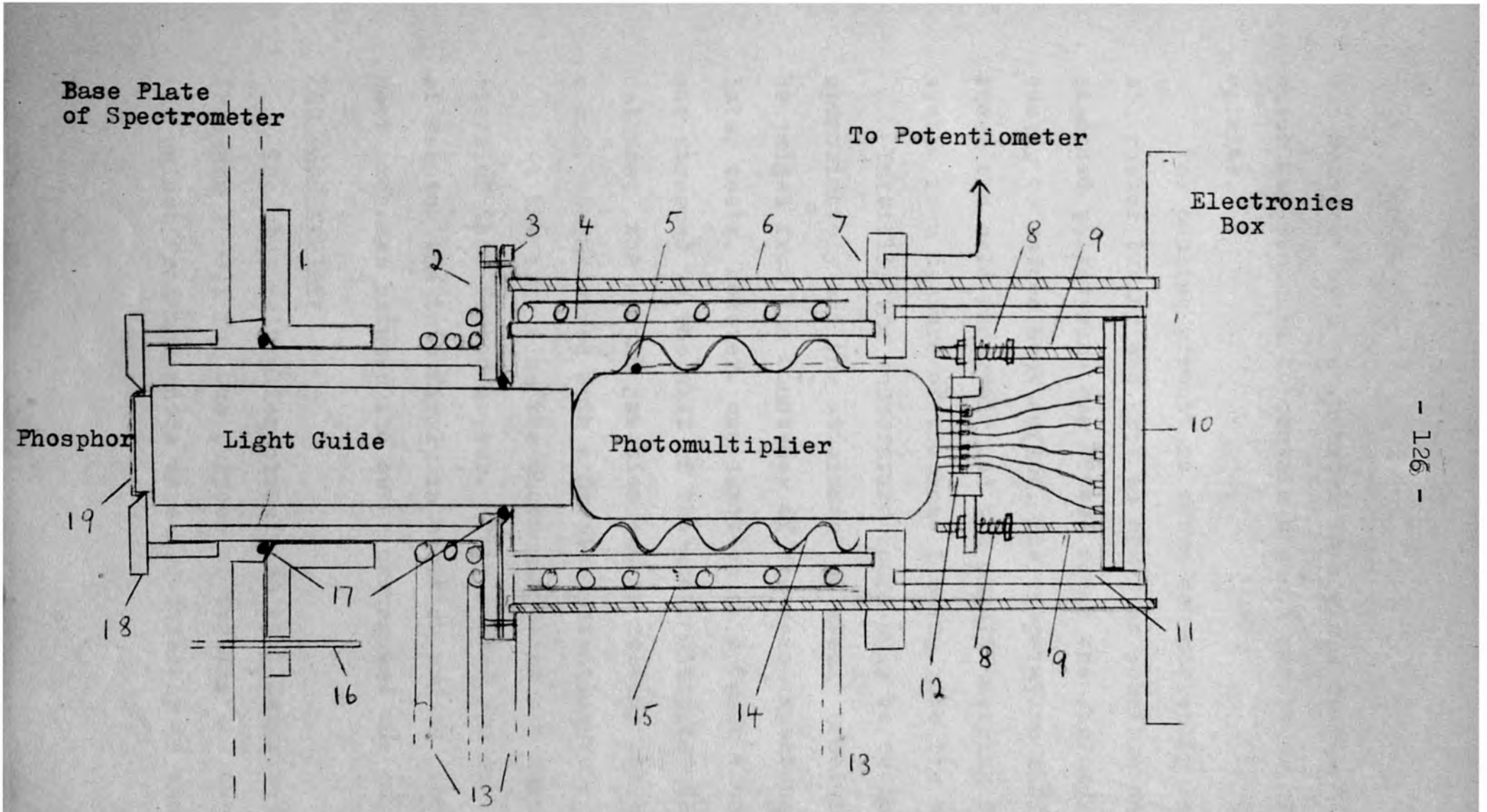

Fig. 4.4. Detector Mounting for Small Spectrometer.

1. Flanged Sleeve
2. Brass Tube
3. Brass Ring
4. Brass Tube
5. Thermocouple
6. Studding
7. Paxolin Disc
8. Spring
9. Studding
10. Photomultiplier Base.
11. Brass tube
12. Photomultiplier socket.
13. Copper Pipe
14. Fluted Cu.Support
15. μ-metal shield.
16. Control Rod for sli
17. O Rings
18. Knife Edge Support for Phosphor.
19. Reflecting Film.

was measured by a thermometer in a glass double-U tube, which was designed to contain a small reservoir of methylated spirits.

The cooling circuit is shown schematically in figure 4.5. All rubber tubing was kept as short as possible and some expanded polystyrene was fitted round the photomultiplier casing to reduce heat inflow. The temperature difference between the cold reservoir and the liquid emerging from the system is a measure of the heat flowing into the system.

Initially the temperature could only be estimated approximately and the attainment of steady conditions had to be judged from the constancy of the noise spectrum. For the later tests, however, one junction of a Cu-Co thermocouple was strapped to the side of the photomultiplier near the cathode; the second junction was in melting ice and the e.m.f. was measured with a Cropico potentiometer.

At the same time the photomultiplier was surrounded by a piece of thin fluted copper. This served the dual purpose of keeping the tube firmly in position and of improving the heat exchange between the outer casing and the tube.

The Electronics.

The photomultiplier circuit is that described by Freeman (Freeman 1960); for the purpose of testing the cooling system the pulses from the anode were fed directly to the cathode

Fig. 4.5. Schematic Diagram of Cooling Circuit.

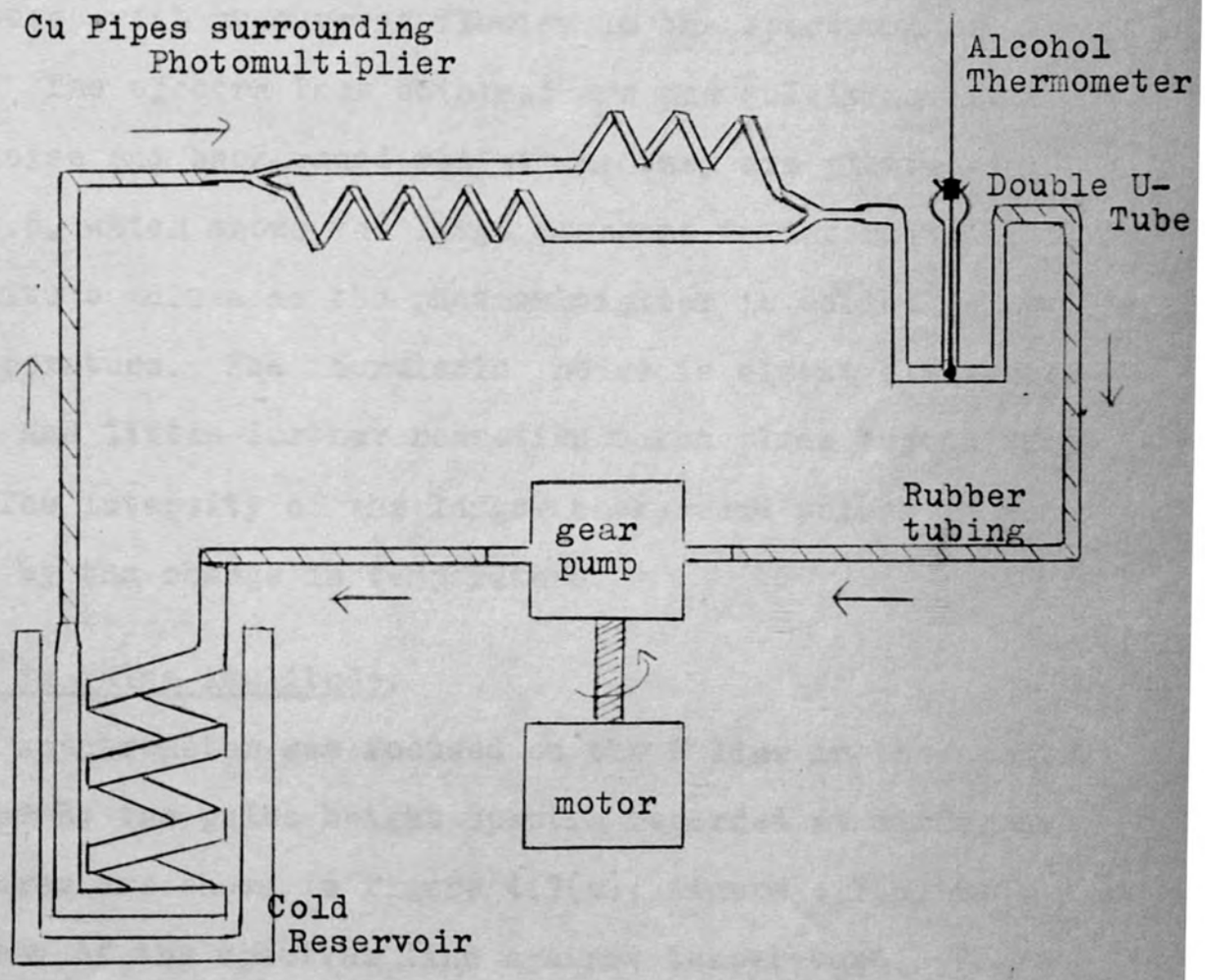

Methylated Spirits circulates in Direction indicated by Arrow.

follower and thence to a phase inverter before being fed to the Intertechnique Pulse Height Analyser, which recorded the pulse height spectrum directly.

4.3.3. Results of Cooling the Photomultiplier.

Pulse height spectra were recorded at several different temperatures with no current flowing in the spectrometer winding. The spectra thus obtained are due solely to instrumental noise and background radiation; they are plotted in Figure 4.6, which shows the large decrease in intensity of the low amplitude pulses as the photomultiplier is cooled below room temperature. The thermionic noise is almost eliminated at $-15^{\circ}C$ and little further reduction takes place beyond this point. The intensity of the larger background pulses is not affected by the change in temperature.

Increase in Pulse Amplitude.

The spectrometer was focused on the F line in the spectrum of Thorium B; the pulse height spectra recorded at different temperatures are shown in figure 4.7(a); figure 4.7(b) is a plot of the peak of the spectrum line against temperature. There is a marked increase in pulse height as the tube is cooled, which amounts to approximately 50% over the range + 20 to $-50^{\circ}C$.

There is evidence of a deterioration in the energy

Fig. 4.6. Noise Spectrum for Photomultiplier at different Temperatures.

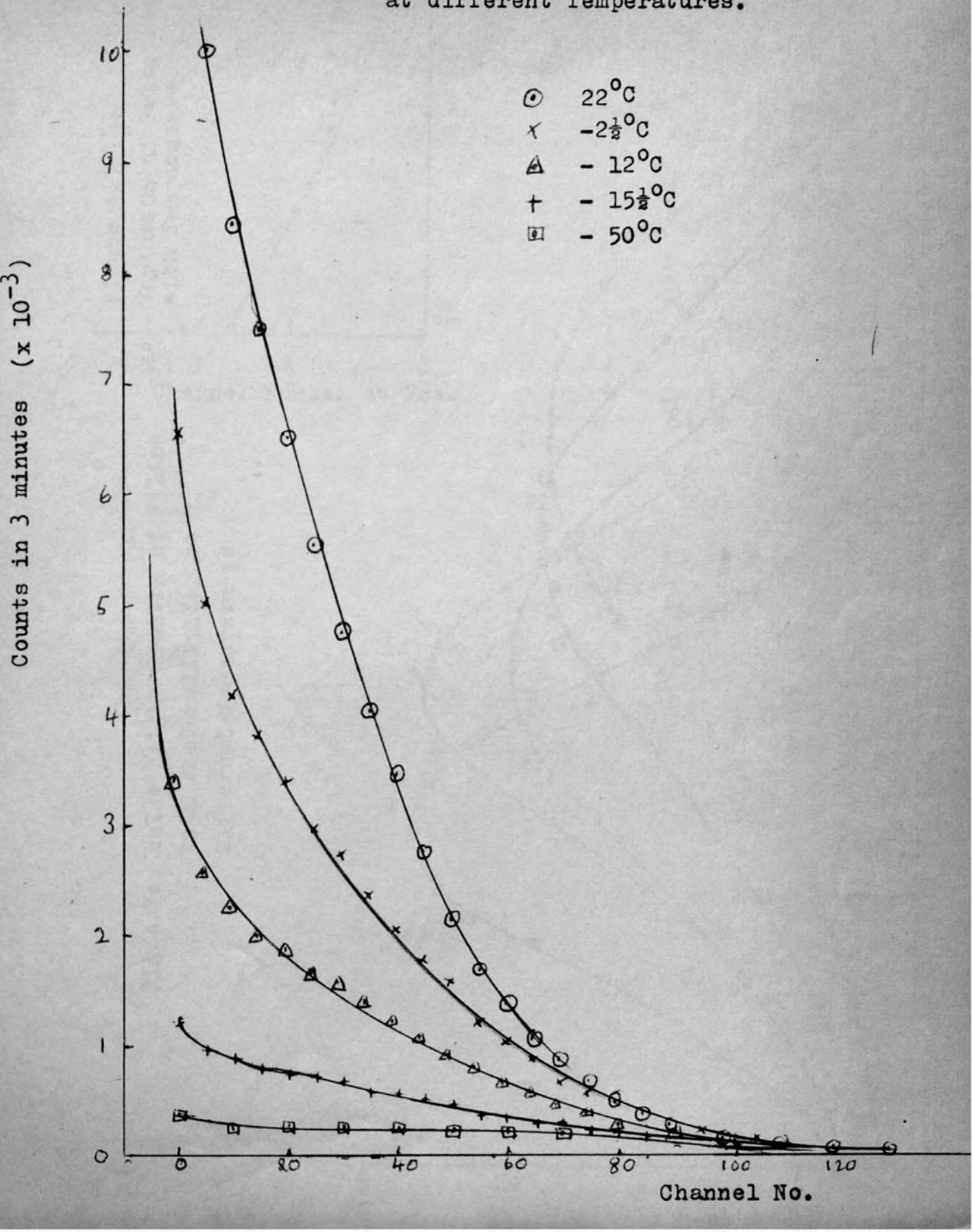

Fig.4.7a. Pulse Height Spectra of F Line With Photomultiplier at Different Temperatures

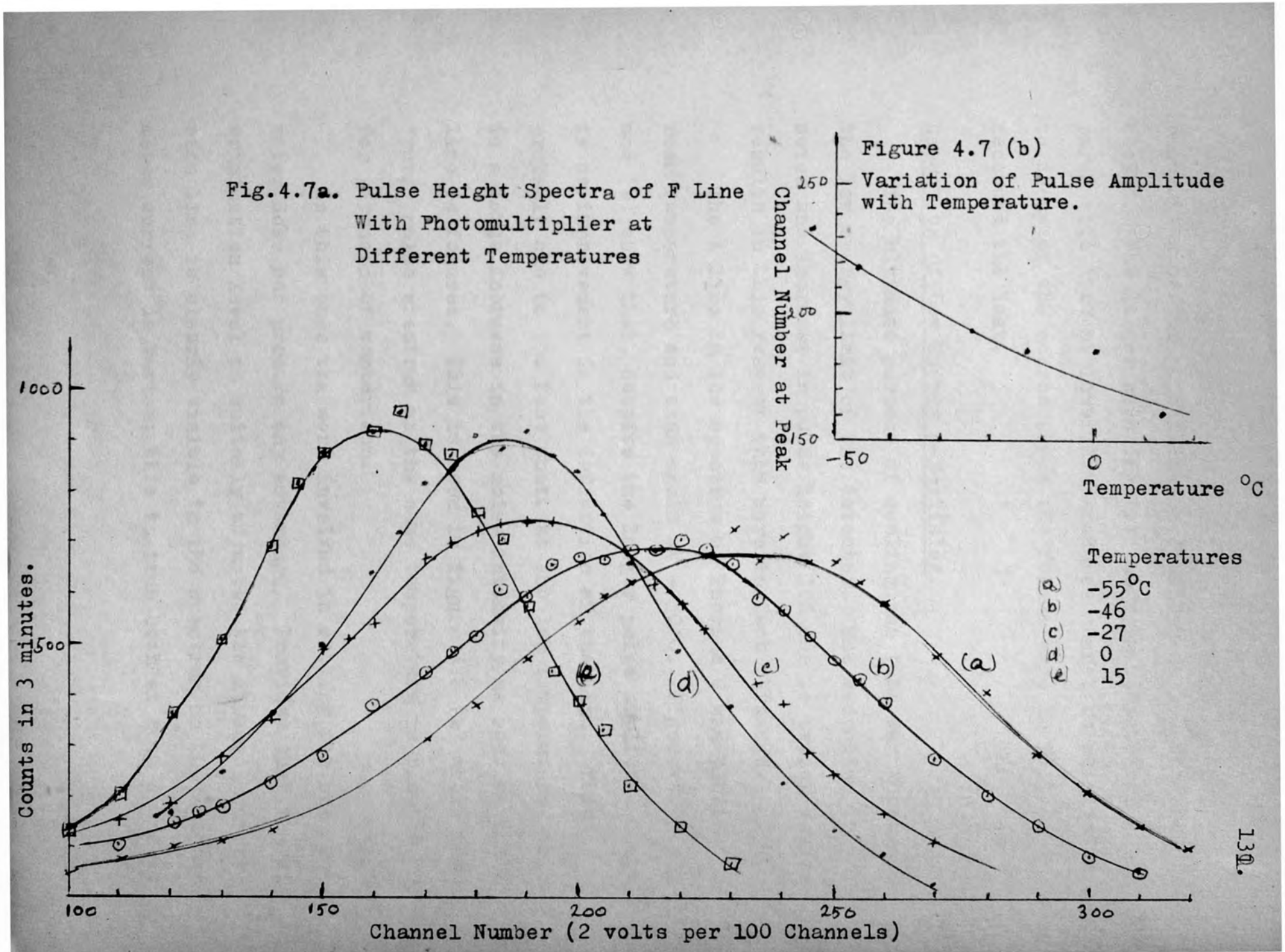

Figure 4.7 (b)
Variation of Pulse Amplitude with Temperature.

resolution of the scintillation detector as the tube is cooled. The larger counting rate at room temperature compared with that at lower temperatures cannot be attributed to decay of the source since the former were in fact recorded the last.

Detection of Low Energy β-Particles.

The ultimate purpose of cooling the tube was to extend the low energy limit of the detector. The reduction in noise and increase in pulse height led one to expect better results in this respect than were in fact obtained.

The A line in the spectrum of Thorium C was plotted at room temperature and then again at - 50°C. Figures 4.8 (a) and (b) show that, despite the larger pulse amplitude there is no improvement in the definition of the line. This is probably due to the fact that, at the low temperature, there is a large increase in the noise intensity as soon as the A line is focused. This is seen in figure 4.8 (b) where the "pure" noise spectrum at the same temperature is plotted for purposes of comparison.

In this case the work involved in cooling the spectrometer does not procure any advantage. Provided that the discrimination level is suitably adjusted the strong A conversion line is clearly visible in the spectrum as the spectrometer current is varied; this is true both at room temperature

Fig. 4.8. Pulse Height Spectra due to the A Line (24 keV) compared with the Noise Spectra

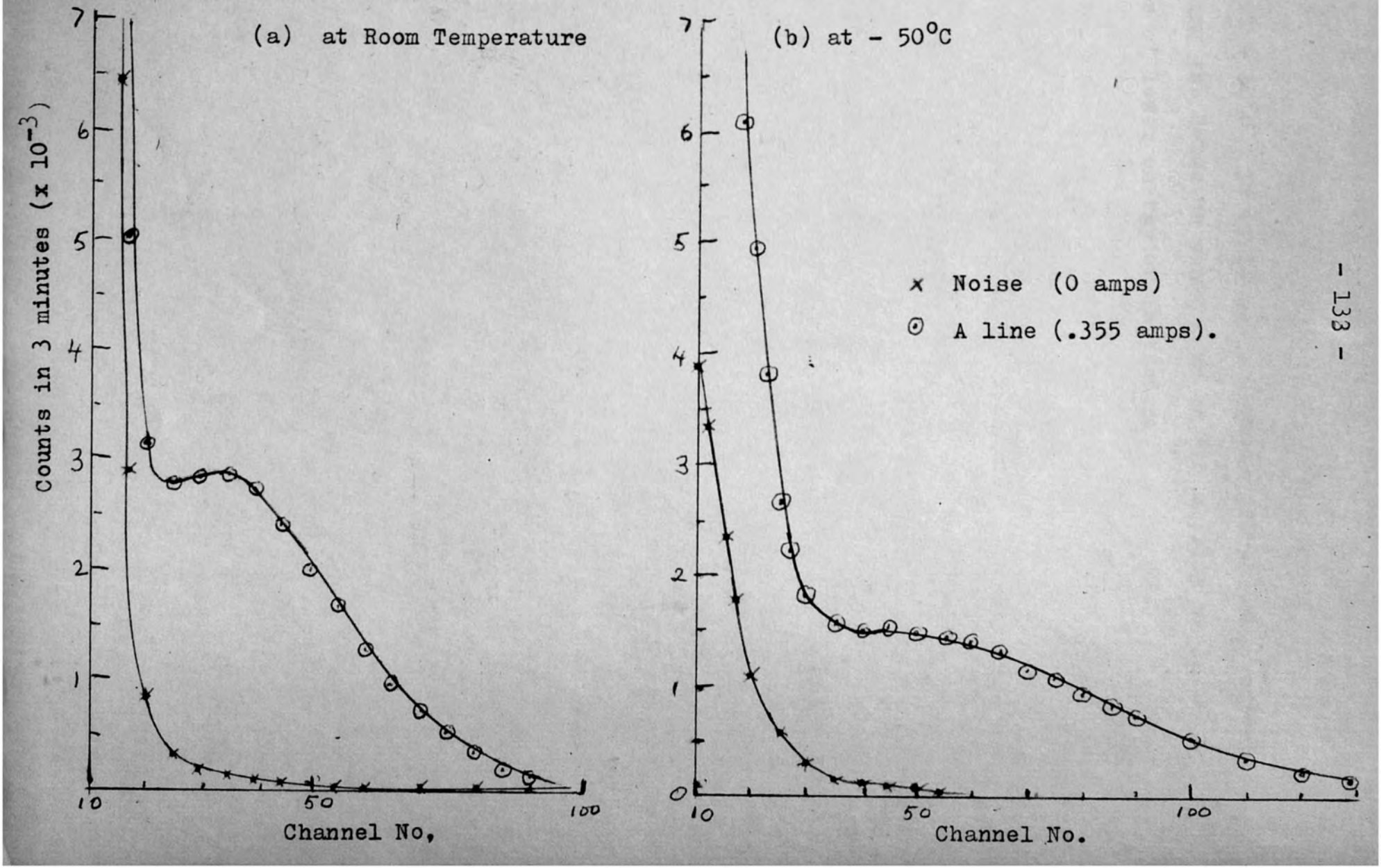

and at - 50°C. It would be interesting to see what effect cooling the detector would have on its ability to detect lines of lower energy or intensity.

CHAPTER 5

Coincidence Circuits

5.1. General Considerations.

5.1.1. Useful Definitions and Concepts.

Coincidence circuits are used in the identification and study of coincident or quasi-coincident nuclear events such as occur for example when an excited nucleus decays to its ground state in several stages by emitting successive "coincident" γ-rays of different energy, or when the de-excitation of a nuclide follows close on the emission of the β-rays which accompanied its formation. The circuits are such that there is an output pulse every time two or more pulses arrive at the input within a short interval of time known as the resolving time 2τ. The circuits are characterised by their resolving time which is in general made as short as possible. Circuits with small resolving times give more precise information and have a lower background of random events. There are in general $2n_1n_2\tau$ such random coincidences per second due to particles which happen by chance to arrive at the particle counters within 2 seconds of each other; whereas true coincidences are the result of a particular pair of transitions occurring within the same

nucleus. The aim is always to make the ratio of true to random coincidence as large as possible; n_1, n_2 are the number of particles per second registered by each of the counters.

The effective resolving time of a coincidence system may be taken as the full width at half maximum height of its prompt curve. The prompt curve is a plot of the number of recorded coincidences against the delay, as the artificial delay between the two incident pulses, whose time separation is known to be much less than the resolving time, is varied. Ideally the prompt curve should be rectangular in shape; in practice time uncertainties at various points in the system give the curve a bell-shaped profile.

When, as is frequently the case, the pulses are derived from a scintillation phosphor and photomultiplier tube a lower limit is set to the width of the prompt curve by the decay time of the phosphor and the speed in transit time of the electrons in the photomultiplier. Bell (Bell 1965) has shown that the limiting value of τ for such a system, using the fastest available phosphors, and multipliers is given by $2\tau = \frac{2.7}{\sqrt{E}} \times 10^{-10}$ sec. where E is the energy lost in the phosphor in Mev. For optimum time resolution the coincidence circuitry should be actuated by approximately the first 25% of the integrated output pulse. Semiconductor

devices, because of their larger electron yield, are theoretically capable of better time resolution but technical difficulties have inhibited its realisation.

5.1.2. Types of Coincidence Circuit.

Various types of coincidence circuit have been designed to meet different experimental requirements. Sometimes one pulse is used to open a gate which then allows the second pulse to pass through. Alternatively valves or transistors are used in the equivalent of parallel or series switch arrangements. In the parallel arrangement exemplified by the Rossi coincidence circuit current flows through a load resistor unless both switches are operated by the arrival of simultaneous pulses. The rapid fall in current gives rise to an output pulse. In the series arrangement, first used by Bothe, current only flows when both "switches" are closed simultaneously. Typically opening and closing the valve or transistor "switches" is achieved by applying the input pulse to suitably biased grid or base.

A particularly simple type of circuit is that which comprises the three fundamental operations, Limit, Add, Discriminate. The input pulses are standardized using pulse shapers or limiters, the identical pulses are then added and a discriminator which may be a biased diode is set so that single pulses will be rejected but double or sum pulses will

be accepted. Such a system which will be referred to as the Adding Type of coincidence circuit is used in the fast coincidence channel of the well-tried Bell and Petch Fast-Slow Coincidence system.

This system comprises fast and slow channels; the arrangement is shown schematically in fig. 5.1. In the slow channel pulse height analysers are used to isolate monoenergetic pulses due to particles of the required energies; the fast channel singles out particles arriving within $\pm\tau$ seconds of each other. A count is registered only if both conditions are satisfied within the much larger resolving time of the triple slow coincidence unit. In this way time fluctuations associated with the energy analysis of the pulses are not allowed to affect the time resolution of the system and fast coincidences other than those due to the required pair of transitions are rejected. Also the probability of a random coincidence occurring is greatly reduced.

Such a system is particularly useful when, as is the case with a scintillation counter, the whole spectrum of radiation from the source is present at the counter. When, however, electrons of the required energies are pre-selected in a magnetic spectrometer the chief reason for the slow channels is removed. There will be a number of random coincidences occurring due to noise in the counters but this can be reduced

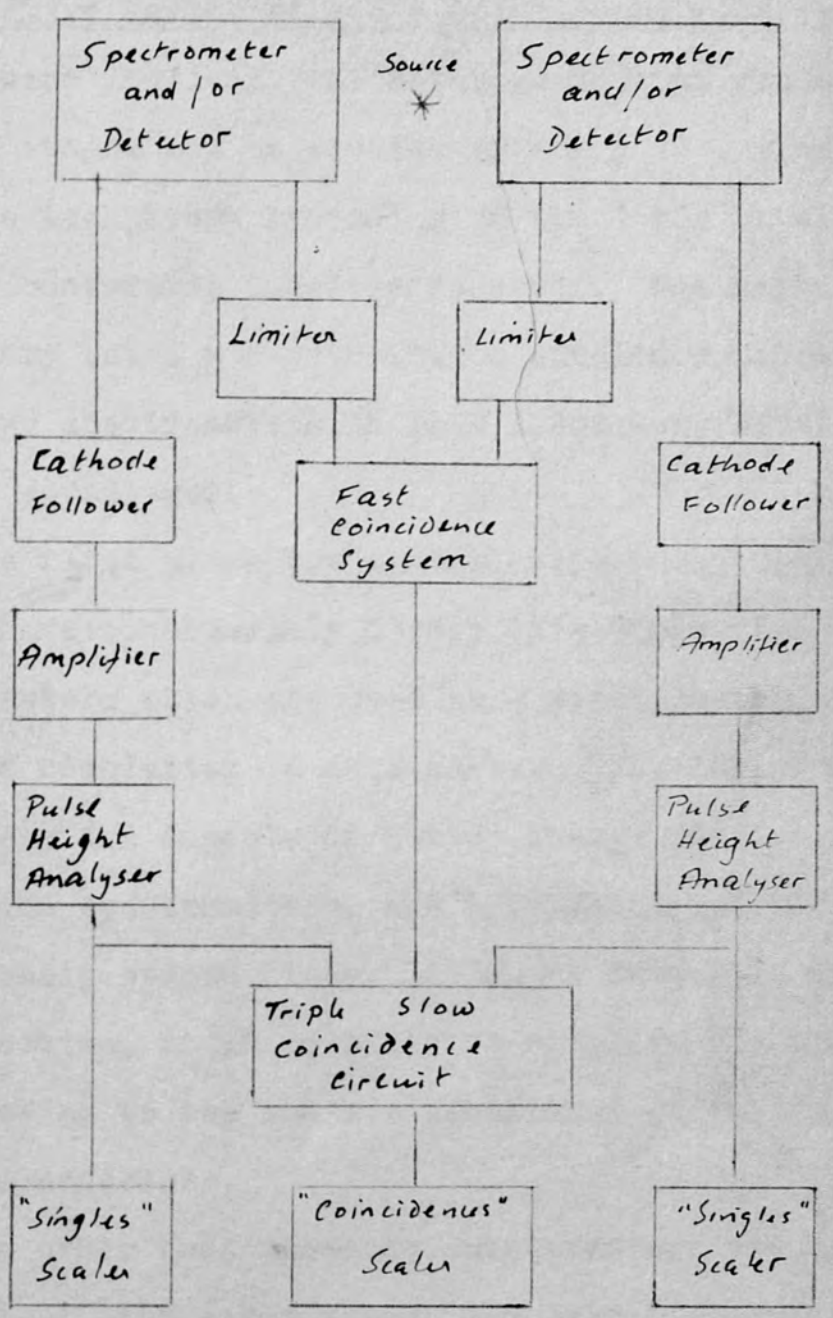

Fig.5.1. Principle of Bell & Petch Fast-Slow Coincidence System

if there is a small discriminating bias at the input to the limiters.

5.1.3. Relative Merits of $\beta - \beta$ Coincidence Measurements.

Processes involving the de-excitation of nuclei in successive stages may be studied by $\gamma - \gamma$, $\beta - \gamma$ or $\beta - \beta$ coincidence techniques according as the γ ray or one of its equivalent conversion lines is observed. The methods are complementary but $\beta - \beta$ coincidence studies which are possible with the two spectrometers in this laboratory offer several particular advantages.

In the first place the best plastic phosphors which are available have considerably faster life times than the sodium iodide phosphors which are used in γ spectrometry, so that better time resolution is obtainable. Further, magnetic spectrometers are capable of better energy resolutions than scintillation spectrometers, and this facilitates the separation of closely spaced lines. Also, as described in the previous section, it is possible to simplify the electronic circuitry owing to the smaller likelihood of random or unwanted coincidences.

On the other hand magnetic spectrometers are considerably less efficient than other types, and even a moderate increase in efficiency usually implies a considerable worsening in energy resolution. This generally leads to a low coincidence

counting rate with correspondingly high statistical inaccuracy. Care must be taken in the spectrometer design to ensure that there is minimum flux leakage from either spectrometer which would disturb the electron paths in the other.

If at least one of the counters detects electrons, the system can be applied to coincidences between the continuous β spectrum and an internal conversion line. It is not, of course, necessary that the β-spectrometer should be of the magnetic type.

5.1.4. Application of Coincidence Techniques.

The usefulness of coincidence techniques extends far beyond the field of β-spectrometry. Some applications of particular interest in this field are considered here.

Identification of lines. Certain weak lines, whose presence is masked by the continuous β-spectrum are more clearly revealed when seen in coincidence. Thus, for example, a γ-ray in the spectrum of ^{61}Cu was first detected in coincidence and only subsequently discovered in the straight-forward γ-spectrum after careful substraction of the background (Wapstra 1965).

Recognition of Cascade Processes. Coincidence measurements also permit recognition of cascade processes, so enabling the relationship of different transitions in a decay scheme to be worked out.

Measurement of Half Lives

The half lives of short lived excited states can be measured by the delayed coincidence method. A time resolution curve is plotted both for coincident radiation (prompt curve) and for the radiations under consideration; the second of these is "delayed" relative to the first by an amount depending on the life-time of the intermediate state. The prompt curve is displaced or distorted and the change enables the life-time to be estimated. The lower limit to the life-times, which can be measured in this way, is set at about 10^{-11} sec by the best time resolutions available.

A valuable modification of this technique is permitted by the use of a Time-to-Amplitude Convertor. This device gives an output pulse whose amplitude is proportional to the time separation of the input pulses. Thus, if the output is fed into a multichannel pulse height analyzer the time resolution curve may be recorded directly.

5.2. Further Consideration of Adding-Type Coincidence Circuit.

5.2.1. Summary of Required Properties.

It is worth while to set down the properties which the components of the Adding-Type Coincidence Circuit should possess ideally; this sets a target for the construction of such a system, even if as discussed later, a compromise has

to be reached in practice.

The Limiters. The limited pulses should be equal in shape and magnitude; they should be independent of the size and frequency of the input pulses. The pulses should be as narrow as possible and the time interval between the arrival of the input pulse and the production of the standardized output pulse should be reduced to a minimum. This time interval should be independent of the size of the input pulse. There should be a facility for discriminating against noise pulses.

Adder and Discriminator. The discrimination level should be adjustable but it must be very stable. Cables and circuits should be properly matched so that there is minimum interference and reflection at the T-junction where the pulses are added. It is desirable that the final output pulses should be of suitable shape and size to trigger the scaler directly.

5.2.2. Effect of Pulse Shape on Time Resolution.

The shape of the "limited" pulses affects the time resolutions of the Adding Type Coincidence Circuit in a straightforward way.

If the limited pulses are perfectly rectangular of width 2τ and amplitude V then the arrival of a second pulse within $\pm\tau$ seconds of the first gives rise to a "sum" pulse

Fig. 5.2. Pulse Shape and Time Resolution.

Shows summing of (a) square, (b) triangular pulses at T-junction. The maximum sum-pulse depends on the time-interval between individual pulses; different intervals are simulated by locating T-junction at different points.

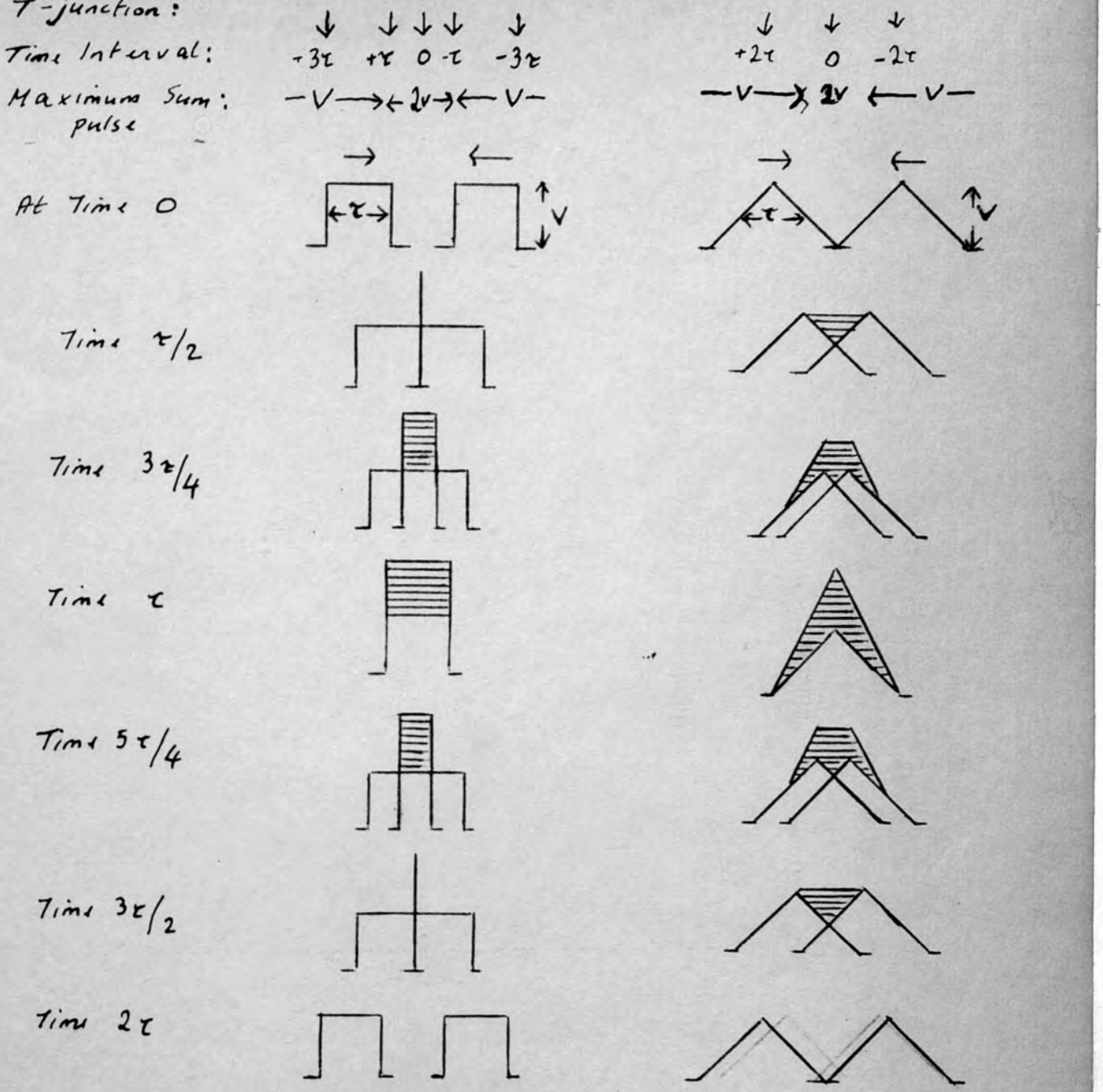

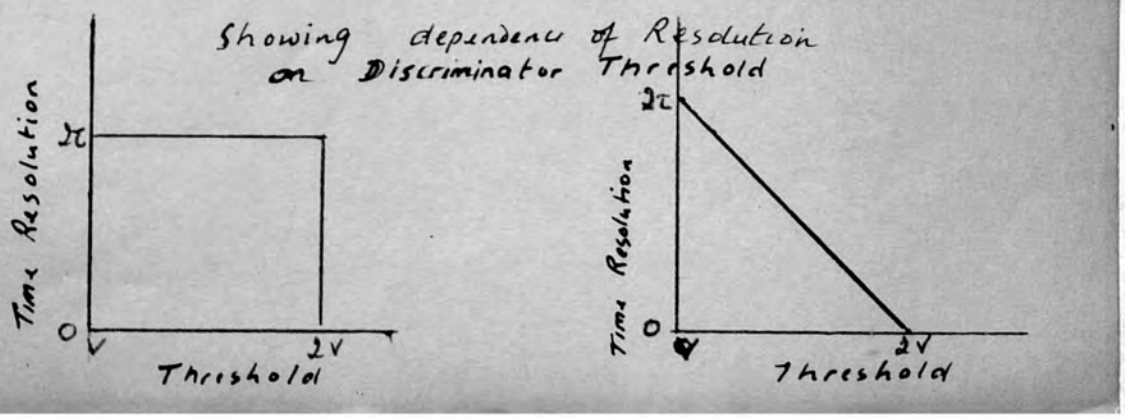

of amplitude 2V. If the discrimination level is set anywhere between V and 2V coincidences are recorded and singles rejected. The resolving time 2τ is determined solely by the width of the pulses.

In practice the pulses have finite rise and fall times and are never perfectly rectangular. In the particular case when pulses are shaped by a differentiating circuit they are more nearly triangular in shape. The amplitude of the sum pulse then depends on the time separation of the pulses, rising gradually from V, when there is an overlap of not greater than t seconds, t being the width of the pulse at half height, to 2V when the pulses are perfectly coincident. Thus by increasing the discrimination level the resolving time may be reduced below that obtainable with rectangular pulses of comparable width. This method of adjusting the resolving time is a useful alternative to that which involves narrowing the pulses.

The relation of time resolution to pulse shape is illustrated schematically in fig. 5.2.

5.3. Replacement of Coincidence System

5.3.1. Previous Coincidence System.

Previous systems used in this laboratory have been modifications of the Bell and Petch Fast-Slow Coincidence arrangement, using pentode valves as the limiters and a

reversed biased diode as discriminator. The limited pulses were shaped by means of clipping lines and their width could be altered by varying the length of the line.

Freeman (Freeman 1960) studied $\beta - \gamma$ coincidences; he detected slow coincidences between events in the fast coincidence channel and those in a single slow channel in which γ-rays of the required energy had been selected. The heights of the pulses, after discrimination at the diode in the fast channel were in the ratio 8:1 for coincident to non coincident pulses respectively, and further discrimination was therefore necessary. The minimum resolving time obtained was $2\tau = 8$ nanoseconds for pulses of 3 ns width.

Michelson (Michelson 1961) studying $\beta - \beta$ coincidences used a similar system but omitted the slow coincidence unit entirely. She used 10 ns clipping cables which she found gave the optimum ratio for coincident to non-coincident pulses but with correspondingly poorer time resolution.

5.3.2. Simplified System using Avalanche Transistors.

The coincidence circuitry described by Jackson (Jackson 1964) using avalanche transistors appeared to offer advantages over the existing system, not least in its extreme simplicity.

Avalanche transistors are operated at high collector voltages; they usually have narrow and lightly doped base

regions so that in the quiescent state the collector depletion layer extends nearly to the base-emitter junction. If holes are ejected from the emitter into the base they quickly reach the collector depletion layer, where they are accelerated under the large field; they produce further electron-hole pairs on collision with atoms in the lattice and an avalanche of charge quickly reaches the collector, causing a rapid rise in potential. A positive pulse with a very fast rise time is transmitted across the capacitor C. This pulse is differentiated in the practical circuit to give a narrow clipped pulse whose width depends on the chosen values of R and C. (see fig. 5.3). The base is positively biased to prevent self-oscillation; on applying a negative signal of sufficient magnitude holes are injected into the base region and this initiates the avalanche.

Three such transistors with their associated circuitry form the complete coincidence unit. Two of them serve as limiters; the third which acts as a discriminator is biased so that the threshold input signal is above that provided by the pulses from a single limiter. Unlike the diode discriminator the transistor does not merely allow a "double" pulse to pass through but it develops a large output pulse once it has been triggered. This can be used to operate a scaler.

5.3.3. Advantages of using Avalanche Transistors.

Coincidence circuits using avalanche transistors are capable of very good resolving times as a result of the very fast output pulses.

Further since single input pulses do not give rise to any output, and there is negligible capacitative feed-through, the ratio of the heights of coincident to non-coincident output pulses is effectively infinite and no further discrimination is required. The transistors are subject to catastrophic failure but this is preferable to the slow deterioration in the performance of valves.

In practice certain factors render the performance of the system less than ideal, but it remains superior to that of the valve circuitry and very much more compact.

5.4. Construction of Coincidence Circuit.

5.4.1. Single-Stage Limiters.

The performance of the limiters whose circuit diagram is given in fig. 5.3 (a) were tested using input pulses from a Cossor Millimicrosecond Pulse Generator (Model C G 200). The output pulses, whose profile as seen on an oscilloscope (Solatron CD 1220) is given in fig. 5.3 (b), could be narrowed by reducing the value of R, though this also caused a reduction in pulse height.

Figure 5.3 (a). Circuit Diagram of Single Stage Limiters.

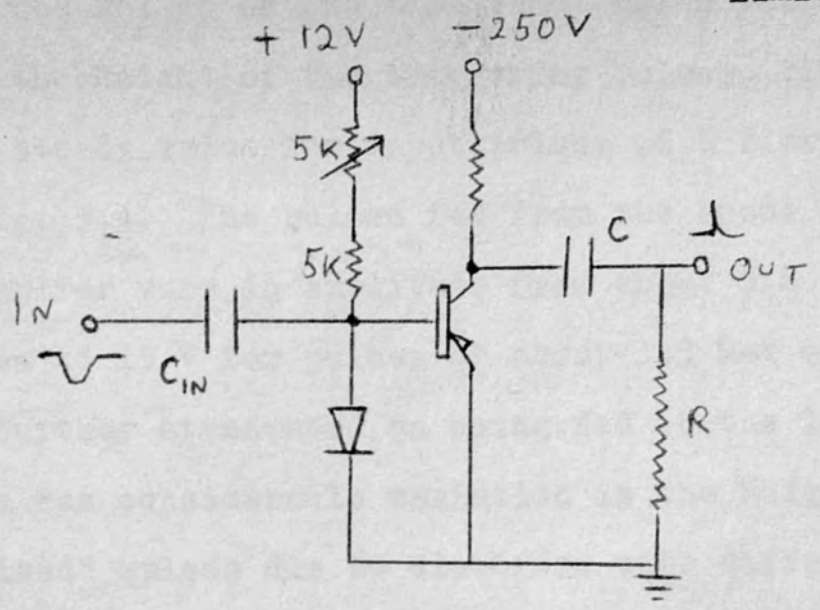

Figure 5.3 (b). Output Pulse .

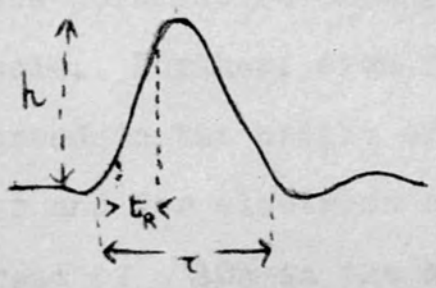

$h = .65\,V$
$\tau_R = \sim 6\,nS$
$\tau \sim 20\,nS$

Figure 5.4. V_{in}:V_{out} Characteristic of Single Stage Limiters.

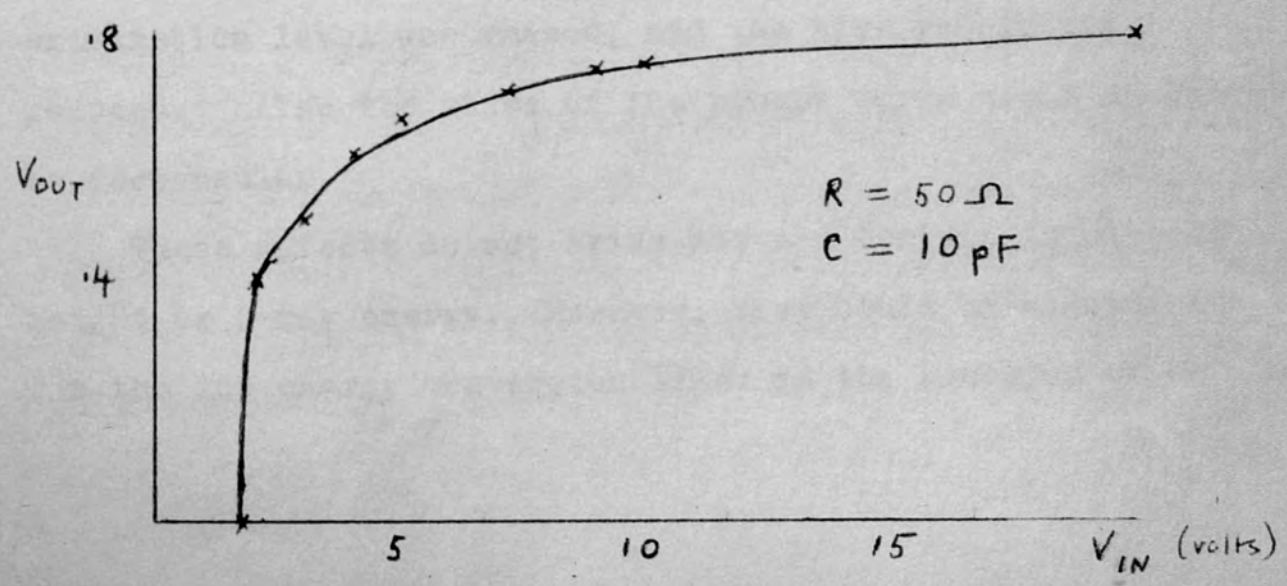

The height of the "limited" pulses was found to vary with the height of the triggering pulses, rising only slowly to a steady value for input pulses of 8 V or more, as shown in fig. 5.4. The pulses fed from the anode of the photo-multiplier vary in amplitude from about 0.8 V for noise pulses to 15 V for pulses of about 1.5 Mev energy, and they are further attenuated on being fed to the limiters. Thus there was considerable variation in the height of the "limited" pulses due to electrons with different energies in the range up to a few hundred Kev. This might be expected to cause a corresponding variation in the time resolution of the complete coincidence arrangement at a given discrimination threshold. Further, even for monokinetic electrons, there is a spread in the height of the pulses at the input to the limiter and for electrons of about 150 Kev this gave rise to a spread of 10% in the height of the "limited" pulses. The spread in pulse height would lead to a gradual falling off in coincidence counting efficiency as the discrimination level was raised, and the time resolution reduced. Also the sides of the prompt curve would no longer be rectangular.

These effects do not arise above a certain input pulse height or β-ray energy. However, they could be significant for the low energy conversion lines in the spectrum of Ce^{144}

which was to be studied and it was therefore considered desirable to try to improve the performance of the limiters in this respect.

Explanation of Effect

The variation in the height of the limited pulses is a function of the differentiating circuit at the output. The pulse developed at the collector is strictly "limited". When an input signal reaches the base, holes are injected from the emitter and these initiate the avalanche. The current flow to the collector increases rapidly until the transistor "bottoms", and thereafter it is limited by the external circuitry. The voltage at the collector rises rapidly, thus causing the avalanche to cease, but the voltage is maintained at its peak value by the discharge of holes which have been stored in the base. Increasing the input pulse height increases the number of stored holes, thus lengthening the pulse without increasing its height.

The height of the differentiated pulse, however, is determined by the rate at which the collector voltage rises; this is determined in the first instance by the initial rate at which holes are injected into the base i.e. by the magnitude of the triggering pulse. For larger input pulses other factors intervene to determine the rate of rise of the voltage pulse at the collector. Thus the rate at which the charge

is liberated will be determined by the properties of the lattice in which the electron-hole pair multiplication takes place, and the value of R and C determine the rise-time of the corresponding voltage pulse.

Such an interpretation is consistent with the observation that for a given transistor and circuit parameters the magnitude of the pulse gradually increases to assume a constant value as the input pulse is increased (fig. 5.4.). It is to be expected that by increasing the RC time constant this steady value will be attained more rapidly. This was found to be the case as shown in fig. 5.5. However, since the time constant had to be kept very short in order to maintain the narrow pulses, it was not possible to improve the limiting action in this way and some alternative solution had to be looked for.

Effect of Input Capacitance.

Since the rate at which charge is fed into the base is determined by the input capacitor it was thought that by increasing its value the performance could be improved. The result of such a change, plotted in fig. 5.6 shows that the output voltage corresponding to a given signal was indeed increased, and thus the β-ray energy below which the "limited" pulse height starts to fall was reduced.

However, even with such a large increase in capacitance

Figure 5.5. Effect of Values of R and C on V_{in}:V_{out} Characteristic of Single Stage Limiters.

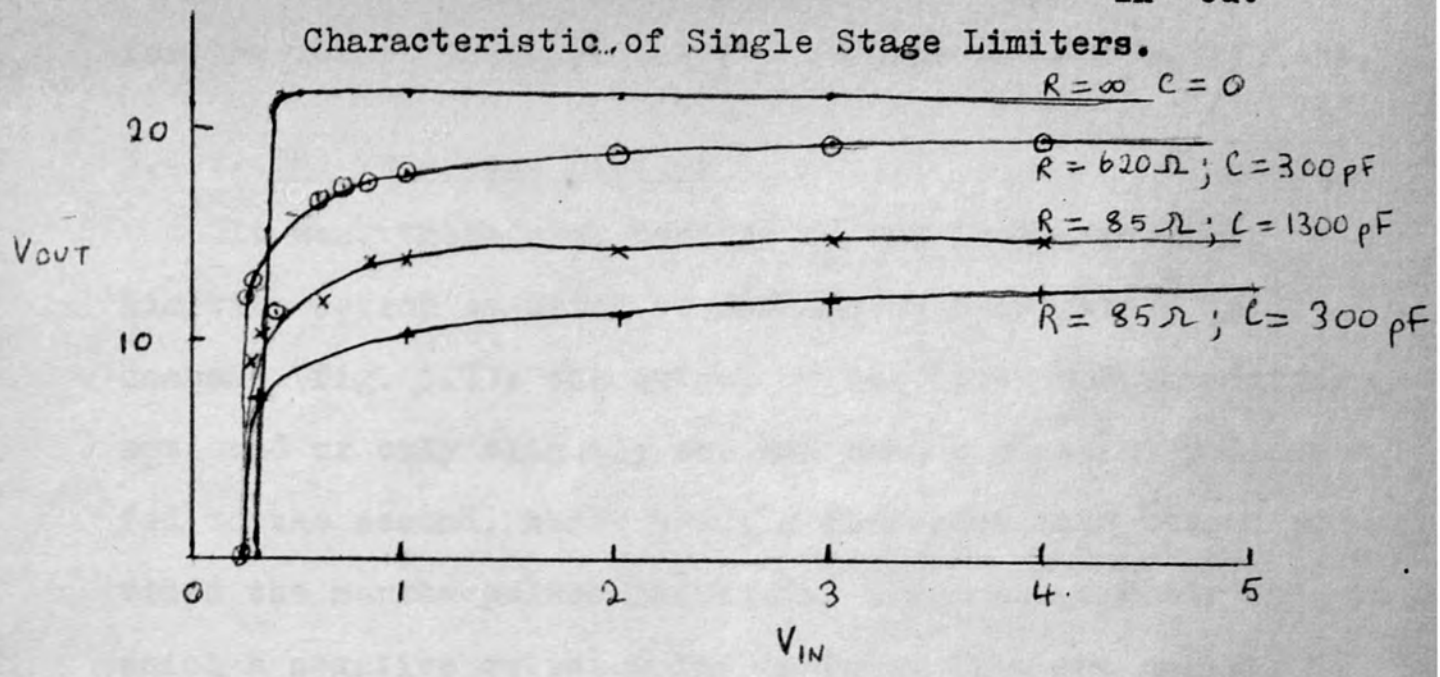

Figure 5.6. Effect of C_{in} on Characteristic of Single Stage Limiters.

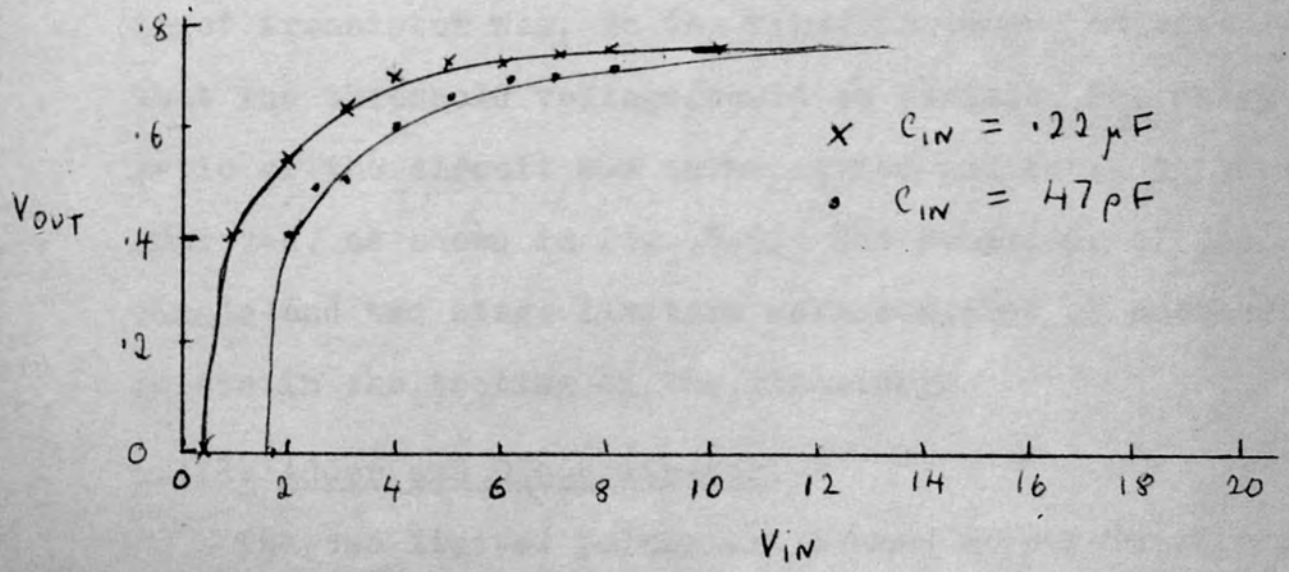

the general shape of the characteristic was unaltered and for the lowest energies the improvement was not sufficient.

5.4.2. The Two-Stage Limiter

It was, therefore, decided to try to improve the limiting action by using two avalanche transistors in cascade (fig. 5.7); the output of the first was not differentiated or only slightly so, and thus a constant pulse was fed to the second, whose sharply differentiated output provided the narrow pulses required. Since the circuit in which a negative output pulse is taken from the emitter of the transistor was found to be subject to oscillation, it was decided to use a ferrox cube transformer to invert the positive output at the collector to obtain the negative pulse required to feed the base of the 2nd transistor. The d.c. bias at the base of the 2nd transistor was just above the threshold for self-oscillation; that at the base of the first transistor was, in the first instance, adjustable so that the threshold voltage could be varied. The characteristic of the circuit was investigated and found to be much improved, as shown in fig. 5.8. The behaviour of the single and two stage limiters were compared at subsequent points in the testing of the circuitry.

5.4.3. Adder and Discriminator.

The two limited pulses are summed at a T-junction at

Figure 5.7. Circuit Diagram of Two-Stage Limiter.

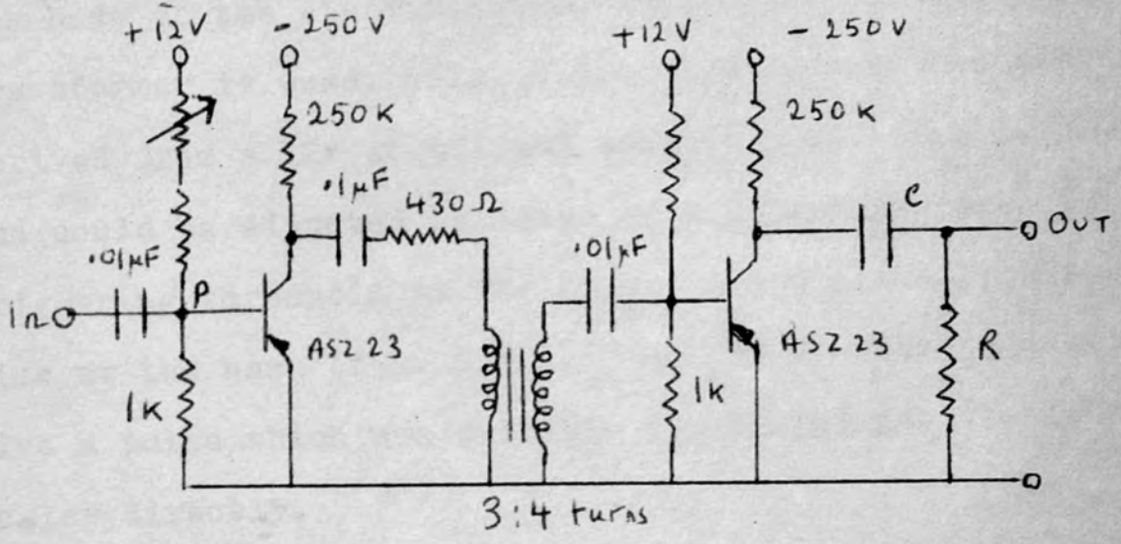

Figure 5.8. V_{in} : V_{out} Characteristic of Two-Stage Limiter for Different Bias Voltages.

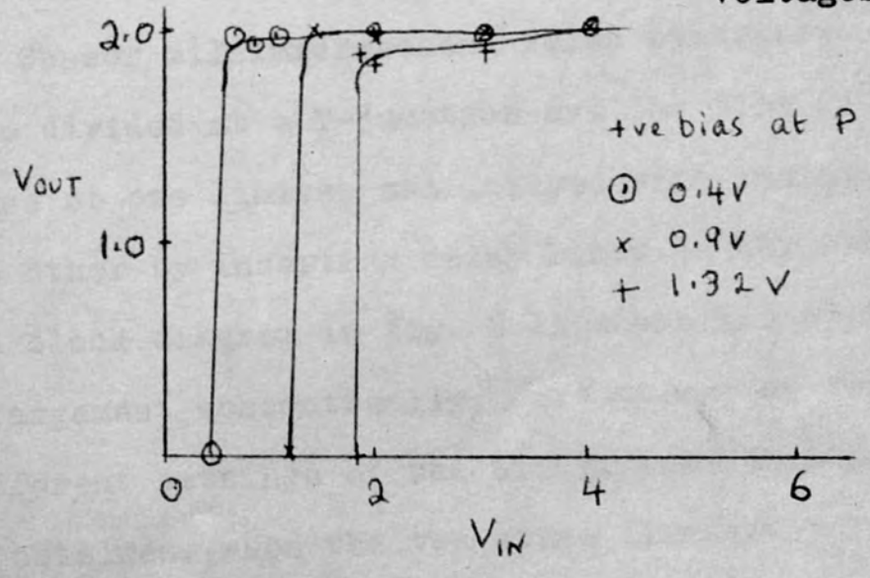

the input to the discriminator, after travelling down variable lengths of 100Ω co-axial cable.

The summed pulse must be inverted before being fed to the base of the discriminating transistor and a ferrox cube transformer is used. (fig. 5.9). The bias at the base was derived from a 12v stabilized power supply. (M.E.L. YL 6101) and could be adjusted by means of a potentiometer. The triggering threshold at the input varied linearly with the bias at the base (fig. 5.10). R and C were adjusted to give a pulse which was suitable for triggering the I.D.L. scaler directly.

5.5. Preliminary Testing of Coincidence Circuitry.

5.5.1. Using Artificial Pulses.

Initial tests of the complete coincidence circuitry were made using the standardized fast pulses delivered by the Cossor Millimicrosecond Pulse Generator. The pulses were divided at a T-junction and the time of arrival of the pulse at one limiter was delayed with respect to that at the other by inserting delay lines in the path of the pulse. The block diagram in fig. 5.11 shows the experimental arrangement schematically. Prompt curves were plotted for different settings of the discrimination bias. The curves so obtained, when the two stage limiters were used, are

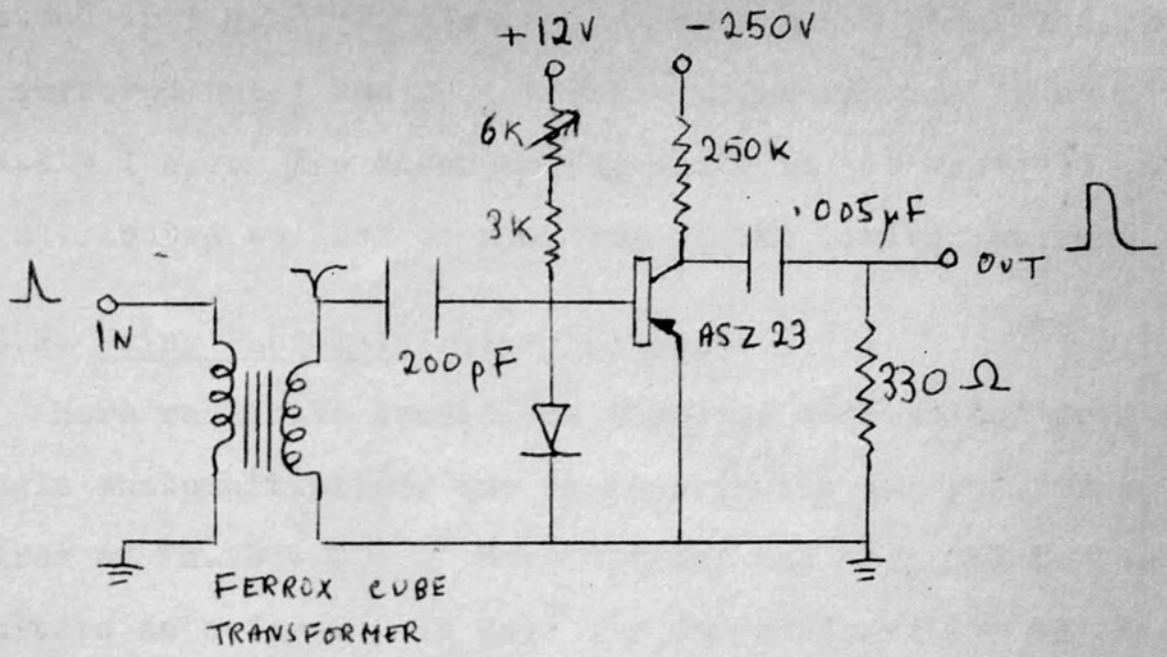

Figure 5.9. Discriminator Circuit.

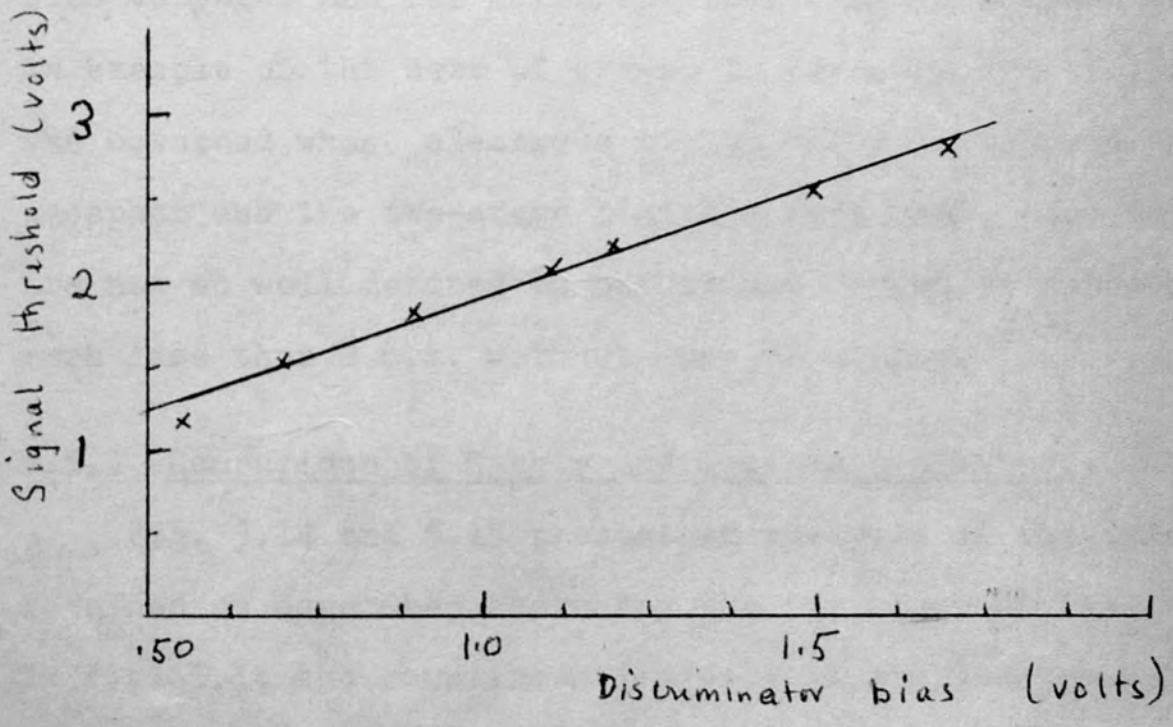

5.10. Variation of Signal Threshold with Discriminator Bias.

plotted in fig. 5.12. The curves have sharp sides and can be narrowed until the full width at half maximum is approximately 1 n.s. The accompanying shift in the centroid can be attributed to lack of symmetry in the limiter pulses.

5.5.2. Using Photomultiplier Pulses.

More realistic conditions obtained when pulses from a single photomultiplier, due to monokinetic β-rays from a source of Th. B + C + C^1 were divided and then fed to the limiters as before. In this way any contribution to the time resolution due to "jitter" in the coincidence circuitry could be noted independent of effects caused by time spreads in phosphor and photomultiplier.

Prompt curves were plotted at different discriminator bias voltages and for different spectrometer current values. An example of the sets of curves is given in fig. 5.13, which was obtained when electrons of 148 keV were focused on the phosphor and the two-stage limiters were used. The curves are not so well defined as before and cannot be narrowed to much less than 2 n.s. without loss of counts.

5.5.3. Comparison of Single and Two-Stage Limiters.

Fig. 5.14 and 5.15 present an analysis of the data obtained as described above for the two types of limiters. In fig. 5.14 the counting efficiency is plotted against the discriminator bias for different values of the focused

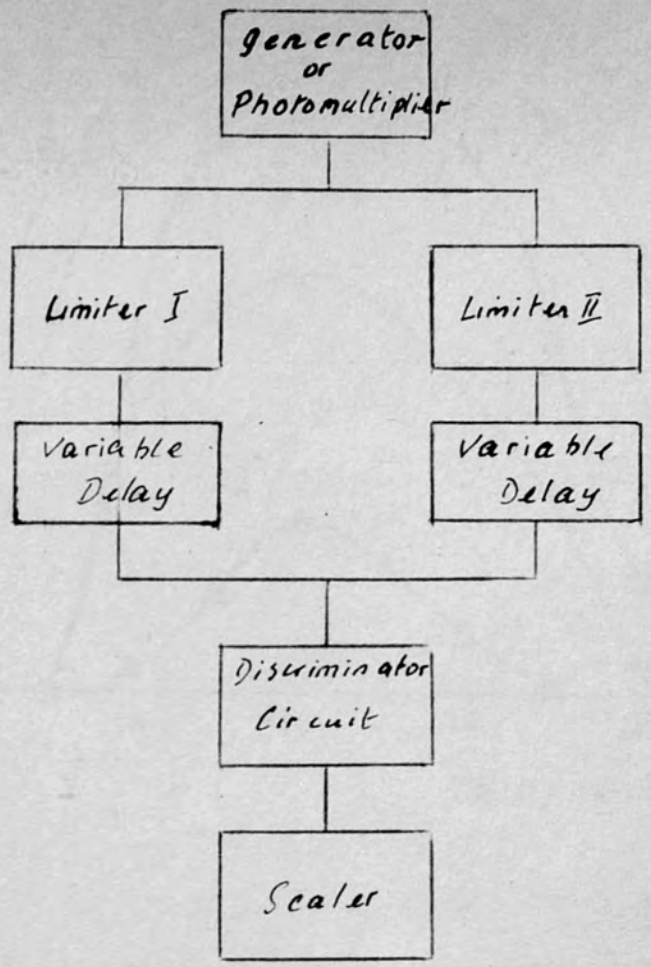

Fig.5.11. Experimental Arrangement for Testing Coincidence Circuits.

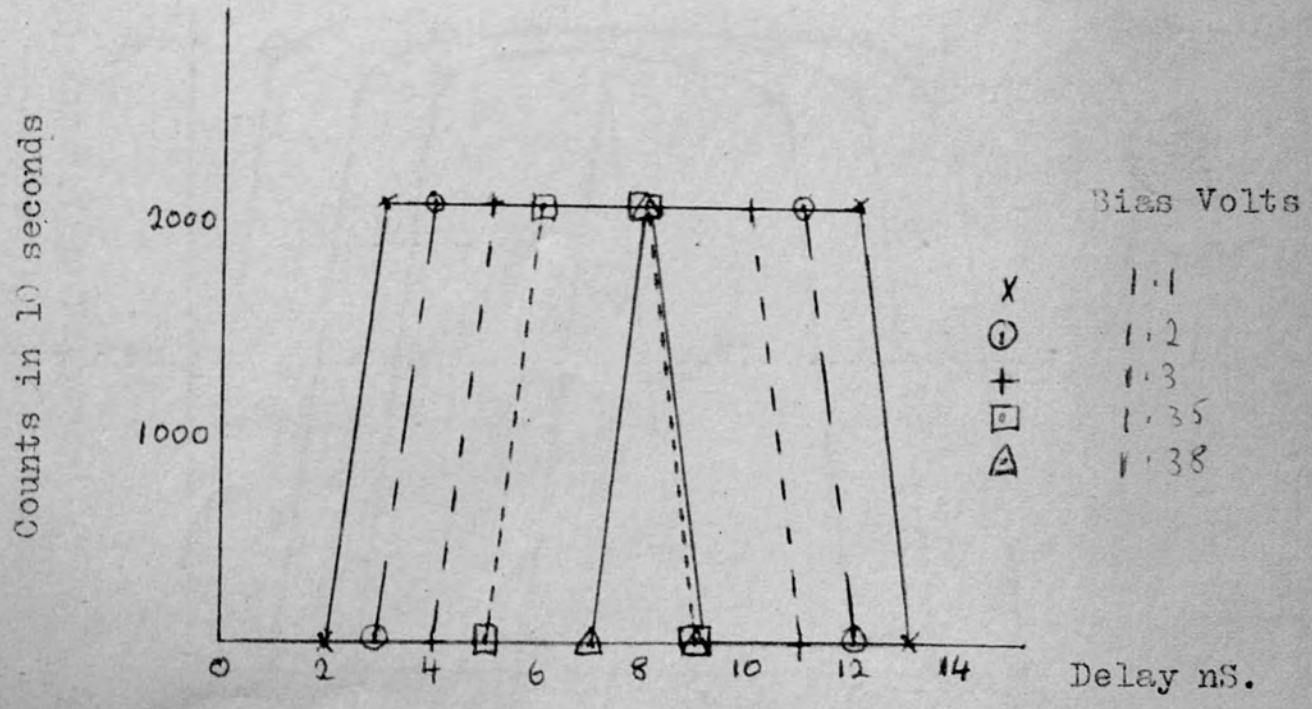

Fig.5.12. Prompt Curves using Artificial Pulses: Two Stage Limiters.

Fig.5.13. Prompt Curve: Pulses derived from one Photomultiplier, due to Electrons of 148 KeV.

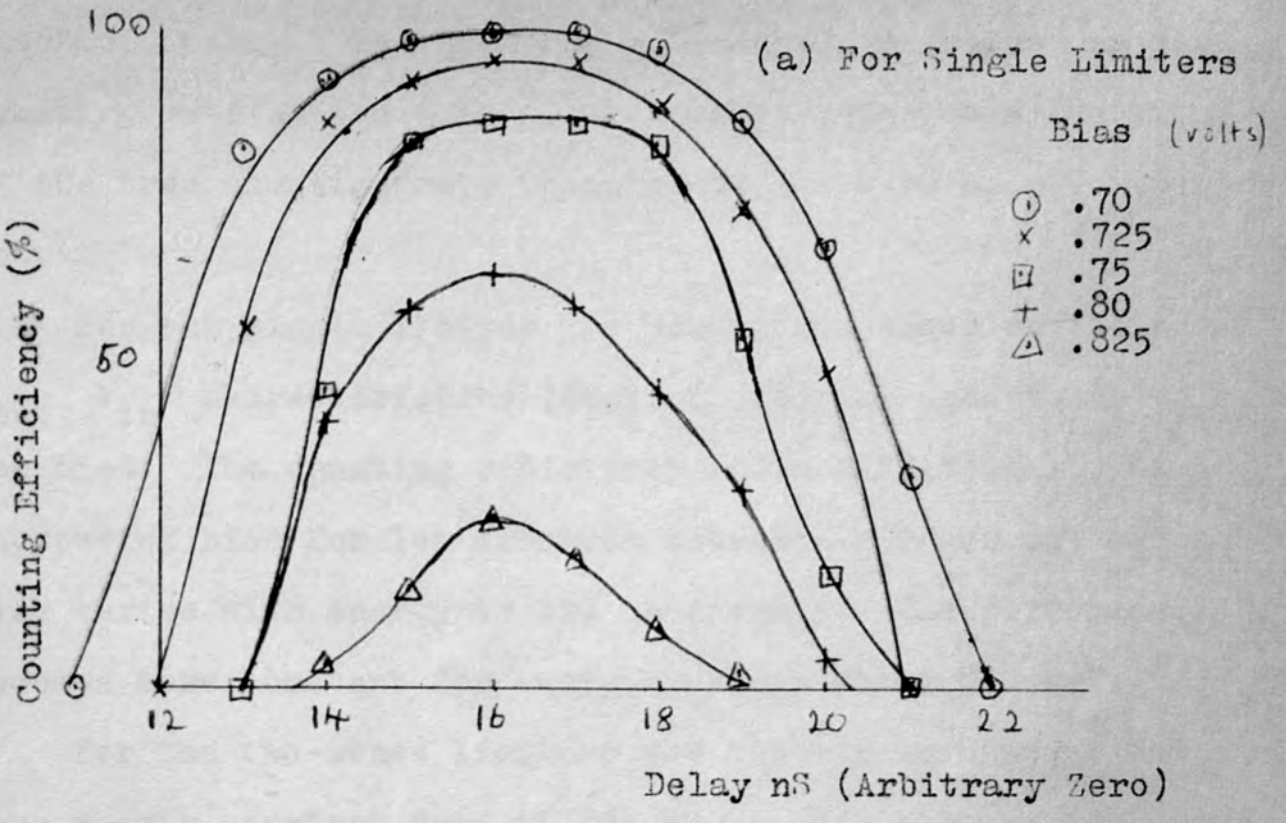

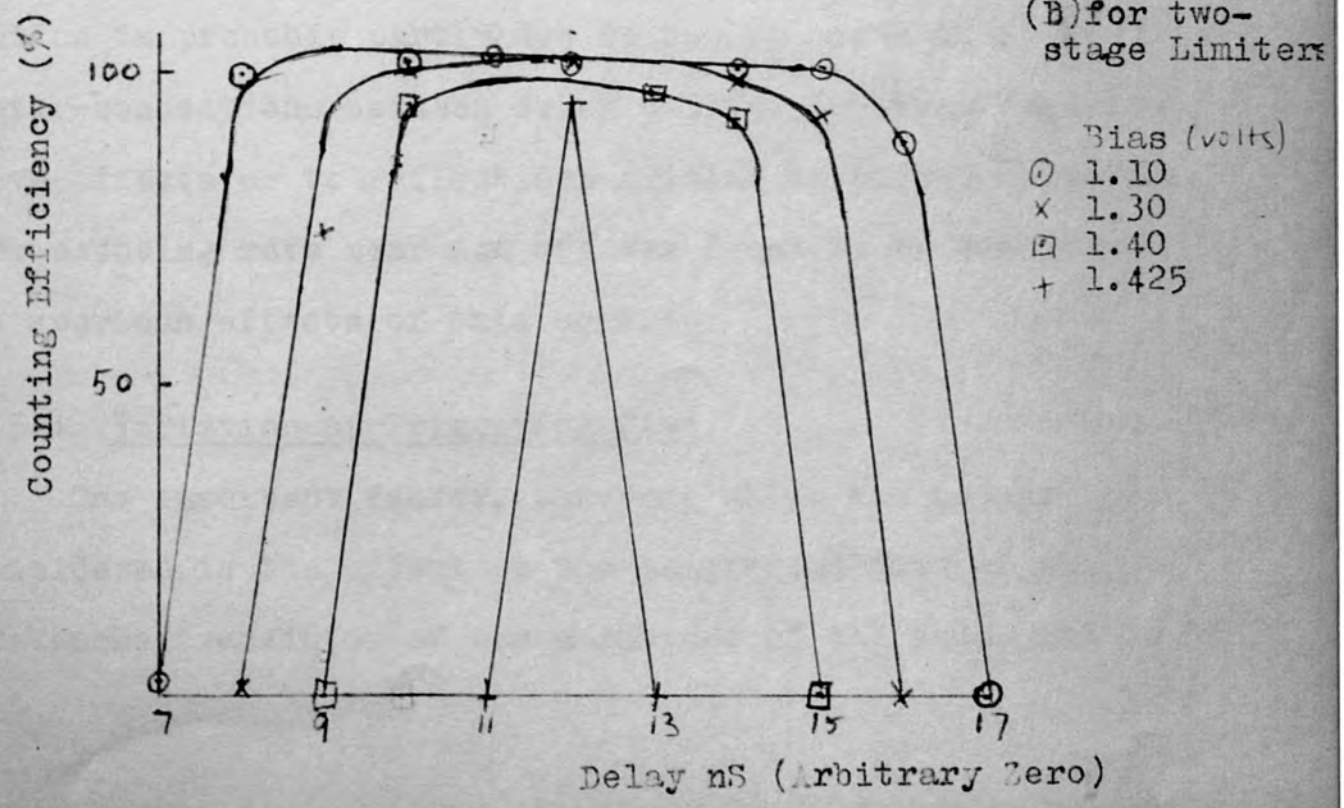

electron energy. The counting efficiency is defined as the counting rate at the peak of the prompt curve as a fraction of the true counting rate measured at the same spectrometer setting.

For the single limiter the prediction based on their $V_{out} : V_{in}$ characteristics (section 5.4) are seen to be verified. The counting efficiency falls off gradually with increasing bias for low electron energies and the cut-off bias varies with energy in the same range. The performance becomes more constant for energies above about 850 keV.

For the two-stage limiters the cut-off is sharper and more nearly constant down to low energies; also better time resolutions are obtainable at the same counter efficiency (fig. 5.15). The behaviour is more acceptable though still less good than could have been hoped for. The finite resolution is probably partly due to faulty contacts at the inter-connections between delay cables, to stray capacitative effects or to reflections arising at different points. The counting rate near cut off was found to be sensitive to spurious effects of this sort.

5.5.4. Variation of Triggering Time.

One important factor, however, which has not yet been considered is the effect on the triggering time of the avalanche transistor of the amplitude of the pulse fed to

its base. Gygi and Schneider (Gygi 1963) and Jackson (Jackson 1964) have reported that the triggering time increases quite sharply as the amplitude of the triggering pulseddecreases below a few volts. Thus under the above conditions there would be a time spread of the "limited" pulses corresponding to the amplitude spread of the input pulses.

The triggering time of the transistor also depends on the value of the positive bias at the base; Jackson pointed out, that the centroid of the prompt curve is shifted if the bias at the base of one of the limiters is altered and our experience confirmed this. The effect is reduced by reducing the bias to a minimum but it must be kept above the value at which self-oscillation takes place and if possible above the noise level as well. Any variation in the bias would thus cause a jitter in the coincidence circuitry and this may well be another factor contributing to the width of the prompt curve. The discrepancy between the results plotted in fig. 5.13 and the analysis of fig. 5.14 which was based on a previous set of measurements may be due at least in part to the fact that the positive power supply was changed between the two sets of measurements.

Jackson reports time resolutions $\sim$ 1 n.s. at 100%

Figure 5.14. Variation of Counting Efficiency with Discriminator Bias for Different Values of Focused Electron Energy.

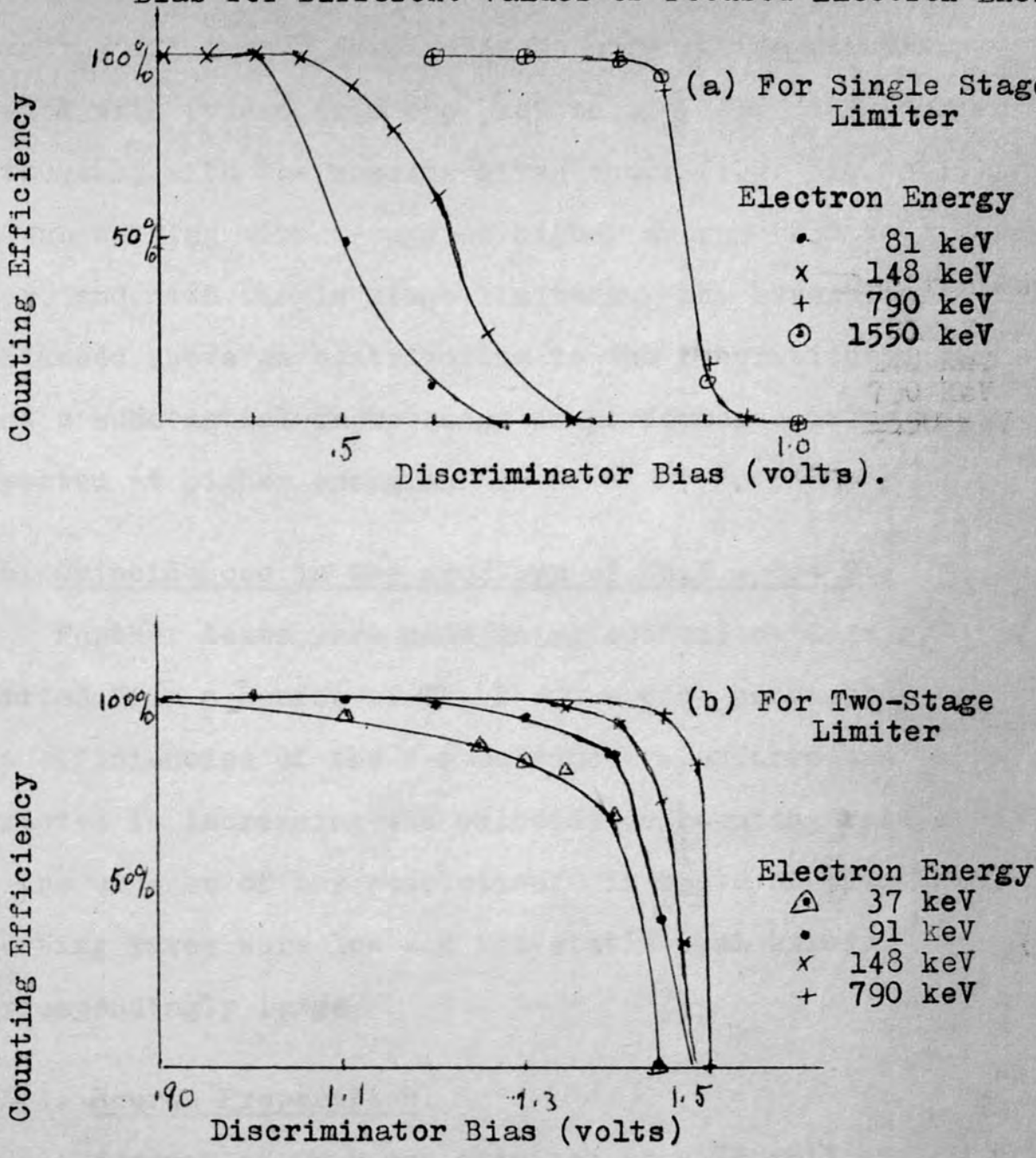

Figure 5.15. Variation of Counting Efficiency as Time Resolution is Improved, for electrons of 148 keV.

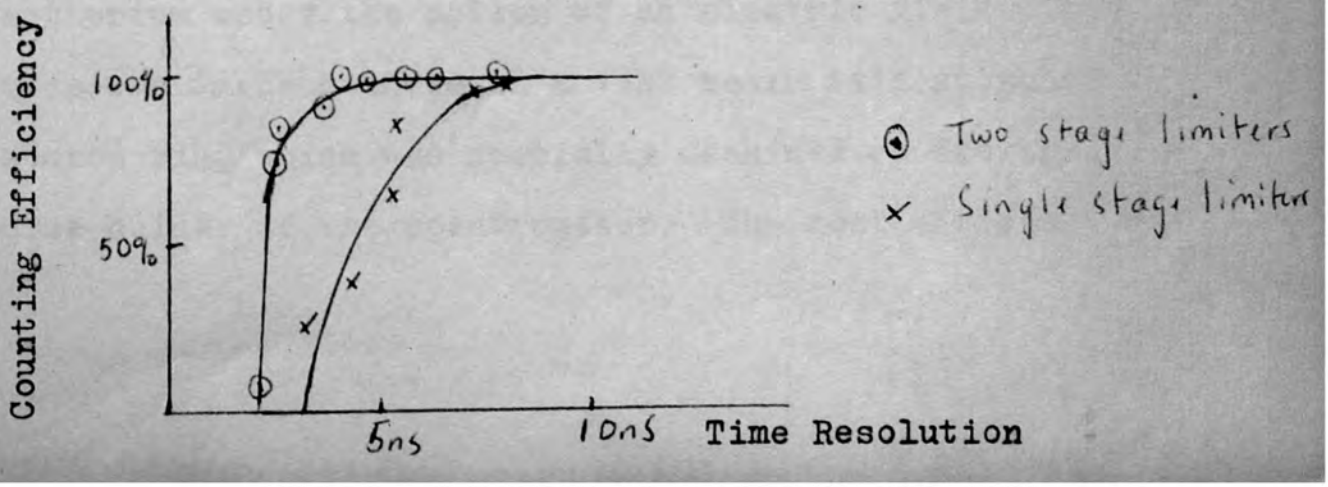

counting efficiency for avalanche coincidence circuitry tested with pulses from one photomultiplier; this compares favourably with the results given above (e.g. fig. 5.13). He was working with β-rays of higher energy (230 keV), however, and with single stage limiters. The several effects mentioned above as contributing to the resolution suggest that a substantial improvement in performance is to be expected at higher energies.

5.6. Coincidences in the spectrum of Th.B + C + C';

Further tests were made using coincident β-rays, emitted from a source of Th. B + C + C'; because of the low efficiencies of the β-spectrometers, efforts had to be directed to increasing the coincidence counting rate even at the expense of the resolution; in spite of this the counting rates were low and the statistical errors correspondingly large.

5.6.1. Source Preparation.

A deposit of Th.B was obtained on a 3" coil of Platinum wire by exposing it to the radiation from mesothorium under the action of an electric field. The source was to be mounted on a VYNS resin film attached to a source ring which was specially machined to fit the source holder of the spectrometer. The most efficient way

of transfering the deposit to the film was found to be by placing the wire on the film and dissolving off the deposit in situ. A few drops of dilute HCl were pipetted on to the wire at the centre of the film, which was already mounted on the source ring in the holder. The liquid was evaporated off under light from an infra red lamp; the wire was carefully lifted off before the wire was completely dry.

5.6.2. Spectrometer Settings.

Both spectrometers were focused on the strong F conversion line in the spectrum of Th.B. In this way there was a double coincidence rate: that between the continuous β-spectrum detected in one spectrometer and the conversion line in the other and vice versa.

The slit of the big spectrometer was opened to setting 60, corresponding to a resolution of about 1.8%.

A rough calculation enabled an estimate of the difference in path lengths in the two spectrometers to be obtained. The actual value of the delay which had to be inserted in the path of pulses from the small spectrometer before coincidences could be observed was found empirically.

5.6.3. Prompt Curves.

Prompt curves were plotted using first the single limiters fig. 5.16 then the two stage limiters (fig.5.17 (a) & (b). In (b) the pulses had been narrowed

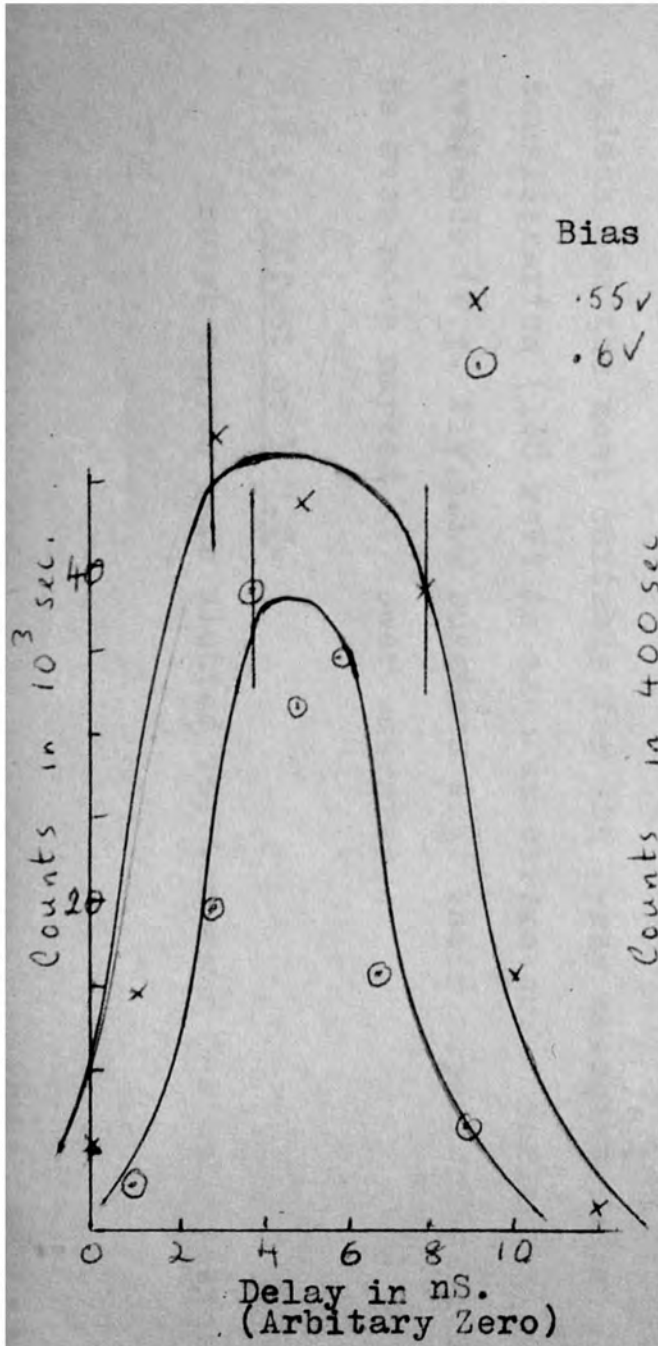

Fig. 5.16. Prompt Curves: Single-Stage Limiter

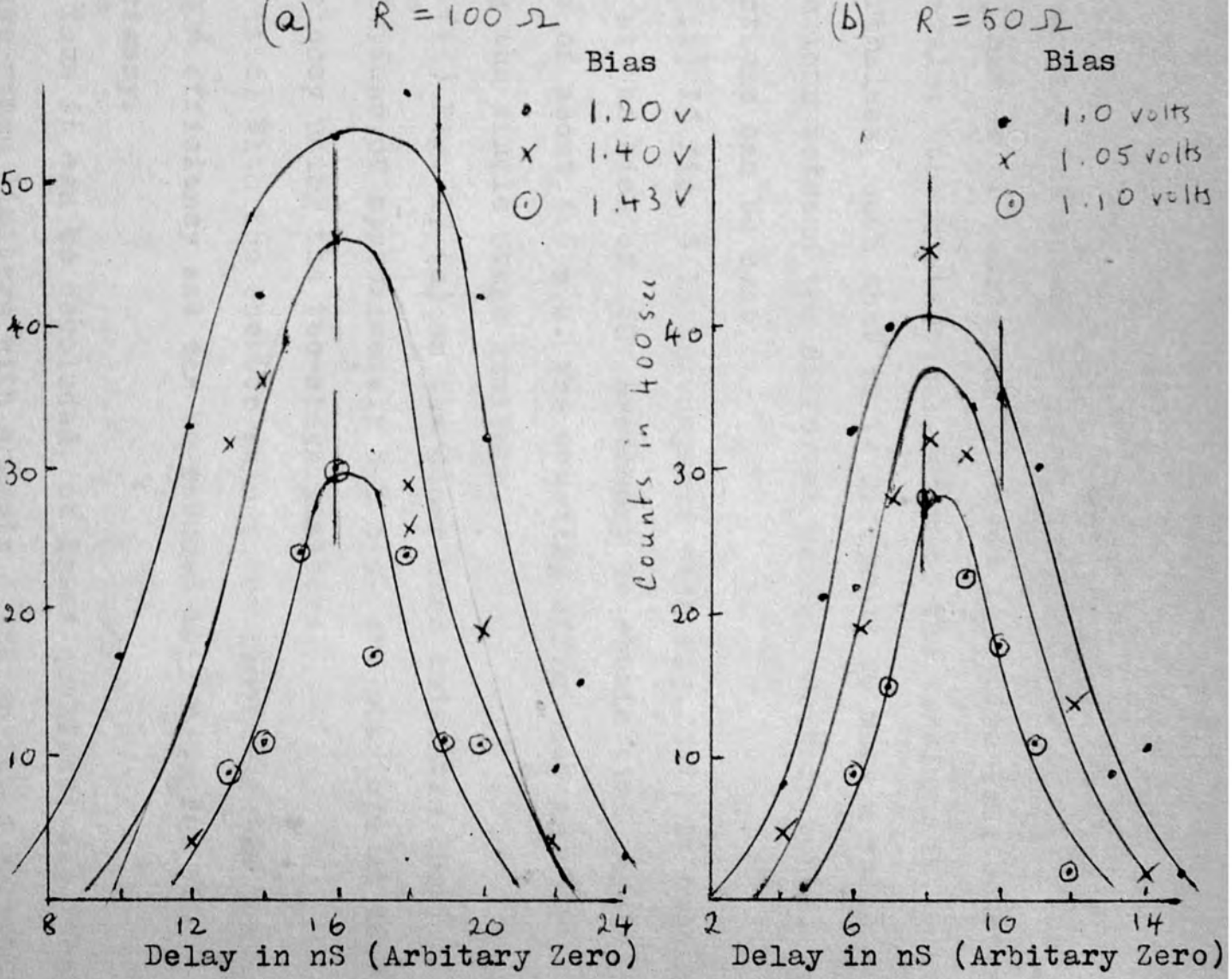

Fig.5.17. Prompt Curves for Two-Stage Limiters.

by reducing the output resister from 100Ω to 50Ω. The total number of counts was low even for quite long counting intervals; the statistical error of the readings is, nevertheless, such that it is difficult to make a valid comparison between the different cases. Certain tentative deductions can be made.

(i) If fig. 5.16 is compared with fig. 5.14 it appears that at the bias of .60v necessary to obtain time resolutions of about 4.5 n.s. the counting efficiency is ~ 50% using the single stage limiters.

(ii) Fig. 17 (a) on the other hand indicates that resolutions of approximately 5.5 n.s. are possible at 100% efficiency using the two-stage limiters.

(iii) With the shorter pulses the resolution is 5 n.s. at 100% efficiency and can be reduced to 3 n.s. for 70% efficiency.

Thus it can be concluded, at least qualitatively, that the two-stage limiters with sharply differentiated output pulses are the most suitable for the β-ray energies under consideration (148 keV) in each spectrometer. Earlier evidence (e.g. fig.5.14) suggests that their superiority will be even more marked at lower energies.

5.6.4. Effect of E.H.T.

Prompt curves were plotted for the same β-β coincidences

Fig. 5.18. Delay Curves at different E.H.T.

E.H.T. Large Spectrometer 2.0 kV.
E.H.T. Small Spectrometer E_s

	E_s kv	Discriminator Bias (volts)
x	1.75	1.10
⊙	1.85	1.00
△	1.95	1.10
•	2.0	1.10

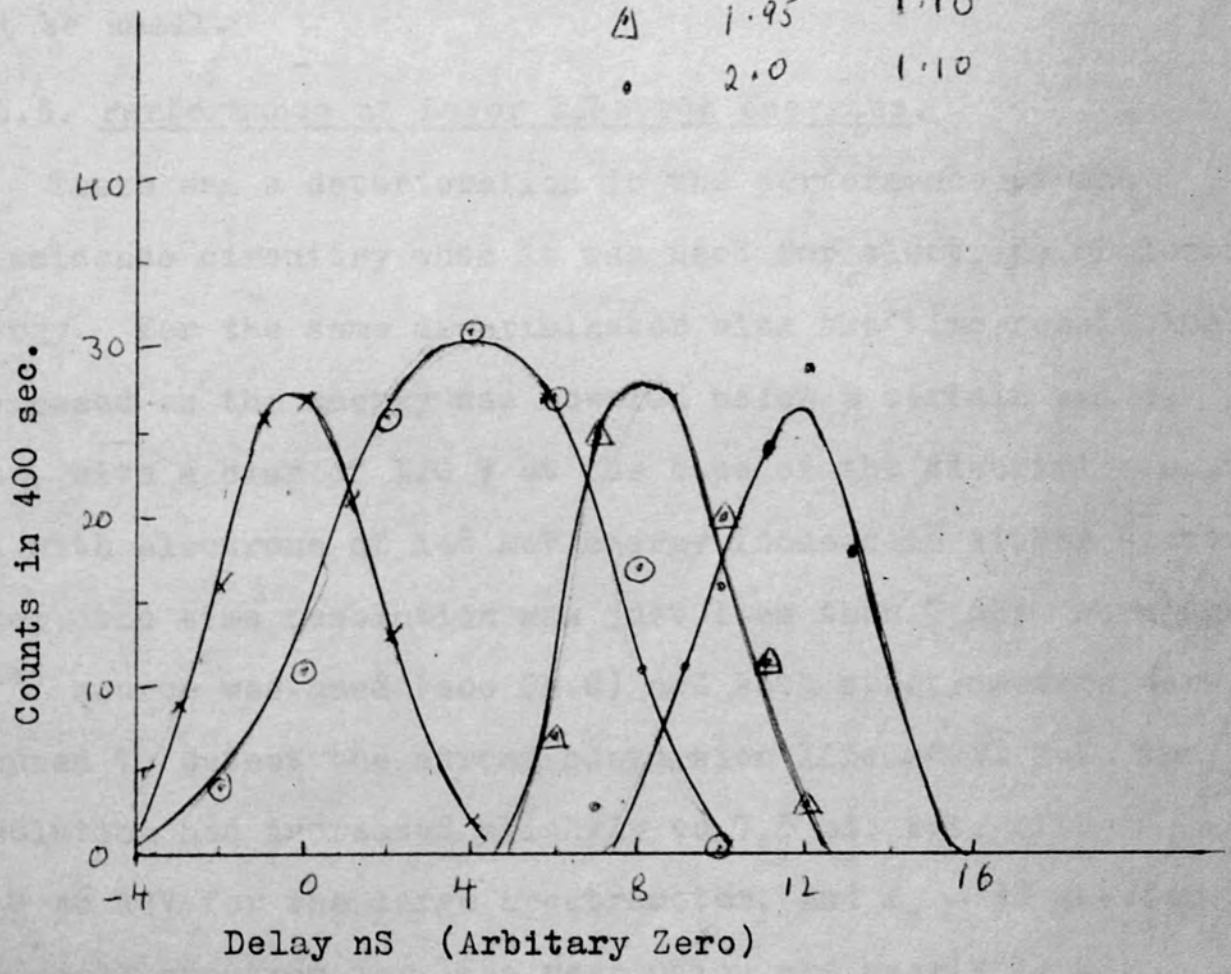

but at different values of the E.H.T. applied to the two photomultipliers. (fig. 5.18). There was a considerable shift in the positions of the centroid of the curve for each 0.1 KV change in the voltage. On the other hand, the time resolution for the same discrimination level remained effectively constant. The shift in the position of the curve is possibly due to change in the transit time of the electrons in the photomultiplier. The fact that the time resolution remains constant suggests that any contributions to this shift, due to the change in triggering delay with pulse amplitude, must be small.

5.6.5. Performance at Lower Electron Energies.

There was a deterioration in the performance of the coincidence circuitry when it was used for electrons of lower energy. For the same discriminator bias the time resolution increased as the energy was lowered below a certain value. Thus, with a bias of 1.0 V at the base of the discriminator, and with electrons of 148 keV energy focused in either spectrometer, the time resolution was just less than 7 nS; when the Ce^{144} source was used (see Ch.6) and both spectrometers were focused to detect the strong conversion line at 91 keV, the resolution had increased slightly to 7.5 nS; but, with E_β = 46 keV for the large spectrometer, and E_β = 38 keV for the small spectrometer, the resolution was nearly 11 nS.

Further, it was noticed that at the lower energies there was a much sharper decrease in counting efficiency as the bias voltage was raised. These effects can probably be attributed to the transit time effects described above (Section 5.5.4.).

5.7. Conclusion.

The avalanche coincidence circuitry described in this Chapter has the advantage of great simplicity, and is potentially very fast. However, the time resolution obtainable in practice for small input pulses is limited by the spreads in output pulse height and transit time described in Sections 5.4.1 and 5.5.4, respectively. The former effect has been overcome by the use of two transistors in cascade in the limiter circuits; it is probable that the transit time effect accounts for the deterioration in time resolution as the energy is lowered.

CHAPTER 6

Decay of Ce^{144}

6.1. Introductory

The decay of the nuclide Ce^{144} has been the object of many investigations; it is of particular interest since the energy levels of the odd-odd daughter nuclide Pr^{144} should provide information about the neutron-proton interaction in a heavy nucleus.

While certain features of the decay are well established, others are still disputed. There is general agreement derived from γ and conversion line studies that de-excitation transitions with the following energies take place in the daughter nucleus: (1) 33 keV; (2) 41 keV; (3) 53 keV (4) 59 keV; (5) 80 keV; (6) 100 keV; (7) 133 keV. Furthermore, different authors agree that there are at least three components in the β-decay of Ce^{144}, whose energies are approximately 310, 230 and 180 keV, and these are generally supposed to feed levels at 0, 80 and 133 keV in Pr^{144}. This information, combined with corroborative evidence from γ-γ, γ-electron, and γ - β coincidence studies has led to the almost universal acceptance of a decay scheme of the general form shown in fig. 6.1 (a), but whereas some authors (Geiger et al.1960, 1961) maintain that these are the only energy levels excited

Figure 6.1. Decay Scheme of Ce^{144}

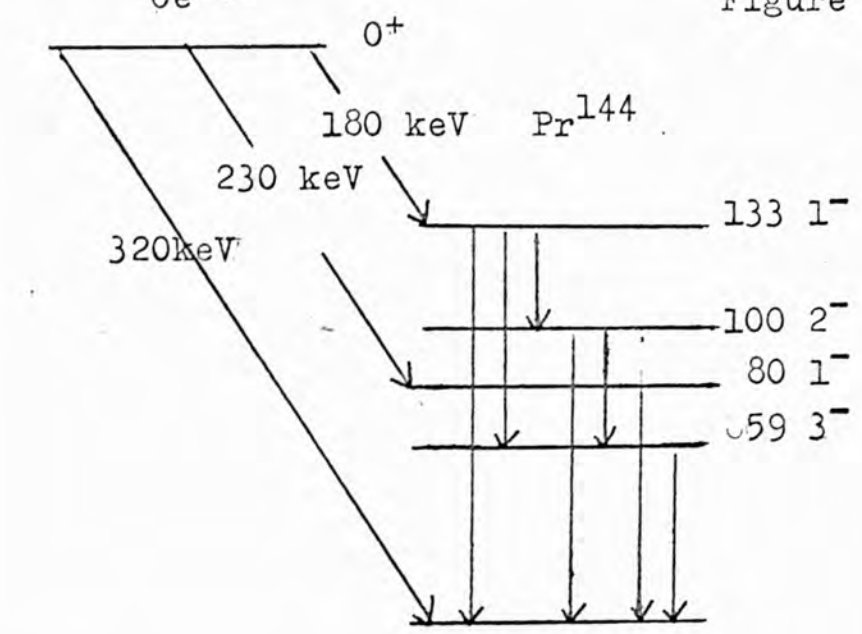

(a) Generally accepted features of decay.

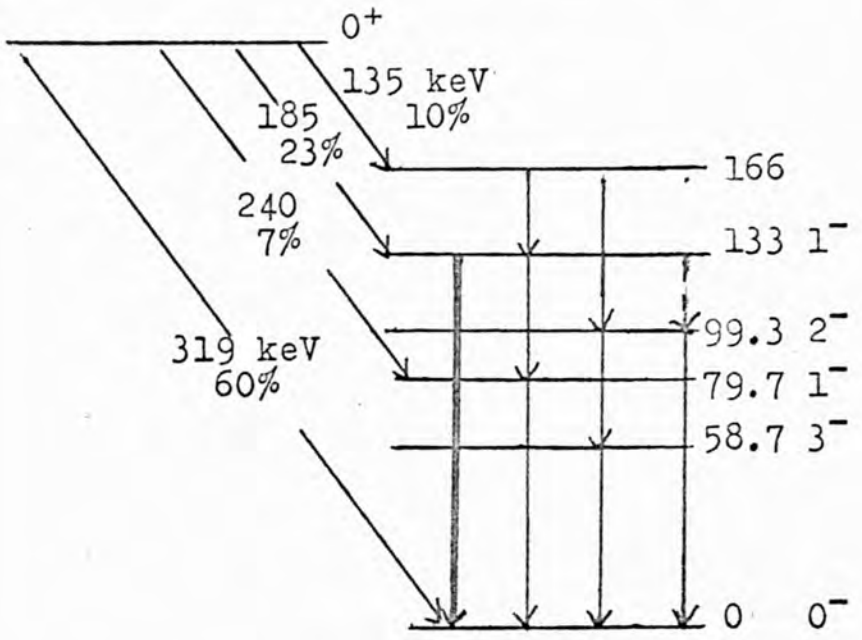

(b) Scheme due to Freeman.

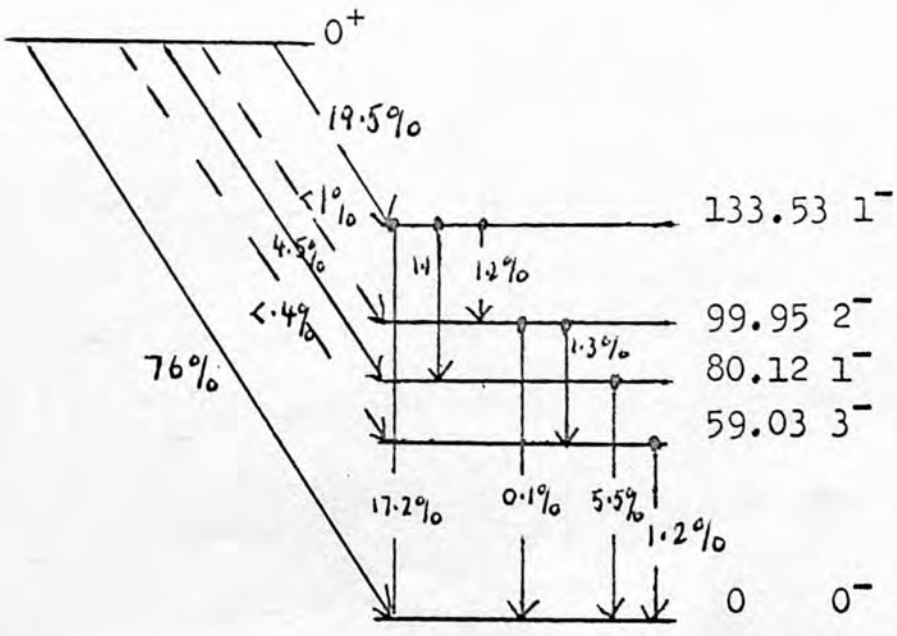

(c) Scheme due to Geiger et al.

in the decay, others (Freeman 1959, Forafontov 1962, Iwashita 1963) claim evidence for higher energy excited states; this evidence, derived from γ, β, and conversion electron investigations is discussed in the next section. The possibility of transitions of energy less than about 20 keV is not excluded, though with existing techniques it has proved difficult to identify them above the noise of the detectors. The assignment of 0^- for the ground state spin and parity of Pr^{144} is not seriously disputed; the evidence comes from $\beta - \gamma$ angular correlation and coincidence β-spectrum shape studies of the Pr^{144} decay. The assignments for other levels which have received a measure of agreement are included on fig. 1. They are the result of measurements of internal conversion coefficients, conversion line intensity ratios, and angular correlations (Geiger 1960, Freeman 1959, Iwashita 1963).

Attempts have been made to interpret the given data in terms of different nuclear models. On a single particle shell model, and using the energy level sequence derived from neighbouring nuclei, one would expect the angular quantum numbers of the odd neutron and proton in the ground state to be 7/2 and 5/2 respectively; this model, therefore, fails to account for the observed spin of 0^-.

It is possible to interpret the known levels in terms of

a more comprehensive shell model in which the combined angular momentum of the three neutrons outside the closed shell at N=82 is considered, but more than one theoretical configuration is capable of explaining the experimental results.

Interpretation in terms of a unified model is also possible, as has been shown by Geiger et al. (op.cit.) though here also the interpretation is not without ambiguity.

Iwashita et al prefer to retain a shell model interpretation on the ground that the Pr^{144} nucleus clearly lies outside the region of deformed nuclei. They make use of neutron and proton spin assignments given by Burde et al (Burde 1962), who deduce values on the basis of their measurements of the life times of excited states. The fact that they are forced to postulate mixed configurations for the 80 keV and 133.5 keV energy levels is perhaps itself an indication that the shell model is no longer applicable in this case.

Some of the ambiguity in the theoretical treatment might well be removed if the existence of other energy levels were to be definitely established. The conflicting evidence as to the existence of a level above 133 keV is reviewed in the next section and the rest of the chapter

is devoted to the results of further investigations of the decay with the present equipment.

6.2. Evidence for Excited States in Pr^{144} at Energies Greater than 133 keV.

6.2.1. The β-rays in the decay of Ce^{144}.

The existence of a β-ray (β_3) of end-point energy less than 180 keV would be definite evidence in favour of an excited state at energy greater than 133 keV in the daughter nucleus. Such a β-ray has been reported by Freeman (β_3 = 128keV), by Parfenova (β_3 = 130 keV), as well as by other workers. (Freeman 1960; Parfenova 1959), Geiger (Geiger 1960) has suggested the possibility that these observations are the result of back-scattering in the source, though Freeman's experiments, with different thicknesses of source backing, would seem to exclude this explanation. However, the value of $\beta_2 - \beta_3 \sim$ 50 keV obtained by Freeman does not agree with his assignment of an energy level at 166 keV (see below), unless this level be itself fed from another higher level.

6.2.2. The γ-rays and Internal Conversion Lines.

There is little direct evidence of γ-rays or conversion electrons corresponding to transitions of energies

greater than 133 keV; the evidence in favour of higher excited states is derived mainly from coincidence studies. Freeman interprets certain weak conversion lines as being due to transitions of 66 keV and 85 keV, which would be consistent with the existence of a level at 166 keV; Geiger failed to detect these lines despite a careful search with the high resolution spectrometer at Chalk River.

Forafontov et al (Forafontov 1962) claim clear evidence for a conversion line peak at 106 keV in the integral coincidence spectrum with β s of energy less than 200 keV; this disappears for β s of energy greater than 400 keV, thus excluding the possibility that it is due to the decay product Pr^{144}, which is itself β-active. This 106 keV level is thought by these authors to be the K line of a 147 keV transition.

6.2.3. Coincidence Studies.

(a) Possible Level at 166 keV.

A peak at 26 keV (33K) in the electron spectrum in coincidence with the 133 keV γ-ray led Freeman to postulate a level at 166 keV. Geiger et al (Geiger 1962) failed to detect such a level when they investigated the γ spectrum coincident with (a) the $L_1$33.7 keV conversion line (b) the $L_1$133.5 keV conversion line, and (c) the γ 133.5 keV line. They do not, however, completely exclude the

possibility of a transition of 33 keV in coincidence with the 133.5 keV, but specify that it must be extremely weak. More recently Iwashita et al in Japan report definite evidence in favour of a coincidence between γ 33 and γ 133.5 as well as between γ 66 and γ 100, thus lending support to Freeman's findings. Forafontov et al, on the contrary, found no evidence of such coincidences in their electron - γ coincidence investigations. The results obtained at Chalk River are probably the most reliable, both because of the instruments available and because of the thoroughness of the search; still, the converging evidence from different sources as to the existence of the 166 keV level, means that the question still lies open to investigation.

(b) Possible Level at 175 keV.

Evidence in favour of a coincidence between the γ 133.5 and L 41 conversion lines was reported by Forafontov and Sorokin (Forafontov 1959), but remained undetected by Geiger et al (Geiger 1961). A more recent paper by the original authors (Forafontov 1962) omits mention of a level at 175 keV altogether, and it, therefore, appears probable that the existence of this level may be discounted.

(c) Level at 147 keV.

In their more recent paper Forafontov et al put forward evidence for a level at 147 keV, of spin and parity 2^-.

The 106 keV line in the coincidence spectrum has been mentioned above. Further the presence of a peak at 24 keV (K 66) in the e^- - γ coincidence spectrum when E_γ = 80 keV, showed that the 148 keV level de-excited by a (66 + 80) keV cascade. Their peak, however, scarcely lies above the normal statistical scatter of coincidence counts; also, it is open to doubt whether with a β - spectrometer of resolution 3.3% one could expect to be able to distinguish clearly between a line at about 24 keV and the known conversion line (L 33, E = 26.7 keV), which might well be in coincidence with γ80. (see Fig. 6.1).

6.3. Experiments with Ce^{144}.

6.3.1. The Source

The source used in the subsequent experiments was prepared by depositing a drop of a solution of CeCl in HCl on a VYNS resin film and evaporating it to dryness. The film had previously been painted with a thin strip of Aquadag to provide a conducting path to earth. The source had a diameter of 6 m.m. and a strength of about 20 μ C. With this rather crude method of preparation, one could not hope to get a very thin, uniform source; broadening of spectrum lines on the low energy side is to be expected but this need not necessarily prevent the detection of coincidences between lines of known energy.

6.3.2. Procedure.

The spectrum lines involved in the cascade to be investigated were first located, whenever possible, in the singles spectrum. The identification was based on the momentum values derived from previous studies of the isotope, and on the momentum: current calibration for the spectrometers obtained from the known Th B lines (e.g. see Ch.3).

In counting coincidences a compromise had to be reached between the counting efficiency on the one hand and the energy and time resolutions on the other. For the detection of fairly weak coincidences the minimum number of counts was about 100 in periods of about one hour. With smaller numbers of counts the statistical variation ($\gtrsim 10\%$) might well have masked any genuine variation in counting rate, and with longer counting intervals the process of plotting through a spectrum line would have become excessively long; also, the reliability of counts extending over longer intervals would be limited by the stability of the system, in particular, of the current I_2 in the small spectrometer.

Suitable values of the discriminator bias, and of the two slit widths were chosen empirically for each coincidence investigated, so as to satisfy the above requirements while maintaining as low a resolution and chance: true coincidence ratio as possible.

The prompt curve was plotted for the energies to be studied so that the time interval between the arrival of pulses from the detector of either spectrometer could be estimated and allowed for. The counting rate for chance coincidences was taken as the counting rate at the fringe of the prompt curve (see fig. 6.2). This was found to agree with the value based on the counting rate when both spectrometers were set on the high energy tail of their respective lines; also it was in approximate agreement with the value $N = 2 n_1 n_2 \tau$ derived from the singles counting rate n_1, n_2, and the width of the prompt curve. The momentum resolution was determined by plotting the strong 91 keV conversion line.

The coincidence spectrum was plotted as the current in the large spectrometer was increased through one of the lines. This was done when the small spectrometer was focused first on the peak, and then on the high energy tail of the other line.

6.4. Coincidence between the 53 keV and 80 keV transitions.

6.4.1. Settings.

The known coincidence between the 53 keV and 80 keV transitions was investigated as a test case. The 80 keV conversion line at 38 keV was focused in the small

spectrometer; the 53L (and 53M) at 47 keV (and 52 keV in the larger one.

The slit of the small spectrometer was about half closed, that of the large spectrometer at a setting of 30, giving a resolution of about 1.5%. The prompt resolution curve (Fig. 6.3) showed that an extra delay of about 14 nS, was required in the lead from the small spectrometer and that the chance coincidence rate was a little greater than 2 per 100 sec. The discriminator bias was set at 0.93 V. The automatic system was set to take 2 steps between readings and the time required for 100 counts was recorded.

6.4.2. Results.

The spectra obtained are shown in fig. 6.2. The following qualitative observations may be made:

(i) The 53L line is expected to occur when the current I_1 in the large spectrometer is 1.08 amps; this line is barely perceptible in the singles spectrum (fig. 6.2.a) but a peak occurs in the coincidence run (b) at this current.

(ii) The peak in (b) at 1.08 amps, when the small spectrometer is focused on the peak of the 80K conversion line is in contrast with (c) where any peak that might be present is well disguised by the statistical fluctuations

of the points.

(iii). Two causes may contribute to the increase in coincidence rate ΔN as I_1 is varied through the peak of the 53L line. Besides any increase due to coincidences between the two conversion lines there will be a contribution due to coincidences between the 53L line and the continuous β-spectrum at 38 keV. The latter source of coincidences is present in (c) (see fig. 6.3.) as well as in (b); thus the fact that $\Delta N_b > \Delta N_c$, even allowing for statistical error, is good evidence that the two conversion lines occur in cascade and that the life-time of the intermediate state is not greater than a few nano-seconds at the most.

(iv) The 53M line occurs at 51. 9 keV, and is thus hard to distinguish from the 59L line which is about 6 times as intense. It is this line which shows up in the singles spectrum at 1.16 amps; the peak which occurs at the same current in the coincidence spectrum (b) is probably a combination of the two contributions.

6.4.3. Interpretation in terms of Intensity Assignments.

A very approximate value for the ratio $\Delta N_b / \Delta N_c$ may be obtained from the spectra of Figure6.2. and this can

Figure 6.2. 80K: 53L Coincidence.

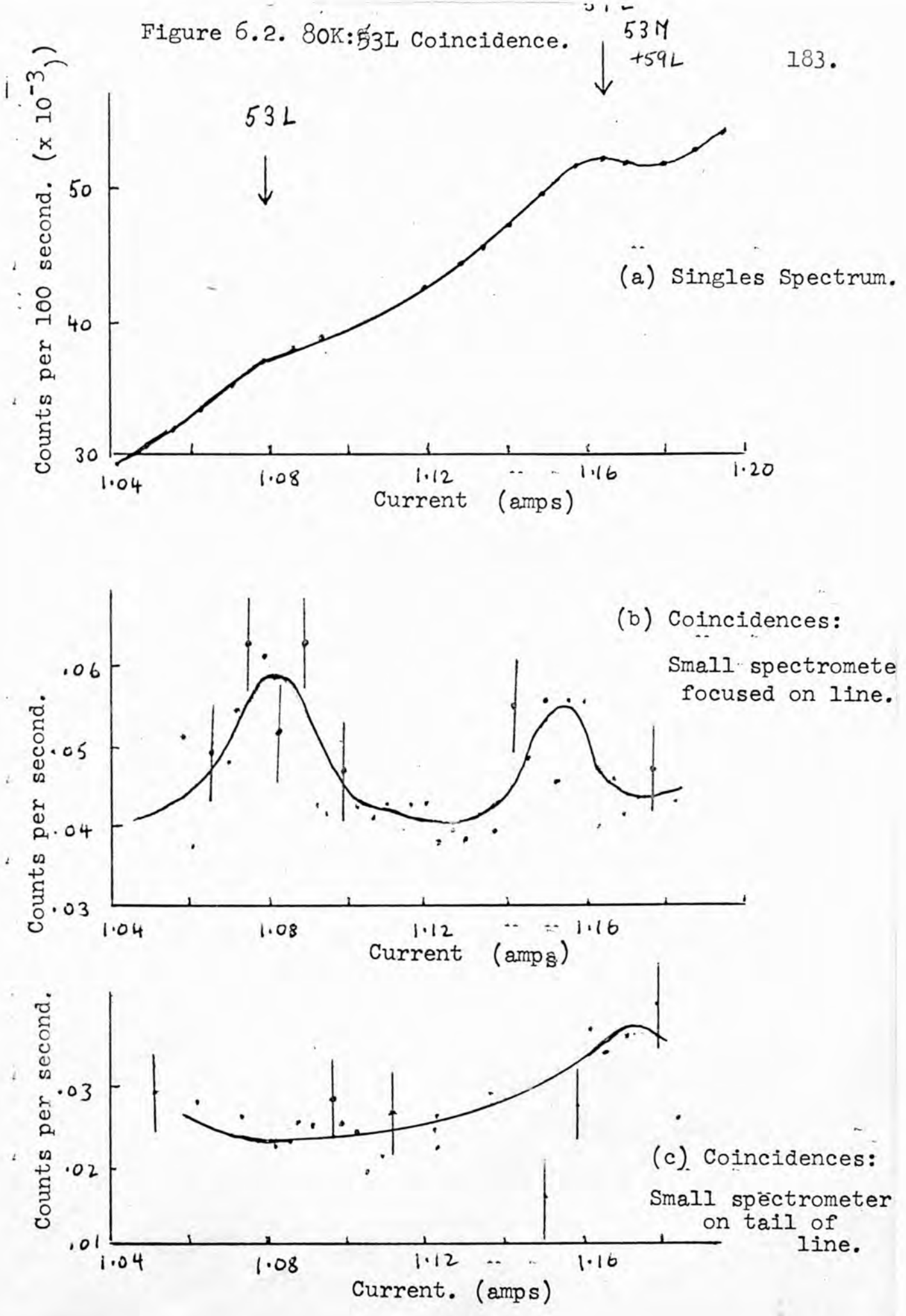

Figure 6.3. Prompt Curve for Coincidences between 53L and 80K lines.

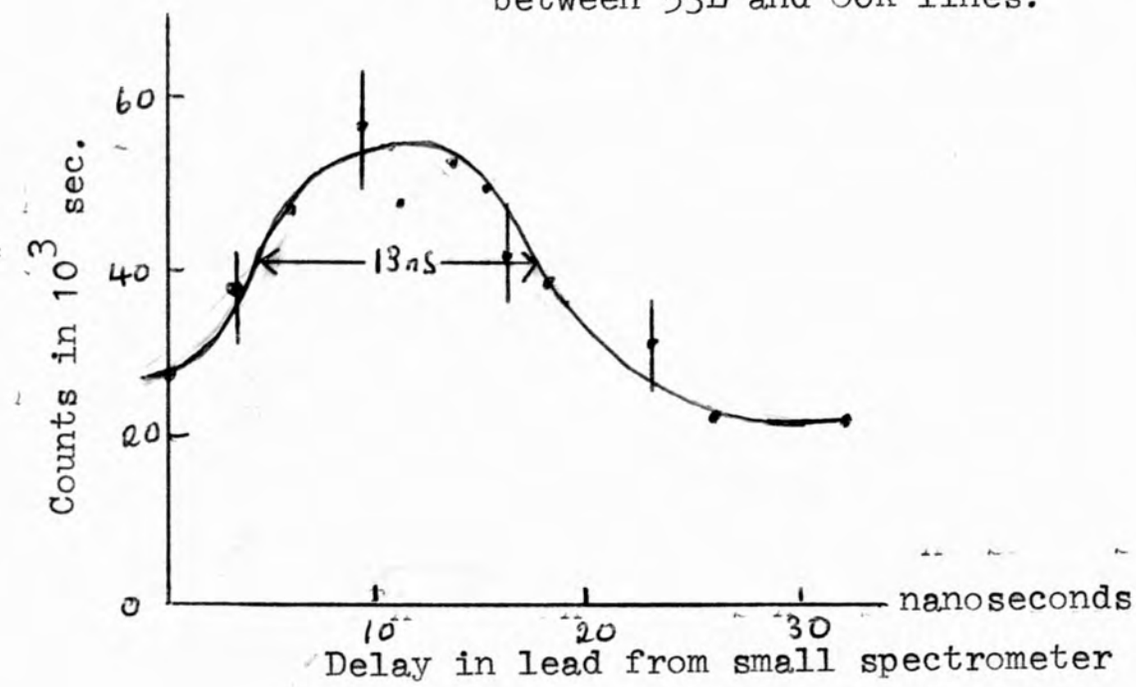

Figure 6.4. 80K Conversion Line plotted with small Spectrometer.

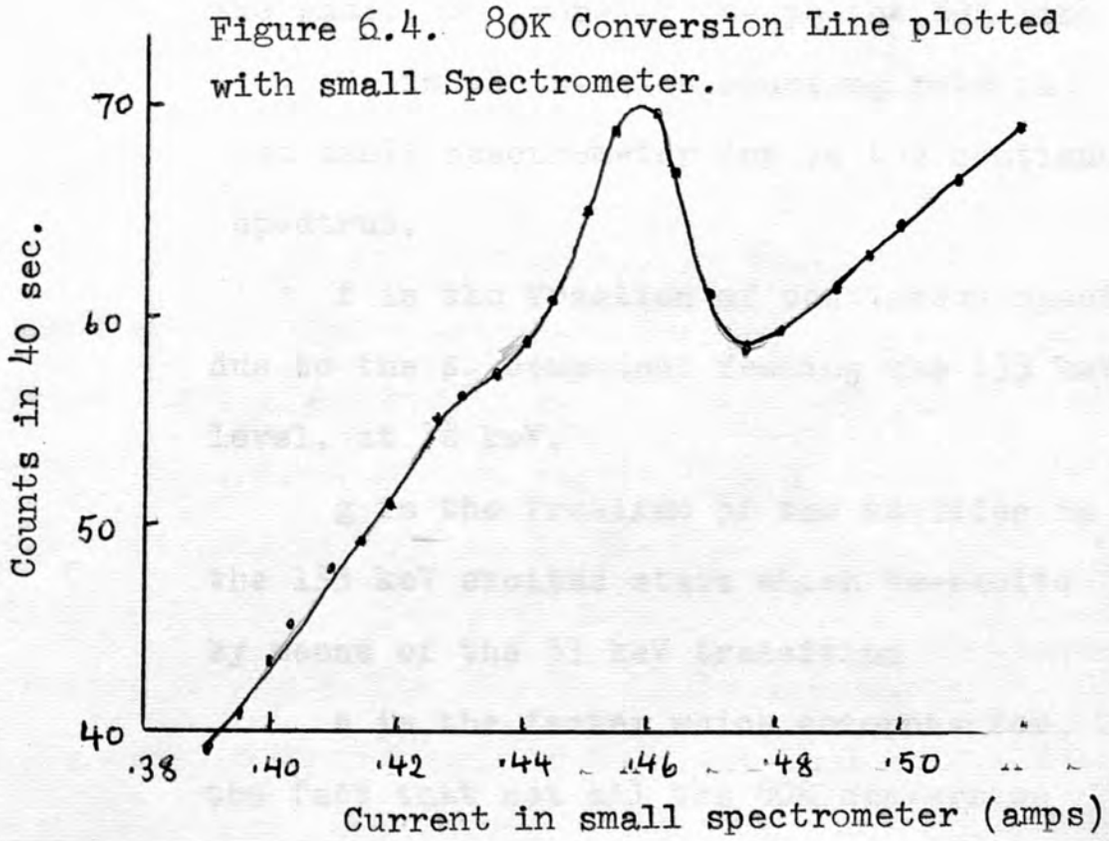

be compared with that derived from existing decay schemes.

If $\Delta N_b = \Delta N_c + n$,

where n is the number of coincidences per second due to the conversion line cascade,

then, $$\frac{\Delta N_b}{\Delta N_c} = 1 + \frac{n}{\Delta N_c} .$$

Also $$\frac{n}{\Delta N_c} = \frac{C_1 \times z}{C_2 \times f \times g}$$

where C_1 is the singles counting rate in the small spectrometer due to the 80K line

C_2 is the singles counting rate in the small spectrometer due to the continuous spectrum,

f is the fraction of continuous spectrum due to the β_2 component feeding the 133 keV level, at 38 keV.

g is the fraction of the nuclides in the 133 keV excited state which de-excite by means of the 53 keV transition

z is the factor which accounts for the fact that not all the 80K conversion lines are emitted in cascade with the 53keV transition.

From the decay scheme of Geiger et al, given in Fig.6.1. it can be seen that $g = 1.1/19.5$, and $z = 1.1/4.5$; Freeman's results, on the other hand lead to values of $g = 0.5/16.4$ and $z = 0.5/7.$; f was estimated from Freeman's Fermi analysis to be 0.29. C_1 / C_2 was determined from the singles sp ectrum of the 80KV line (Figure 6.4), and found to be $\sim 1/5$. Thus the value for $\Delta N_b / \Delta N_c$ is 1 + 3.0 using Geiger's intensity ratios, or 1 + 1.6 using Freeman's values.

In the present case $\Delta N_b \sim .016$; the height of the peak above the background was found by fitting the experimental points to the nearest Gaussian curve. It can be seen from fig 6.2(c), that ΔN_c must certainly be less than .005. Thus the ratio $\Delta N_b / \Delta N_c$ must be greater than 3.2, and so agrees better with the values quoted by Geiger than those given by Freeman. It can hardly be considered as conclusive evidence, however, since the statistics of the experiment are so poor, and the value for C_1 / C_2 , deduced from Figure 6.4. does not take into account any distortion of the line caused by back-scattering in the rather poor source, nor the fact that the number of electrons, due to the continuous β-spectrum, is greater on the tail of the line than on the peak.

6.5. Search for a 133keV - 133 keV Cascade.

The coincidence reported by Freemand and by Iwashita, between the 33 keV and 133 keV transitions, was looked for by a procedure similar to the above. However no conclusive evidence was obtained, neither when the 33 L line was focused in the small spectrometer, and the 133 K line in the larger instrument, nor when the opposite was the case.

It must be concluded that much longer counting intervals would be necessary before definite evidence about weak coincidences could be obtained with the present apparatus. Alternatively, some method of improving the performance must be found; one such improvement would be the use of a slow coincidence channel to eliminate any coincidences due to noise pulses, without the necessity of applying positive bias at the input to the limiters; more drastically, it might be necessary to replace the avalanche coincidence circuitry by another design, in which the time resolution was maintained down to lower energies. In any case it would be an advantage to replace the photomultipliers by some of the more recent faster models. Any modifications to spectrometers or detectors which aimed at improving the momentum resolution or the light collection efficiency, would be important aids in the detection of β-β coincidences between the transitions which are of interest in the decay of Ce^{144}.

[illegible]

[illegible]

[illegible]

[illegible]

(g) [illegible]

(h) Impex Electrical [illegible] Switch Type No. [illegible]

(i) Impex Electrical Gear Box, Type No. [illegible]

(j) Weir Electronics 1/2 amp Transistor Power Supply [illegible]

(k) [illegible] Power Supply Assembly [illegible]

APPENDIX I

Details of Commercial Equipment used in Construction of Automatic System - (section 3.2)

(a) I.D.L. Scaler 1700/A.

(b) I.D.L. Programme and Read-Out Unit Type 2007/C.

(c) Addo-X Printer

(d) Impex Electrical Stepping Motor Type No. AU 5105/81.

(e) N.S.F. Ledex Rotary Solenoid and Circuit Selector (4 load sections)

(f) Newport Magnet Power Supply Type C5.

(g) Borg Micropot 2201B

(h) Impex Electrical Electronic Switch Type No. 2P 72786.

(i) Impex Electrical Gear Box, Type No. AU 5300/80.

(j) Weir Electronics 1/2 amp Transistor Power Supply LVT/CB

(k) M.E.L. Power Supply Assembly YL 6101/01 with YL 6104.

APPENDIX II

Power Supplies.

Figure A.1 shows how the power supplies (j) and (k) are utilised.

The Weir unit (j) delivers - 26v stabilized; the M.E.L. supply has a stabilized output (+ 12v) and an unstabilized output (-18v) which is used to operate the relays.

The power supplies are connected to the Control Unit by means of an 8-way Cable (Cable A). The wiring of the cable A is given in figure A.1.

Interconnections.

The wiring of cables, B, C and D together with their plugs and sockets are given in figure A.2.

The connections to the End connectors of the Ledex Relay and the Panel II are shown in figure A.3.

Panels.

The lay-out on Front Panels I and II is given in figure A.4.

The position of the various plugs and sockets on the back panel is shown in figure A.5.

Legend.

Connections made directly to one of the circuit blocks (Panels I and II, Delay, Ledex) are appropriately marked

and the accompanying numbers refer to the respective diagrams in chapter 3 (figure 3.7,3.11, 3.9, 3.10).

The numbers marked against "current supply" refer to figure 3.3; Prog. refers to the Programme and Read-Out Unit.

The plugs and socket s are referred to by their letters and appropriate numbers prefixed by P or S for plug or socket respectively. Thus S.A.4 refers to the 4th terminal of socket A.

Figure A 1 Use of Power Supplies.
Wiring of Cable A connecting
Power Supplies to Control Unit.

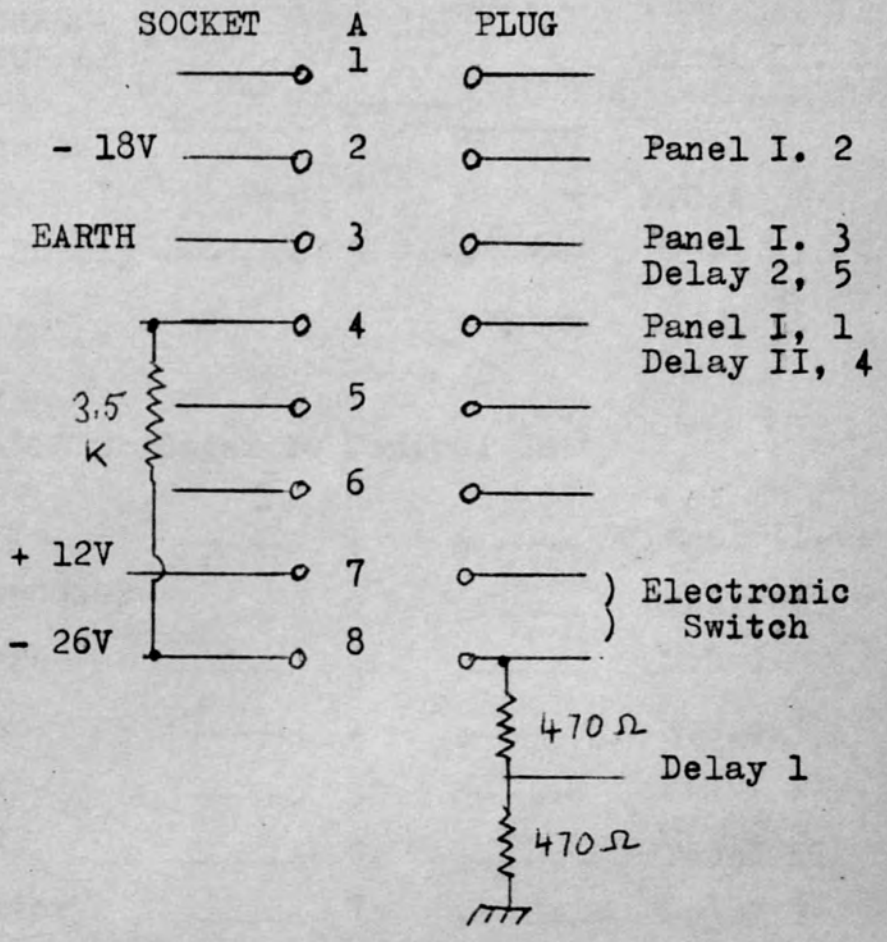

Figure A.2 Interconnections
Wiring Diagram of Plugs, Sockets and Cables.

CABLE B: Current Supply and Power to Control Unit

CURRENT SUPPLY	1		Panel I. 7
	2		Panel II. 8
Labpack −	3		S.C.3
24V +	4		S.C.4
Current Supply	5		Panel II. 9
	6		

CABLE C: Ledex to Control Unit

To	1		Panel II. 1
Corresponding	2		Panel II. 2
Numbers	3		S.B.3.
on	4		S.B.4.
Ledex	5		Panel II. 5
End	6		Panel II. 6
Connector	7		Delay 9
(Figure A3)	8		Delay 10

CABLE D: Programme Unit to Control Unit

Prog. A	1		Delay 4
Prog. G	2		Delay 3
Prog. E	3		Delay 7
Prog. F	4		Earth

Figure A. 3. Further Wiring Diagrams.

(a) End Connector of Ledex

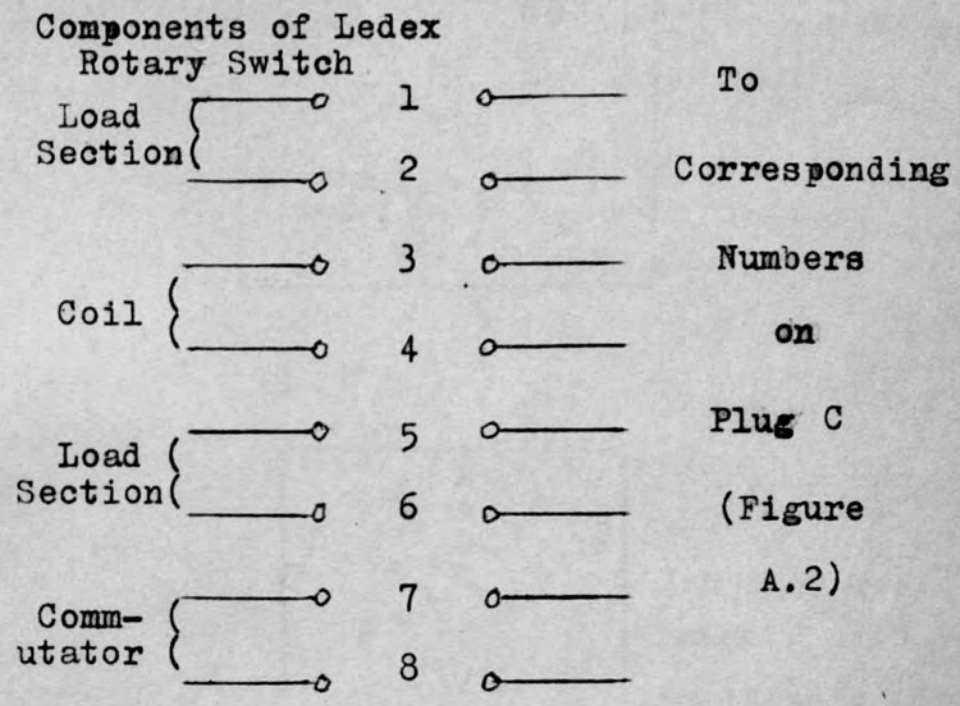

(b) End Connector of Panel II

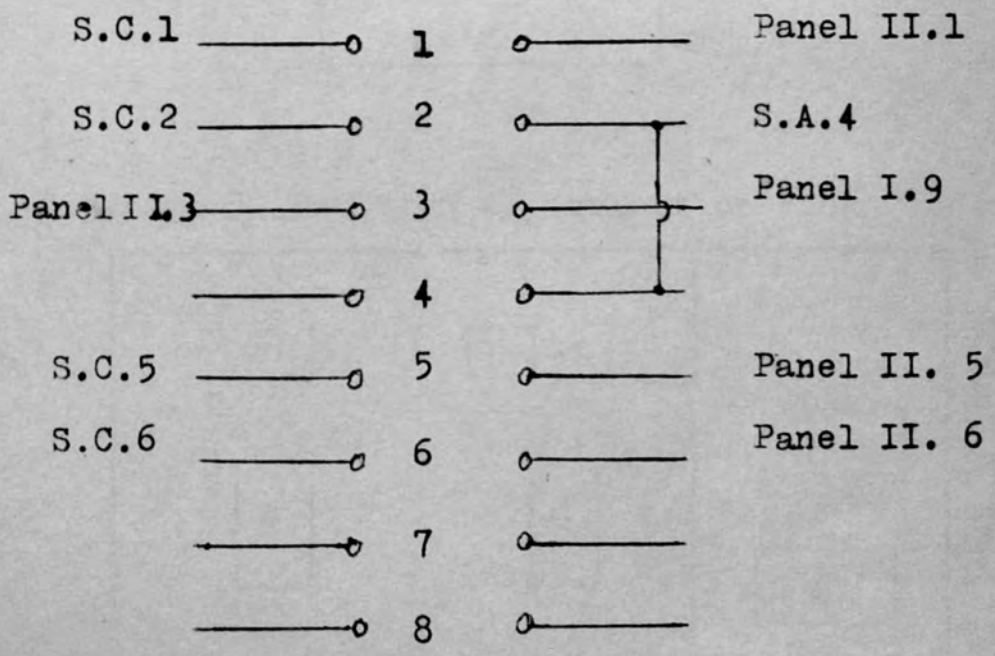

Figure A.4 External Arrangement of Front Panels

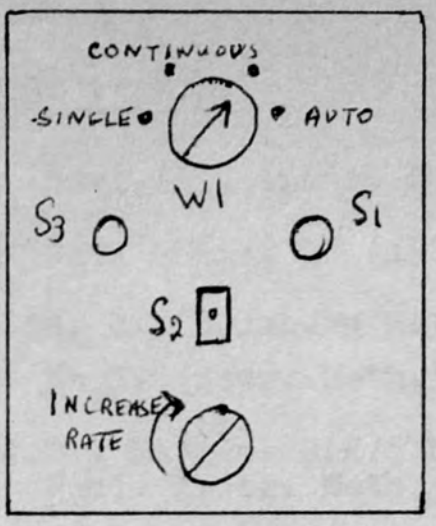

Front Panel I

S_1) Push Buttons
S_3)

S_2 Toggle Switch

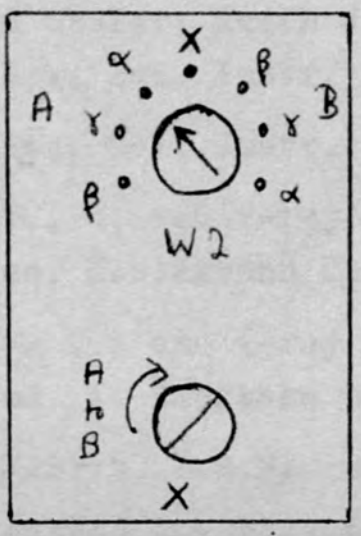

Front Panel II

Range A 0-3.7 Amps

Range B 3.5 - 7.0 Amps

Position X - for Smooth Change Over

Figure A.5 Position of Sockets on Back Panels.

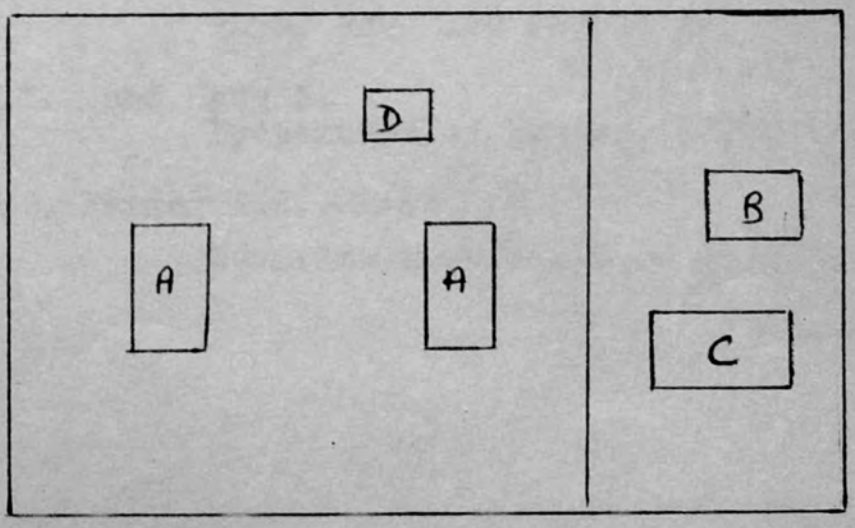

REFERENCES

Alburger, D.E. Rev. Sci. Instr. 27 (1956) 991.

Bäckström, G. Nucl. Phys. 15 (1960) 566.

Bäckström,G., Bäcklin, H., Holmberg N.E., Bergkvist, K.E., Nucl. Instr. Meth. 16 (1962) 199.

Baird G.L., Nall, J.C., Haynes, S.K., Hamilton J.H. Nucl. Instr. Meth. 16 (1962) 275.

Bartlett A.P., Ristinen R.A., Bird, R.P. Nucl. Instr. Meth. 17 (1962) 188.

Bartlett A.P., Howard Shafer, Keith J.R., Rev. Sci. Instr. 35 (1964) 1072.

Bell P.R. Rev. Sci. Instr. 26 (1955) 726.

Bell R.E. α, β, and γ-ray Spectroscopy (1965) ed. K.Siegbahn Ch. 17.

Bergström I., et al. α, β and γ-ray Spectroscopy (1965) ed. K. Siegbahn p.120.

Bertoya H.C. J.Brit. I.R.E. 25 (1963) No.2

Birks J.B. Theory and Practice of Scintillation Counting (Pergamon) 1964.

Burde J., Rakevy M., Engler G. Phys. Rev. 128 (1962) 325

Champion F.C., and Davy N. Properties of Matter. (Blackie) 1941. p.267.

Cramer, J.G., Farmer B.J.,Class C.M., Nucl.Instr. Meth.16 (1962) 289.

Dekker, A.J. Solid State Physics (Macmillan) 1955.

Enge H.A., Wahlig, M.A.
Rev. Sci. Instr. 28 (1957) 145.

Evans, R.D. The Atomic Nucleus. McGraww Hill (1955)

Evans, P.R., Freeman, N.J., McGinty G.K., Armitage, B.H. Richardson, H.O.W.
Proc. Phys.Soc. 72 (1958) 949.

Evans, P.R. * Ph.D.Thesis.University of Exeter (1958).

Ewan G.T., Graham R.L.
β and γ ray Spectroscopy, ed. K.Siegbahn (1965) Ch.18 B.

Forafontov N.V.,Sorokin,J.E.T.P. (U.S.S.R.) 36 (1959) 329.

Forafontov N.V., Shipnel V.S., Vasilev T.S.
Nucl. Phys. 35 (1962) 260.

Freedman M.S., Wagner F. (Jr.), Porter, F.T.Terandy J., Day P.P.
Nucl. Instr. Meths. 8 (1960) 225

Freeman N.J. Proc. Phys. Soc. 74 (1959) 449

Freeman N.J. Ph.D. Thesis. University of Exeter (1960)

Geiger J.S., Graham R.L., Ewan G.T.
Nucl. Phys. 16 (1960) 1.

Geiger J.S.,Graham R.L., Ewan G.T.
Nucl. Phys. 28 (1962) 387.

Geoffrion C., Giroux G.
Can. J. Phys. 34 (1956) 920

Graham R.L., Ewan G.T., Geiger J.S.
Nucl. Instr. Meth. 9 (1960) 245.

Gygi E.,Schneider F. Nucl. Instr. Meth. 20 (1963) 352.

Hä gström S., Nordling C., Siegbahn K.
α, β and γ-ray Spectroscopy, ed. K. Siegbahn (1965), Appendix 2.

Hedgran A. Arkiv f, Fysik. 5 (1952)1.

Iwashita T., Inamura T., Ikemoto Y., Kageyama S., J. Phys. Soc. Japan 18 (1963) 1358.

Jackson D.A. Ph.D. Thesis. University of London. (1964)

Jungerman J.A., Gardner M.E., Patten C.G., Peck N.F., Nucl. Instr. Meth. 15 (1962) 1

Kelman V.M., Peregood P.R., Skopina V.I., Soviet Physics. Techn. Phys. 7 (1962) 1068.

Kelman V.M., Peregood P.R., Skopina V.I., Nucl. Instr. Meth. 27 (1964) 190.

Kinard F.E. Nucleonics 15 (1957) 92.

Koechlin Y. J. Phys. Radium 18 (1955) 849.

Krüsche A., Bloess D., Münnich F. Nucl. Instr. Meth. 33 (1965) 177.

Lanstriat G., Coche A., J. Phys. Radium 19 (1958) 927.

Matveev V.V., Minaeva E.E., Sokolov A.D. Instrum. Exper. Tech. U.S.A. 1 (1962) 146.

Michelson D. Ph.D. Thesis. University of London (1961)

Mitchell A.C.G. α, β and γ-ray Spectroscopy. ed. K.Siegbahn (1965) Ch. 8A.

Neiler J.H., Bell P.R. α, β and γ-ray Spectroscopy ed. K.Siegbahn (1965) Ch.5.

Parfenova V.I., Forafontov N.V., Shipnel V.S.
I S V Akad. Nank. S.S.S.R. Ser. Phys. 21 (1957) 1601

Parker W.L., Slatis H.
α, β and γ-ray Spectroscopy, ed. K. Siegbahn (1965) Ch. 7A.

Petterson H., Grunditz Y., Bäckström G., Bergman O., Antman S., Aasa E.
Institute of Physics, Uppsala. Report(1964)

Richardson H.O.W., Michelson D.
Proc. Phys.Soc. 81 (1963) 553.

Rutherford E. Radioactive Substances and their Radiations. (Cambridge) 1913.

Serson P.H. Can. J. Phys. 35 (1957) 1387.

Siegbahn K., Edvardson K.
Nucl. Phys. 1 (1956) 137.

Siegbahn K., Nordling C., Karlsson S.E., Hagström S., Fahlman A., Andersson L.
Nucl. Instr. Meth. 27 (1964) 173.

Siegbahn K. α, β and γ-ray Spectroscopy ed. K.Siegbahn (1965) p.107.

Symonds J.L. Rep. Prog. Phys. 18 (1955) 102.

Valentin J., Horen D.J., Hollander J.M.
Nucl. Phys. 31 (1962) 353, 373.

de Vriss C., Wapstra A.H.
Nucl. Instr. Meth. 8 (1960) 120.

Wapstra A.H. α, β and γ-ray Spectroscopy, ed. Siegbahn (1965) Ch. 8C.

Yaffe L. Ann. Rev. Nucl. Sc. 12 (1962) 153.